



CO₂ Capture Mongstad - Project B - Theoretical evaluation of the potential to form and emit harmful compounds

Task 2: Atmospheric Chemistry

Dennis Angove, Phil Jackson, Nicholas Lambropoulos, Merched Azzi
and Moetaz I. Attalla

Revision 03
18th October 2010

Enquiries

Dr. Merched Azzi
CSIRO Energy Technology
(02) 94905307
merched.azzi@csiro.au

Copyright and Disclaimer

© 2010 CSIRO To the extent permitted by law, all rights are reserved and no part of this publication covered by copyright may be reproduced or copied in any form or by any means except with the written permission of CSIRO.

Important Disclaimer

CSIRO advises that the information contained in this publication comprises general statements based on scientific research. The reader is advised and needs to be aware that such information may be incomplete or unable to be used in any specific situation. No reliance or actions must therefore be made on that information without seeking prior expert professional, scientific and technical advice. To the extent permitted by law, CSIRO (including its employees and consultants) excludes all liability to any person for any consequences, including but not limited to all losses, damages, costs, expenses and any other compensation, arising directly or indirectly from using this publication (in part or in whole) and any information or material contained in it.

EXECUTIVE SUMMARY

This report is associated with the provision of contracted services by CSIRO in support of the CO₂ Capture Mongstad (CCM) Project. The primary purpose of the work was to improve knowledge concerning the abiotic fate of PCC emissions to the atmosphere.

The work started on the 30th May and was performed to satisfy the objectives specified for Project B Task 2: *Theoretical evaluation of the fate of harmful compounds post emission*, being a component of the principal activity *Protocol for the evaluation of solvents: Process and Atmospheric Chemistry*.

An extensive literature review was performed. A number of publications on the atmospheric chemistry of some alkylamines and to a lesser extent of MEA was found. Apart from the theoretical study by Bråten *et al.* (2008), no publications concerned with the atmospheric chemistry of AMP, MDEA and PZ were found, apart from a limited sub-study of AMP which was included in the Maximum Incremental Reactivity (MIR) Scale study by Carter (2008).

The potential for the formation of nitrosamines and nitramine from amines including MEA was investigated. However, information relevant to the formation of these compounds from AMP, MDEA and PZ in the gas phase was not found. Based on ASPEN modelling amine emission outcomes from Project B Task 1, the ranking of solvents based on their propensity to form *N*-nitroso compounds from highest to lowest is B (AMP/PZ) > A (MEA) > C (MEA/MDEA).

Where OH rate constant data was available, the atmospheric lifetimes of the oxidative degradation products of amines that were identified in Task 1 have been determined.

Aerosol formation from MEA was discussed in light of recent findings by Nielsen *et al.* (2010) and Angove *et al.* (2010). If present in the gas phase, the rapid formation of aerosol from AMP, MDEA and PZ in the presence of HNO₃ or H₂SO₄ is expected. However, no publications concerning this possibility were found.

Based on the observations by Pitts *et al.* (1978) for diethylamine and triethylamine and estimates by Nielsen *et al.* (2010) for MEA, the yields of *N*-nitroso compounds from PCC solvents in the gas phase in the presence of NO_x is likely to be <3%. However, this assumption needs to be tested and verified by experiment.

Results from two MEA theoretical computational studies are presented as **Research Addenda** in this report. Study 1, Jackson and Attalla (2010) predicted branching proportions of C2:50.3%, O: 44.3%, N: 5.4% and C1 << 0.1%. In comparison, in Study 2, Lambropoulos (2010) predicted branching of C2: 1.7%, O: 63.9%, N: 31.9% and C1:2.4%. These results differ markedly with respect to hydrogen abstraction from C1, C2 and N. However, both studies indicate that hydrogen abstraction from the hydroxyl group is a major pathway. Only the Jackson and Attalla (2010) predictions support the conclusion of Nielsen *et al.* (2010) that C2-H abstraction is predominant over C1-H and N-H abstractions.

The overall OH rate constant determined in Study 1 was $1.14 \times 10^{-10} \text{ cm}^3 \cdot \text{molecule}^{-1} \cdot \text{s}^{-1}$ and in Study 2, $2.56 \times 10^{-10} \text{ cm}^3 \cdot \text{molecule}^{-1} \cdot \text{s}^{-1}$. When used to model an experiment performed in the Angove *et al.* (2010) MEA, kinetic matrix study, both these rate constants produced a much improved outcome in comparison to the rate constants used by Carter (2008) and that estimated by Nielsen *et al.* (2010).

At this stage, there is insufficient validated information related to the atmospheric chemistry of amines, hence, the determination of the atmospheric fate of amine emissions can only be performed at this time with high precautions.

To overcome the shortcomings in knowledge a number of recommendations, all of which are strongly linked to the critical objectives and “Protocol Steps” given in the Test Protocol, (Project B task 3), have been made. A summary of these recommendations is as follows:

Summary of Recommendations

- a. To facilitate the design of experiments, it is recommended that a composition matrix (Amine/NO_x) be developed that is representative of the range of concentrations expected from a PCC plant, similar to that employed by CSIRO during the recent MEA study for Norsk Energi/Gassnova.
- b. The collected data can be used to establish a reactivity scale for different amines under different NO_x concentrations to predict major degradation products in the atmosphere.
- c. It is recommended that, using the composition matrix, results from experiments that have been performed in a well characterised smog chamber be used to construct and verify a new or, modify an existing gas phase, explicit chemical mechanism for alkanolamine and diamine, atmospheric degradation. The impact of amine emissions on more representative, ambient atmospheric systems should also be investigated.
- d. It is recommended that isotopic labelling of parent alkanolamines/alkylamines be prepared and used to assist in the elucidation of atmospheric chemical pathways.
- e. In order to understand the chemistry and conditions required to form aerosol from the reaction between alkanolamines/piperazine and HNO₃ and, other acids, it is recommended that gas phase/aerosol partitioning studies be performed on all solvents.
- f. It is recommended that a method be established for the collection of aerosol that minimises changes in morphology and, that after preliminary research, that an analytical method be developed to target species of concern, such as nitrosated compounds and oligimeric components.
- g. Once the aerosol has been characterised to >80% of its mass has been identified, it is also recommended that an aerosol formation mechanism be developed drawing on results from the elucidated explicit gas phase mechanism and new aerosol partitioning studies.
- h. After the updated chemical mechanism has been validated and optimised, it will need to be embedded in a selected air quality model to predict the spatial and temporal concentrations fields over a selected modelling domain. The predicted concentration profiles of the selected pollutants can be used to assess the exposure and potential environmental impacts of these pollutants. This model can be used as a step in the protocol developed in Project B Task 3.
- i. It is recommended that the Quantum Chemistry (QC) computational methods employed be reviewed and where suitable, applied to AMP, MDEA and PZ systems.

It is further recommended, that such studies be performed in a benchmarked environment to assist their development, thus ensuring a systematic approach when applied to amine chemistry. Where possible, outcomes from computational methods should be verified by experiment.

ABBREVIATIONS

AMP	2-amino-2-methyl-1-propanol
CB05	Carbon Bond Model 2005
CSIRO	Commonwealth Scientific and Industrial Research Organisation
DEA	diethanolamine
FTIR	fast Fourier transform infrared spectroscopy
HPLC	high pressure liquid chromatography
INRS	French National Research and Safety Institute
IR	infrared
LC/MS	liquid chromatography/mass spectrometry
MDEA	methyldiethanolamine
MEA	2-aminoethanol, monoethanolamine
MIR	maximum incremental reactivity
NILU	Norwegian Institute for Air Research
NIOSH	United States National Institute of Occupational Safety and Health
NO _x	oxides of nitrogen
OSHA	United States Occupational Safety and Health Administration
ppb	parts per billion (by volume)
ppmv	parts per million (by volume)
PCC	post-carbon capture
PZ	piperazine
R	correlation coefficient
SAPRC	Statewide Air Pollution Research Centre
SOA	secondary organic aerosol
TAPM	The Air Pollution Model
TEA	triethanolamine
VOC	volatile organic carbon
US EPA	United States Environmental Protection Agency

CONTENTS

EXECUTIVE SUMMARY	i
1. Introduction	10
2. Atmospheric Amine Chemistry	12
2.1 Literature Overview	12
2.2 Chemical and physical properties of MEA, MDEA, AMP and PZ	13
3. Gas phase decomposition of MEA - Pathways	16
3.1 Summary of MEA Studies	16
3.2 Chemical Reactions (applicable to MEA)	16
3.2.1 C1, C2 and N atom-centred hydrogen abstractions	16
3.2.2 Peroxy radical self-termination	25
3.2.3 Imine formation	26
3.2.4 Amino radical removal.....	27
3.2.5 Ammonia generation	28
3.3 Nitrosamine and nitramine formation	28
3.4 Aerosol formation and partitioning.....	30
4. Atmospheric Lifetimes	31
5. H&E Relevance of process and Atmospheric Chemistry	37
6. Ranking of Solvents	41
7. Computational Chemistry Studies	43
8. Recommendations	46
8.1 Modelling Context	46
8.2 Characterisation of PCC emissions to atmosphere	47
8.3 Elucidation of chemical mechanism	47
8.4 Verification of explicit and reduced gas-phase mechanisms	47
8.5 Aerosol formation	48
8.6 Predictive dispersion modelling using the embedded mechanism	48
8.7 Computational chemistry	49
8.8 Summary of recommendations	49
9. Acknowledgements	50
10. References	51
Research Addendum – STUDY 1	55
Theoretical study of the atmospheric fate of 2-aminoethanol (MEA)	55
<i>Authors: Phil Jackson and Moetaz I. Attalla</i>	55
Summary	55
Introduction	56
Computational methods	56
Results	57
Hydrogen abstraction at O	59
Hydrogen abstraction at N	60
Hydrogen abstraction at C1	60
Double-bond formation?.....	61
Peroxo and oxo species.....	63
Cx-oxoMEA (oxidanyl radicals) and associated unimolecular decomposition.....	65

Decomposition of Cx-peroxoMEA	66
Fate of •CH ₂ OH (hydroxymethyl) radicals	67
Fate of •CH ₂ NH ₂ (aminomethyl) radicals.....	68
Formation of C- and N-nitroso species.....	69
Formation of C- and N-nitro, nitrite species.....	74
Aminyl (•NH ₂) radicals.....	76
References to Study 1.....	78
Research Addendum – STUDY 2.....	79
First principles determination of rate constants – MEA degradation.....	79
<i>Author: Nicholas Lambropoulos</i>	79
Introduction	79
Transitions state search methods.....	79
Model scenarios investigated	81
Computational methodology	82
Derived rate constants using synchronous direct methods	83
Observations	87
Improved NEB - The Dynamical Matrix Approach	87
Preliminary Recommendations	90
References to Study 2.....	91

LIST OF TABLES

Table 1 Summary of physical properties for MEA, MDEA, AMP and PZ	14
Table 2 Summary of products predicted to form during the atmospheric degradation of MEA as considered by Bråten et al. (2008).....	17
Table 3 Summary of available MEA+OH rate constants	20
Table 4 Atmospheric lifetimes of nitrosated-compounds of interest	31
Table 5 Atmospheric lifetimes of oxidative degradation products of amines identified in Project B Task 1	33
Table 6 Atmospheric fate of degradation products of amines (degradation products identified from Kennard and Melsen, 1985; Strazisar, 2003; Goff and Rochelle, 2004; Bello and Idem, 2005; Supap, 2006; Bedell, 2009; Freeman, 2009; Lepaumier, 2009, Jackson and Attalla, 2010).....	39
Table 7 Atmospheric emissions of generic solvents and their contribution to the production of atmospheric pollutants	42

List of Figures

Figure 1 Modelling simulations for CSIRO MEA experiment E514 using SAPRC using MEA+OH rate constants presented in Table 3	21
Figure 2 Modelling simulations for CSIRO MEA experiment E514 using CB05 using MEA+OH rate constants presented in Table 3	21
Figure 3 Scheme 1: C1-hydrogen abstraction and resulting theoretical mechanism, adapted from Bråten et al. (2008)	22
Figure 4 Scheme 2: C2-hydrogen abstraction and resulting theoretical mechanism, adapted from Bråten et al. (2008)	23
Figure 5 Scheme 3: N-hydrogen abstraction and resulting theoretical mechanism, adapted from Bråten et al. (2008)	24
Figure 6 Scheme 4: Peroxy radical self-termination.....	25
Figure 7 Scheme 5: Formation of an imine derivative via the Leuckart Reaction between MEA and cyclohexanone	26
Figure 8 Scheme 6: Proposed formation of unidentified products of m/z 74, 88, 102 and 104 as detected by Nielsen et al. (2010).....	27
Figure 9 Scheme 7: Reaction of amino radicals with NO and NO2.....	27
Figure 10 Scheme 8: Proposed reaction for the formation of ammonia from the ethanol ammonium nitrate cation.....	28

Revision	Description	Issue Date
01	Draft	9 August 2010
02	Resubmitted Draft	7 September 2010
03	Corrected with CCM comments	18 October 2010

1. INTRODUCTION

In the case of fossil-fired power stations, absorption-desorption technologies are being developed to capture CO₂ in a post-combustion capture process (PCC). The absorber contains solvents, such as alkanolamines, that can chemisorb CO₂. Widely used solvents include monoethanolamine (MEA), diethanolamine, (DEA), triethanolamine (TEA), methyldiethanolamine (MDEA) and the diamine, piperazine (PZ). Ammonia and 2-amino-2-methyl-1-propanol (AMP) are also being trialled. With the widespread rollout of PCC technology, it is expected that the number of formulations used will increase exponentially, as solvent providers seek niche markets for patented assets.

Although the process technology has been in wide use since the 1930's (Kohl and Nielsen, 1997), the application of this technology to control CO₂ emissions from coal-fired and gas-fired power stations requires an increase in the scale of the process well beyond previous experience. As a result, expected emissions of alkanolamines and their degradation products may pose an environmental risk, which will need to be addressed. Hence, the purpose of this short-time project is to close the knowledge gap, in this case, for the most widely used amine, MEA.

The chemistry of CO₂ absorption by alkanolamine solutions is complex. It depends on the nature of the amine absorbent (primary, secondary or tertiary), and involves an equilibrium between aqueous HCO₃⁻, aqueous carbamate (primary and secondary amines only) and gaseous CO₂. The alkanolamine is regenerated by releasing the CO₂ at an elevated temperature. A useful introduction to CO₂/alkanolamine chemistry can be found in McCann *et al.* (2008; 2009). Process plant design information such as vapour pressure curves etc. can be found in the advanced textbook by Kohl and Nielsen (1997).

The alkanolamine solvent solution used as the CO₂ absorber does not only react with CO₂ present in the flue gas but also with other acid constituents. These secondary reactions may produce different types of chemical species that can affect the selectivity and the absorption capacity of the amine solvent. The CO₂ capture plant releases the treated flue gas from the top of the absorber to the atmosphere. These emissions depend on the operating conditions of the absorber top. Amines, ammonia, aldehydes and carboxylic acids are the major compounds expected to be released from the plant. Once emitted to the atmosphere, these compounds undergo different complex chemical reactions to produce different types of pollutants.

There are a lot of gaps in the knowledge related to the atmospheric chemistry of these compounds. The loss of solvent by chemical degradation mechanisms and its subsequent *emission to the atmosphere* represents a significant challenge for the operation of amine-based, carbon capture plants. One purpose of this review is to identify such knowledge gaps.

Project B Task 2 had the following objectives:

- Update literature review of atmospheric chemistry of the selected solvents and provide recommendations for further research to close gaps in available information
 - Potential to form nitrosamines, nitramines and particles/aerosols to be considered as a minimum
 - Partitioning of substances between the gas and aqueous/aerosol phases
- Estimations of yields, formation rates and lifetimes in the environment where/if possible:
 - Carry out quantum-chemical calculations for selected amines including solvation (water component)
 - Compare and evaluate rate constants using novel solid state physics approach

- Evaluate importance of process versus atmospheric chemistry with respect to H&E impact
- Update ranking of solvents from Project B Task 1

As a result of the literature review performed as part of this Task, studies of the atmospheric chemistry of 2-amino-2-methyl-1-propanol (AMP), methyldiethanolamine (MDEA) and piperazine (PZ) were not identified, except for the theoretical study performed by Bråten et al (2008). This lack of information has limited our efforts to discuss the atmospheric chemistry of AMP, MDEA and PZ and to identify their atmospheric degradation products in this report.

In relation to the application of amine solvents to PCC, this Task focussed on the atmospheric chemistry of 2-aminoethanol (monoethanolamine and MEA).

2. ATMOSPHERIC AMINE CHEMISTRY

2.1 Literature Overview

Estimating lifetimes of amines and their degradation products requires the knowledge of the rate constants of the chemical reaction pathways that control the sink and production of species. The major identified atmospheric reactions controlling the degradation of amines are reactions with OH, O₃, NO₃ and HNO₃. The amines are known to react rapidly with OH radical where the rate constant controlling this reaction is still not fully determined. Also, there is less knowledge about other pathway rate constants. These difficulties are related to the fact that it is very complex to manipulate these solvents because of their chemical characteristics.

In the US in the late 1970's and early 1980's there was concern about the use of amines in jet engine fuels and consequently the formation of carcinogenic compounds such as nitrosamines in the atmosphere. Some smog chamber studies have been performed on the photochemical degradation of amines in air in the presence of oxides of nitrogen (NO_x). Pitts *et al.* (1978) studied the photochemical oxidation of diethylamine and triethylamine and observed the formation of nitrosamines, nitramines and amides as well as secondary organic aerosol (SOA). Lindley *et al.* (1979) conducted rate studies of reactions between the dimethylamino radical and O₂, NO and NO₂. Tuazon *et al.* (1984) determined the k_{OH} for N-nitrosodimethylamine and dimethylnitramine. Additional amine/OH rate constant studies have also been determined by Atkinson *et al.* (1978) for dimethylamine; (CH₃)₂NH₂, trimethylamine; (CH₃)₃N and ethylamine; C₂H₅NH₂. Grosjean (1991) generated detailed mechanisms for the atmospheric chemistry of amines which included diethylamine, triethylamine and dimethylamine. Grosjean (1991) also stated that nitramines do not photolyse and are expected to accumulate in the atmosphere. Schade and Crutzen (1995) proposed photochemical reaction schemes for mono-, di- and trimethylamine. The formation of imine products appeared to be common to their reaction schemes.

More recently, amines have been detected in ambient urban aerosol samples prompting more interest in aerosol formation from amine precursors. Murphy *et al.* (2007) studied SOA formation from aliphatic amines and concluded that non-inorganic aerosol formed was more stable than nitrate salts. The role of triethylamine as an urban SOA precursor was studied by Silva *et al.* (2008), who concluded that amines could contribute significantly to the SOA burden in urban areas if the nitrate radical concentration was high enough. The nitrate radical photochemistry with simple aliphatic amines was also investigated by Malloy *et al.* (2009). They observed SOA formation after rapid nucleation, in all cases.

Carter (2008) performed smog chamber experiments to determine the maximum incremental reactivity (MIR) values for MEA and AMP that are related to potential ozone formation. It was concluded that MEA would have positive and relatively high impact on ozone formation, whereas, AMP would act as ozone inhibitor. In addition, Carter (2008) reported that AMP and MEA had high PM formation potentials. As stated by Carter (2008), these conclusions were made under problematic conditions because precise MIR coefficients could not be determined since initial and subsequent removal of the MEA or AMP could not be measured reproducibly. This is also evidenced by the reported range of amine injection by volume which was 5-60% of that expected.

Bråten *et al.* (2008) recently completed a theoretical study for the Norwegian Institute for Air Research (NILU), on the atmospheric chemistry of amines. Importantly, they proposed MEA, AMP, MDEA and PZ gas-phase degradation as well as nitrosamine and nitramine formation mechanisms which have yet to be fully tested experimentally. Initiated by this study, Nielsen *et al.* (2010) and Angove *et al.* (2010) recently completed MEA/NO_x smog chamber study.

These studies that are discussed in Section 4 includes the formation of formaldehyde, acetaldehyde and glycolaldehyde.

The literature is scant on atmospheric and/or gas phase studies of AMP, MDEA and PZ. Consequently, a comparison between the atmospheric reactivities of these compounds and their degradation products could not be performed. The theoretical study by Bråten *et al.* (2008) includes products formed as a result of atmospheric gas-phase oxidation, such as acetamide from AMP, all of which require validation and verification by experiment.

It is known that amines react in the atmosphere through reactions with hydroxyl radicals (OH), ozone (O₃) and nitric acid (HNO₃). Amines do not photolyse in the upper actinic region (290 to 400 nm) of the spectrum (Pitts *et al.*, 1978). The reaction with OH is generally much faster than with O₃. For example, in the case of dimethylamine, OH radicals react seven orders of magnitude faster than ozone (Finlayson-Pitts and Pitts, 2000). The reaction with HNO₃ is thought to occur more readily in more polluted urban areas. The products of atmospheric amine degradation formed depend on the oxidising species, including NO_x, as well as ammonia which competes for acidic molecules. Similar to ammonia, amines can also undertake chemical reactions with either nitric or sulphuric acid to form the corresponding nitrate or sulphate salts (Murphy *et al.*, 2007).

An important class of gas phase degradation products of amines are nitrosamines and nitramines. The former are known to be potent carcinogens (Spiegelhalder, 1984). The latter are suspected carcinogens. Nitrosamines are expected to be in higher concentrations at night since they photolyse rapidly in daylight (Pitts *et al.*, 1978). This may be an important issue for PCC plant operation in winter, and particularly at high latitudes. Nitrosamines can be formed in the gas phase in the presence of NO_x and nitrous acid (HONO) or, photochemically in the presence of NO_x alone. It is hypothesised that surface reactions play a role in the formation of nitrosamines; hence, heterogeneous reactions on existing aerosol particles may also be important (Glasson, 1979). This latter postulate is yet to be tested experimentally although amines have been observed in urban aerosol collections (Silva *et al.*, 2008).

The atmospheric chemistry of six amides has recently been investigated by Barnes *et al.* (2010) by reviewing existing kinetic and mechanistic data in combination with new photoreactor studies. They include OH rate constants for formamide and acetamide in their paper.

In summary, the mechanism of the atmospheric oxidation of amines is still not well understood as only a limited number of theoretical and experimental studies have been undertaken. This is especially so for alkanolamines such as MEA and in particular, AMP, MDEA and PZ. The following statement by Finlayson-Pitts and Pitts (2000) is still current and sets the research challenge for studies of the atmospheric chemistry of amines:

“It should be noted, however, that in studies of amine photo-oxidations, it is generally true that a significant fraction of the reacted parent amine remains unaccounted for in the identified products. Clearly, the mechanisms and products are complex and warrant further investigation”.

2.2 Chemical and physical properties of MEA, MDEA, AMP and PZ

A characteristic that makes amines difficult to work with is the ease with which the parent amine can transform into a stable salt at pH < 7 and back again at pH > 7. Whilst the amine can be volatile or semi-volatile, the salt form has a very low vapour pressure. This occurs as a result of the ability of the un-bonded electron pair on nitrogen to readily protonate, which also makes it a highly reactive centre in an amine molecule. This polar nature also renders amines soluble in water up to 6 carbons, and greater than 6, sparingly soluble. It is true that analytical techniques can use these properties to advantage, but it is important within an

environmental context that the original nitrogenous state be known after application of the environmentally relevant, analytical technique and not masked by artefact formation caused by the reactivity of the amino nitrogen (or other substituents). This means that reliable and representative sampling is an issue, as well as the identification of previously unknown products formed during amine degradation.

As the degree of substitution onto the amino nitrogen increases the vapour pressure decreases markedly. The addition of one or more hydroxyl groups to the amine to form an alkanolamine also causes the vapour pressure of the amine to drop significantly. Consequently, due to their low vapour pressures, investigation of the atmospheric gas phase properties of the amines in PCC solvents A, B and C is made more complex, because injection method development is needed to move them from the liquid to gas phase without losses caused by condensation into an aerosol phase and/or onto investigative surfaces, such as smog chamber walls. For example, it is unlikely that MDEA will be studied in the gas phase, but rather in the aerosol phase, which is more likely to be its primary emission form.

Table 1 lists some of the physical properties of MEA, MDEA, AMP and PZ (source: CAS-SCIFINDER).

Table 1 Summary of physical properties for MEA, MDEA, AMP and PZ

Property	MEA	MDEA	AMP	PZ
Formula	$\text{CH}_2(\text{OH})\text{CH}_2\text{NH}_2$	$\text{CH}_2(\text{OH})\text{CH}_2)_2\text{NCH}_3$	$\text{CH}_3\text{C}(\text{CH}_3)(\text{NH}_2)\text{CH}_2(\text{OH})$	$[\text{NHCH}_2\text{CH}_2]_2$ cyclic
MW (g/mol)	61.09	119.17	89.14	86.14
Density (g/ml @ 20°C)	1.012	1.03	~0.93	1.1
Boiling Point (°C @ 1 atm.)	171	247.2	165	146
Vap. Pressure (Torr @ 25°C)	0.458	0.0043	0.566	4.1
Freez. point (°C)	10.5	-21.0	31	106
Water Sol. (g/100 ml @ 20°C)	complete	complete	complete	very

In addition, two important issues are the toxicity and general handling/storage of amines as well as related products, such as amides and nitroso- compounds, including in some cases, their explosive nature. The rendering safe of substances such as nitrosamines and their disposal is also of importance from an HS&E stance.

In summary the practical investigative issues when using amines are associated with:

- Ionic nature which is dependent upon pH.
- Reactivity of the lone pair electrons on the amino nitrogen
- Possibility of artefact formation during sampling
- Selection of most appropriate analytical technique for target analyte(s)
- Low vapour pressure (LVP) of PCC amines and VLVP of some degradation products

- Toxicity (including carcinogenicity)
- Specialist handling is required, hence staff training crucial.
- Safe handling and disposal of amines and degradation products which is required

3. GAS PHASE DECOMPOSITION OF MEA - PATHWAYS

3.1 Summary of MEA Studies

While some experimental studies on the atmospheric degradation of aliphatic amines have been performed (Pitts *et al.*, 1978; Schade and Crutzen (1995); Murphy *et al.* (2007); Silva *et al.*, 2008; Malloy *et al.*, 2009), there is very little published on the gas-phase atmospheric degradation of alkanolamines and piperazine, except for MEA.

Amine studies which included MEA were the particle phase smog chamber study by Murphy *et al.* (2007), the MIR smog chamber study by Carter (2008) and the amine/nitrate radical study by Malloy *et al.* (2009). In all three of these studies, MEA consumption is considered to be uncertain. Murphy *et al.* (2007) did not measure MEA and assumed 100% was injected. Carter *et al.* (2008) had difficulty with injection and measurement of MEA while Malloy *et al.* (2009) were unable to detect amine signals with their PTRMS and assumed 100% injection and consumption.

Bråten *et al.* (2008) derived theoretical degradation pathways for MEA as well as AMP, MDEA and the heterocyclic diamine, piperazine (PZ). They considered initial radical formation by hydrogen abstraction by the OH radical from both aliphatic carbons and the amine group. This study initiated the preliminary MEA/NO_x atmospheric chemistry, smog chamber studies by Nielsen *et al.* (2010) at EUPHORE, located in Valencia and the kinetic matrix study by Angove *et al.* (2010) using the CSIRO chamber located in Sydney. These studies were able to measure MEA consumption, albeit with difficulty.

Since the detailed Bråten *et al.* (2008) theoretical study is consistent with the amine mechanisms proposed by Pitts *et al.* (1978), Grosjean (1991) and Schade and Crutzen (1995), it will be used as a basis for discussing the gas phase decomposition of MEA. This is especially advantageous since unlike the earlier studies, it also considers abstraction from the β or C1 carbon.

Bond dissociation enthalpies of aliphatic amines, including MEA, were determined by Lalevée *et al.* (2002). MEA dimer stability was investigated by Vorobyoz *et al.* (2002) and found to be influenced strongly by the OH••N interaction. In a study by da Silva (2002), it was concluded that alkanolamines can form dimers with high formation energies. Galano and Alvarez (2008) used transition state theory to determine that at 298 K, the overall rate constant k_{OH} for ethylamine was $1.19 \times 10^{-11} \text{ cm}^3 \text{ molecule}^{-1} \cdot \text{s}^{-1}$ and that the C1-H, C2-H and N-H abstraction pathway fractions were ~0.02, 0.98 and <0.01, respectively.

3.2 Chemical Reactions (applicable to MEA)

3.2.1 C1, C2 and N atom-centred hydrogen abstractions

Bråten *et al.* (2008) investigated hydrogen abstractions from the C1, C2 and N atom-centred positions of MEA. Theoretical investigations of abstraction of hydrogen from the hydroxyl group are included in this report.

Schemes 1, 2 and 3 are mechanisms adapted from Bråten *et al.* (2008), which describe the pathways arising from hydrogen abstraction from C1, C2 and N atom-centres, respectively.

Table 2 summarises some of the products formed as a result of theoretical atmospheric degradation of MEA initiated by OH radical attack. An ID designation has been allocated to each species to enable ease of identification in the three mechanism schemes.

Table 2 Summary of products predicted to form during the atmospheric degradation of MEA as considered by Bråten et al. (2008)

ID	Product	Formula
A	formamide	(NH ₂)CHO
B	2-hydroxy-acetamide	(NH ₂)C(O)CH ₂ OH
C	2-amino-2-oxo-peroxyacetyl-	(NH ₂)C(O)C(O)OONO ₂
D	amino radical	•NH ₂
E	2-oxo-acetamide	(NH ₂)C(O)CHO
F	2-amino-peroxylacetyl-nitrate	(NH ₂)CH ₂ C(O)OONO ₂
G	2-nitroamino-ethanol	((NO ₂)NH)CH ₂ CH ₂ OH
H	N-nitramino-hydroxy-acetamide	((NO ₂)NH)C(O)CH ₂ OH
I	nitroamino-glycol	((NO ₂)NH)CHOHCH ₂ OH
J	nitrosoamino-glycol	((NO)NH)CHOHCH ₂ OH
K	2-nitrosoamino-ethanol	((NO)NH)CH ₂ CH ₂ OH

Nielsen *et al.* (2010) studied the gas phase photo-oxidation of MEA in NO_x and concluded that >80% of the reaction between OH radicals and MEA occurs at the C2 to H bond. Major products measured were formamide (A) and formaldehyde which is consistent with the C2 hydrogen abstraction mechanism shown in Scheme 2. They also detected amino acetaldehyde and 2-oxo-acetamide (E) which, according to Scheme 1, can be theoretically formed via C1 hydrogen abstraction. They estimated that <10% of the OH/MEA reaction proceeded down this pathway.

Nitrosamine formation was not observed by Nielsen *et al.* (2010) or Angove *et al.* (2010). However, the formation of the nitramine, 2-nitroamino-ethanol (G) was detected by Nielsen *et al.* (2010). This finding indicates that hydrogen abstraction from the N atom did take place. Nielsen *et al.* (2010) estimated that <10% of the OH/MEA reaction proceeded via hydrogen abstraction from N. These branching proportions are consistent with the findings of Galano and Alvarez (2008) for the related compound, ethylamine.

In the MEA theoretical studies presented as **Research Addenda** at the end of this report, Jackson and Attalla (2010) [**STUDY 1**] and Lambropoulos (2010) [**STUDY 2**] used quantum computational methods to investigate hydrogen abstraction by OH radicals from C1, C2, N and O atom-centres at 298K. Jackson and Attalla (2010) also investigated additional product formation pathways and Lambropoulos (2010) calculated hydrogen abstraction rate constants under hydrated-MEA conditions using two water molecules for radical stabilisation.

Jackson and Attalla (2010) predicted branching proportions of C2: 50.3%, O: 44.3%, N: 5.4% and C1 << 0.1%. In comparison, Lambropoulos (2010) predicted branching of C2: 1.7%, O: 63.9%, N: 31.9% and C1: 2.4%. These results differ markedly with respect to hydrogen abstraction from C1, C2 and N but both studies indicate that hydrogen abstraction from the hydroxyl group is a major pathway. Only the Jackson and Attalla (2010) predictions support the conclusion of Nielsen *et al.* (2010) that C2-H abstraction is predominant over C1-H and N-H abstractions.

Other products of interest formed and observed in the Nielsen *et al.* (2010) study include ammonia, acetaldehyde, ethylene glycol, acetamide and glycolaldehyde. Angove *et al.* (2010) also observed and quantified ammonia, formaldehyde and acetaldehyde. Glycolaldehyde was also observed but at low concentration.

The mechanism in Scheme 2 provides for the formation of glycolaldehyde and the amino radical, but this reaction is considered to be thermodynamically unfavourable which suggests the appearance of glycolaldehyde may arise from a surface reaction. The formation of ammonia is discussed in Section 4.3.5.

Similar to that observed by Murphy *et al.* (2007), Carter (2008) and Malloy *et al.* (2009), pronounced aerosol formation was observed in both the Nielsen *et al.* (2010) and Angove *et al.* (2010) studies. Aerosol formation is discussed in Section 4.5.

MEA consumption was measured in smog chamber experiments by both the Nielsen *et al.* (2010) and the Angove *et al.* (2010) studies. In the former, the concentration appeared to decrease uniformly whilst in the latter an initial rapid decrease was observed after the lights were turned on. In the Nielsen *et al.* (2010) study they determined that the product yield for formamide was ~0.8. In the Angove *et al.* (2010) formamide was not detected but this does not preclude that it was formed. In the Angove *et al.* (2010) study, the observed mass of MEA and the aerosol mass determined during this rapid-decrease period did not account for observed consumption of MEA.

One of the difficulties associated with understanding the MEA mass balance is demonstrated with the aid of SAPRC-07 and CB05 modelling of MEA in one of the MEA matrix experiments (E514: 475 ppb MEA; 51 ppb NO_x) performed by CSIRO (Angove *et al.*, 2010).for Norsk Energi and Gassnova. A brief review of the most widely used chemical lumped mechanisms for photochemical smog formation is given below.

The Statewide Air Pollution Research Centre (SAPRC) mechanism developed by Carter (2000) is one of the most widely used chemical mechanisms used to predict photochemical smog oxidants that employ the lumped species approach. This approach represents similar organic species with a particular organic compound or a generalised species. Recently, Carter has developed the new updated SAPRC-07 that has been evaluated against ~2400 environmental chamber experiments using over 120 types of VOCs. The mechanism improvements include updated chemical reactions and rate constants, reduced parameterised aromatic mechanisms and different representation for peroxy reactions allowing for SOA modelling. This mechanism has been peer-reviewed in 2009 by five separate investigations (Azzi, M. *et al.*, 2010). In addition, the model has a representation to MEA atmospheric reactions that was based on smog chamber data described as difficult by the developer. Because of the big number of chemical reactions of the mechanism, Carter produced another simplified version of mechanism that can be used in air quality models.

Another widely used chemical mechanism that has been released in 2005 and recommended by the USEPA for air quality simulations is the Carbon Bond chemical mechanism version 5 referred by CB05. The core of the CB05 mechanism (Yarwood *et al.*, 2005) that has been updated from the version IV of Carbon Bond Mechanism (CB4) (Gery *et al.*, 1989) has 51 species and 156 reactions. The inorganic reactions represented in the CB5 are now extended to simulate remote to polluted urban conditions. Organic species are lumped according to the carbon bond approach where reactions are lumped based on the similarity of carbon bond structure so that fewer surrogate species are needed in the model. For instance, the single-bonded one-carbon-atom surrogate PAR represents alkanes and most of the alkyl groups.

Several common characteristics of these mechanisms can be found. (1) The inorganic mechanisms are very similar. (2) Four organic species (methane, ethene, isoprene, and formic acid) are treated explicitly. (3) Most of the mechanisms use lumping approaches to reduce the great number of organic reactions. At the same time, the chemical mechanisms have some significant differences.

These differences occur in the following characteristics: (1) the lumping approaches for organic species, intermediates and products; (2) assumptions for unknown or poorly studied reactions, such as aromatics chemistry; and MEA chemistry (3) condensing processes for certain organic reactions; (4) pressure and temperature dependence of rate constants, especially for organic chemistry.

The modelling utilised available overall MEA+OH rate constants summarised in Table 3, which also includes ethylamine+OH rate constants determined by Atkinson *et al.* (1978), Carl and Crowley (1998) and computationally determined by Galano-Alvarez-Idaboy (2008), for comparison.

It can be readily seen in Figures 1 and 2 that for both SAPRC-07 and CB05, the recently calculated MEA+OH rate constants by CSIRO more readily account for the observed MEA degradation than the original calculated by Carter (2008) and that estimated by Nielsen *et al.* (2010) The non-hydrated rate constants determined by Jackson and Attalla (2010) and that by Lambropoulos (2010) produced MEA profiles which are more representative of the final concentrations at 6 hours than the others.

However, none of the simulations account for the initial rapid decrease in MEA since not all products formed during MEA photo-oxidation has been identified. In addition, since the computational studies produced different abstraction pathway proportions, definitive experimental pathway studies are required to improve the chemical mechanisms. This is also applies for AMP, MDEA and PZ.

Table 3 Summary of available MEA+OH rate constants

Hydrogen abstraction by OH radical	Rate Constants ($\text{cm}^3 \cdot \text{molecule}^{-1} \cdot \text{s}^{-1}$) at 298K				
	C1	C2	N	O	Overall
CSIRO MEA Study 1 <i>Without hydration</i>	1.95×10^{-14}	5.71×10^{-11}	6.16×10^{-12}	5.03×10^{-11}	1.14×10^{-10}
CSIRO MEA Study 2 <i>Without hydration</i>	6.28×10^{-12}	4.31×10^{-12}	8.19×10^{-11}	1.64×10^{-10}	2.56×10^{-10}
CSIRO MEA Study 2 <i>With hydration</i>	3.90×10^{-10}	3.18×10^{-9}	1.02×10^{-6}	1.18×10^{-3}	1.18×10^{-3}
MEA Nielsen <i>et al.</i> (2010)	2.9×10^{-12} <i>(note 1)</i>	2.8×10^{-11} <i>(note 1)</i>		1.6×10^{-13} <i>(note 1)</i>	0.31×10^{-10} <i>(note 1)</i>
MEA Carter (2008) (original)	-	-	-	-	0.441×10^{-10} <i>(note 2)</i>
Ethylamine Galano and Alvarez - Idaboy (2008)	2.26×10^{-13}	1.16×10^{-11}	4.76×10^{-14}	Not relevant	0.119×10^{-10}
Ethylamine Atkinson <i>et al.</i> (1977)	-	-	-	Not relevant	0.277×10^{-10}
Ethylamine Carl and Crowley (1998)	-	-	-	Not relevant	0.237×10^{-10}

Note 1: Estimates based on critical review of $\text{CH}_3\text{CH}_2\text{OH} + \text{OH}$ reactions

Note 2: Estimate based on structure-reactivity calculations

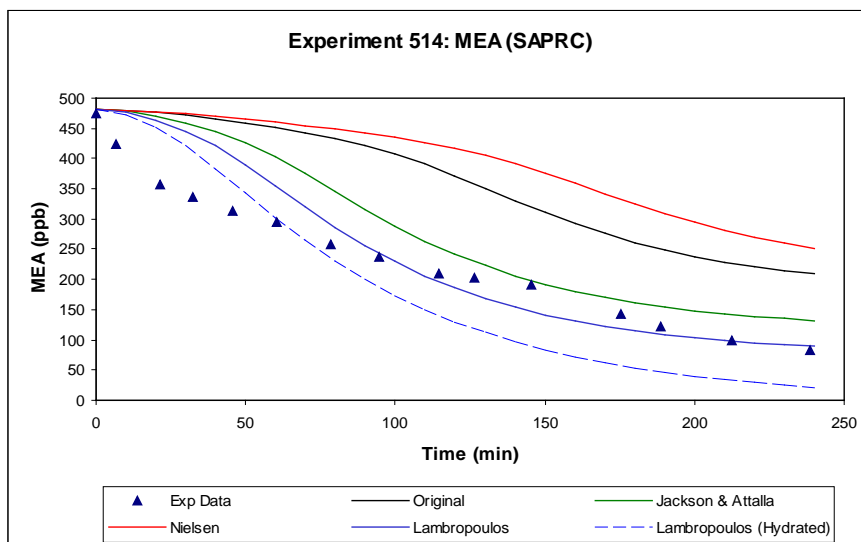


Figure 1 Modelling simulations for CSIRO MEA experiment E514 using SAPRC using MEA+OH rate constants presented in Table 3

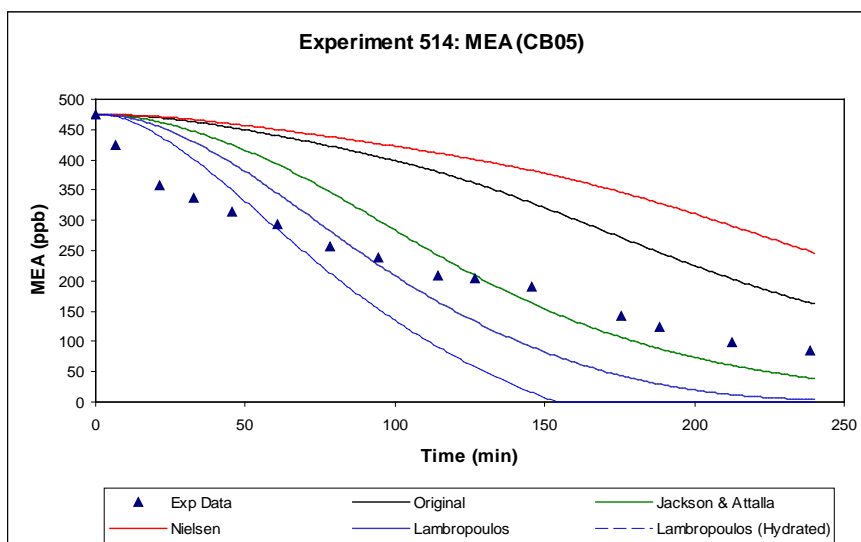


Figure 2 Modelling simulations for CSIRO MEA experiment E514 using CB05 using MEA+OH rate constants presented in Table 3

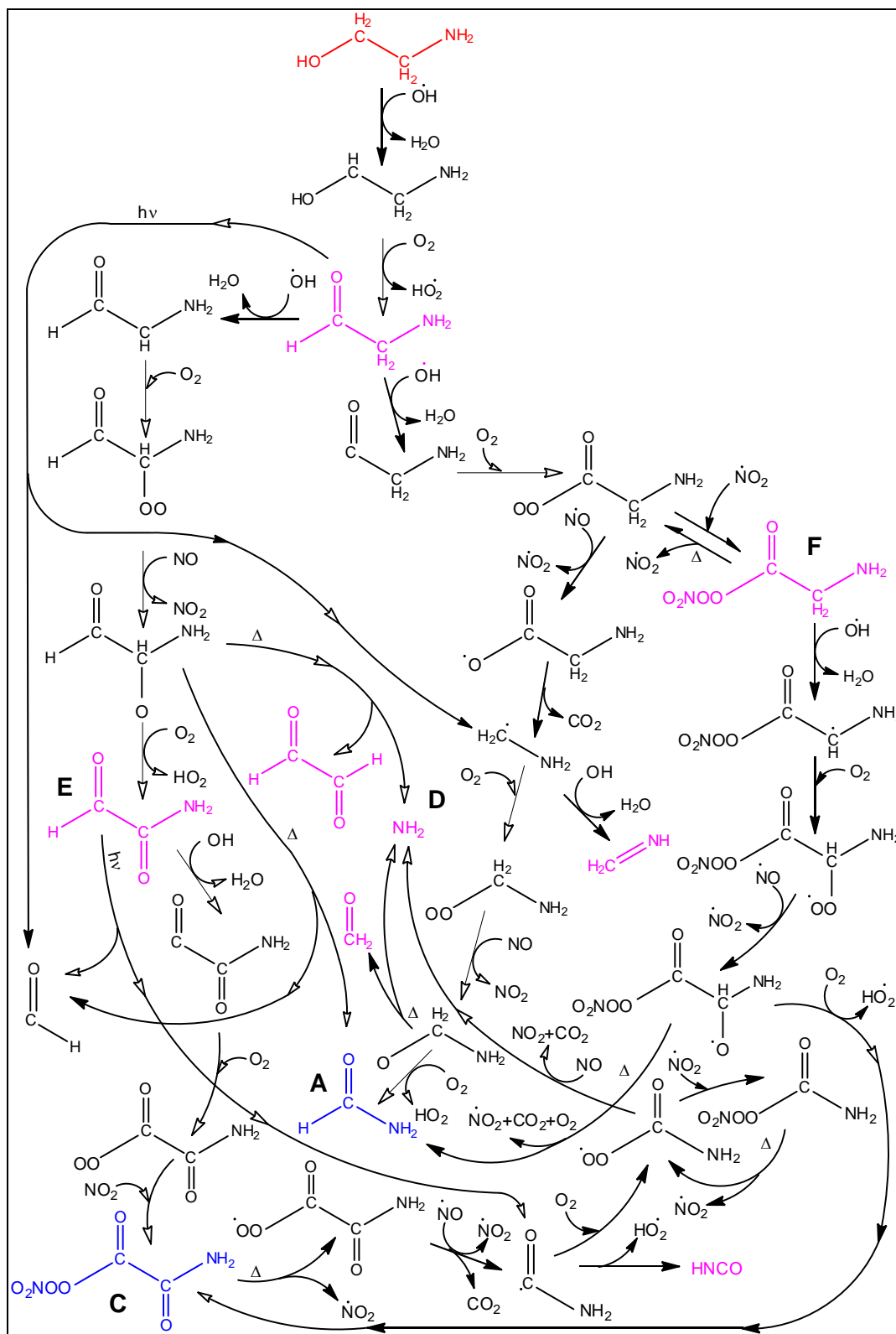


Figure 3 Scheme 1: C1-hydrogen abstraction and resulting theoretical mechanism, adapted from Bråten et al. (2008)

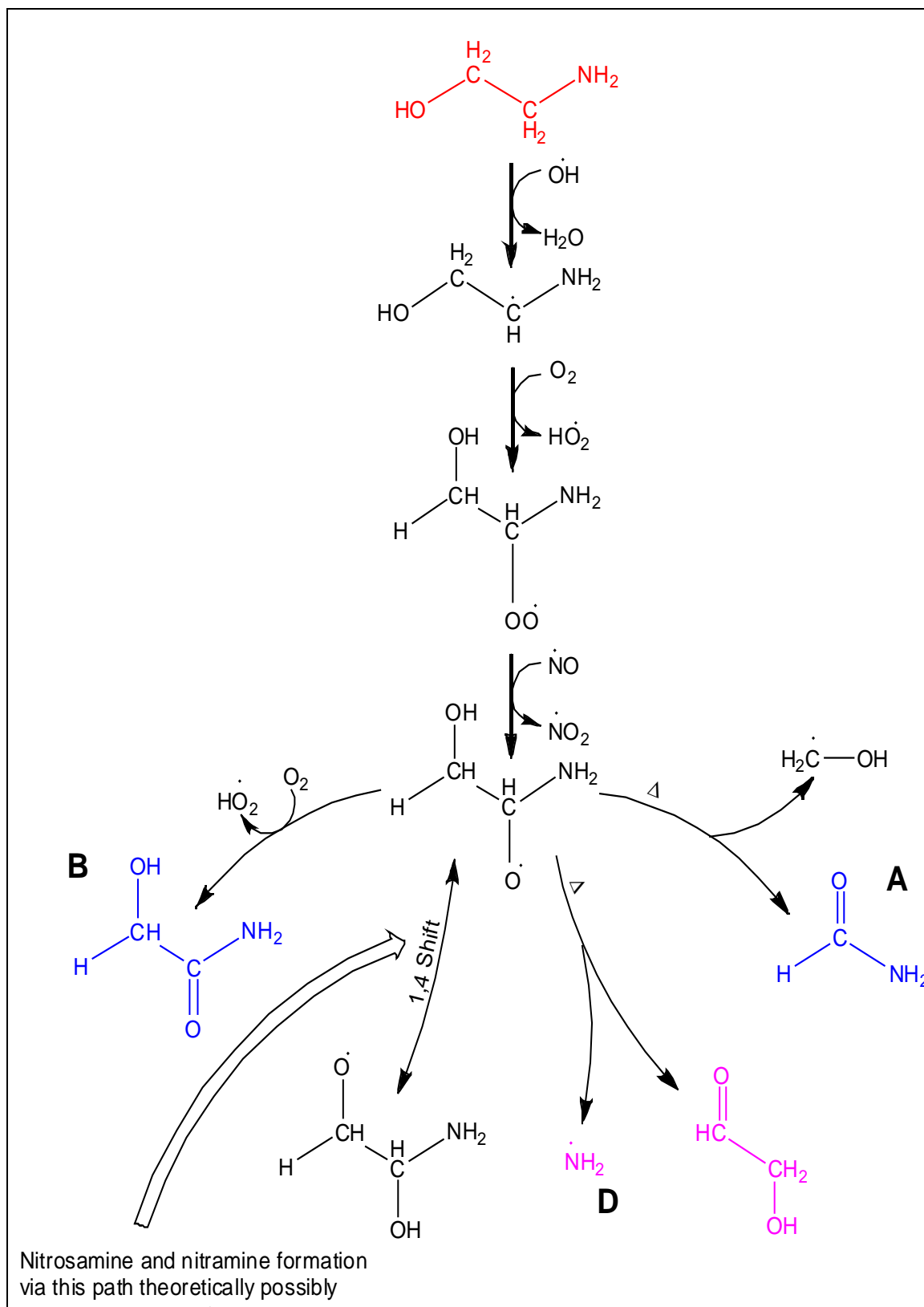


Figure 4 Scheme 2: C2-hydrogen abstraction and resulting theoretical mechanism, adapted from Bråten et al. (2008)

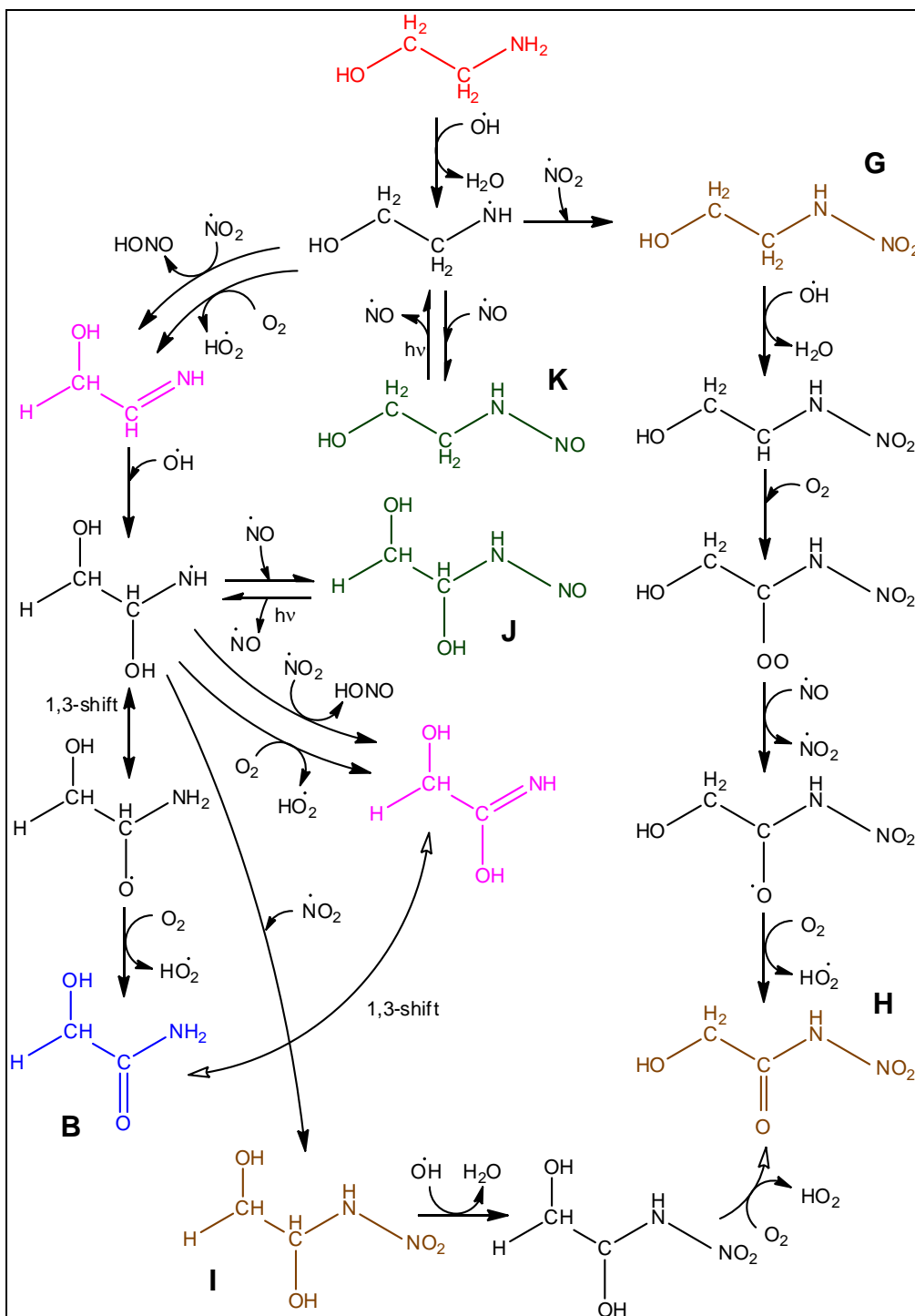


Figure 5 Scheme 3: N-hydrogen abstraction and resulting theoretical mechanism, adapted from Bråten et al. (2008)

3.2.2 Peroxy radical self-termination

Simple sugars (polyols) such as methyl erythritol were originally observed in ambient aerosol samples by Claeys *et al.* (2004). These compounds have also been formed in smog chamber experiments from isoprene (Edney *et al.*, 2005) and 1,3-butadiene (Angove *et al.*, 2006). It was proposed in these studies that they were formed by self-termination of peroxy radicals under low NO_x conditions, or more precisely, when the NO concentration becomes too low to sustain the alkyl-peroxy to alkyl-oxy radical pathway. A similar mechanism was proposed by Malloy *et al.* (2009) for imine formation as part of their aerosol formation mechanism.

Shown in Scheme 4, starting from abstraction of the C2-hydrogen from MEA, the most likely products formed by peroxy radical self-termination are 1-aminoethane-1,2-diol and 2-hydroxyacetamide.

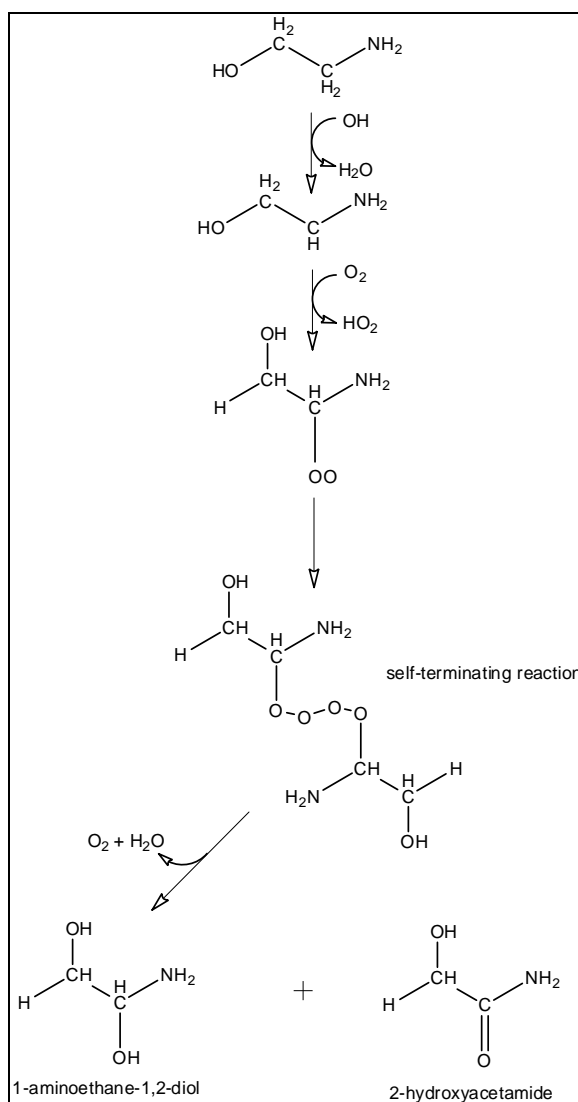


Figure 6 Scheme 4: Peroxy radical self-termination

3.2.3 Imine formation

The formation of imines as a result of OH radical hydrogen abstraction from MEA has been proposed by Braten *et al.* (2008) and, via self-termination of alkylamine peroxy radicals by Malloy *et al.* (2009). Nielsen *et al.* (2010) concluded that one of the products they detected was $\text{CH}_2(\text{OH})\text{CH}=\text{NH}$ which is one of imines predicted to form via the N-H hydrogen abstraction pathway (Scheme 3). Jackson and Attalla (2010) concluded that this species maybe an acetonitrile, MS-artefact.

Malloy *et al.* (2009) detected imines of the form $\text{R}_\text{A}\text{N}=\text{C}(\text{R}_\text{B})\text{NH}_2$ which they concluded was formed via peroxy radical self-termination. The formation of imines has also been observed on levitated aerosol by Hadrell and Agnes (2004).

The formation of imines can also occur via the Leuckart Reaction (Lawrence, 2004). Only mildly acidic conditions are required for the Leuckart Reaction to proceed and it is expected that this would be facilitated by acidic nature of the aerosol. This reaction is widely used to measure gas phase carbonyls using the well established 2,4-DNPH method as prescribed in USA EPA Method TO11 (Winberry *et al.*, 1990). It was also used by Gaiand *et al.* (1992) who developed an elegant method to measure gas phase MEA with greater than 90% recovery. It is likely that this method can also be used for the analysis of other gas phase amines.

In the Gaiand *et al.* (1992) method, the analyte strategy is the reverse of the 2,4-DNPH method since the carbonyl becomes the derivatising reagent and the amine becomes the target. The reaction between MEA and cyclohexanone is given in Scheme 5 and the imine formed is 2-(cyclohexylideneamino)ethanol.

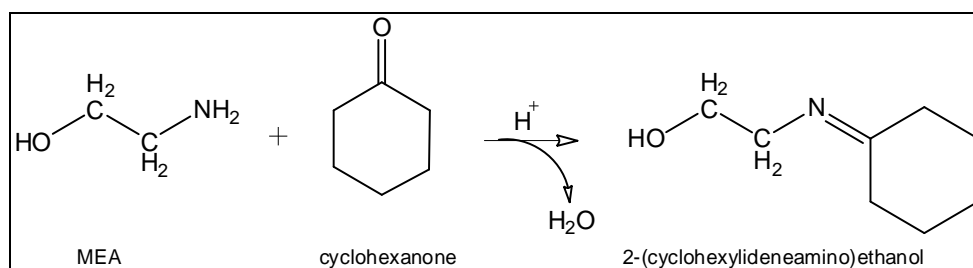


Figure 7 Scheme 5: Formation of an imine derivative via the Leuckart Reaction between MEA and cyclohexanone

In the Nielsen *et al.* (2010) study, a number of products were detected at >1% of the total MEA mass spectrum signal. It was concluded that they were condensation products.

Assuming that some of the simple carbonyls, such as formaldehyde, acetaldehyde, glycolaldehyde and glyoxal detected by Nielsen *et al.* (2010) and Angove *et al.* (2010) reacted with MEA according to the Leuckart Reaction, then some of the detected species maybe assigned according to that presented in Scheme 6.

If these reactions proceeded then the products formed from formaldehyde, acetaldehyde, glyoxal and glycolaldehyde would have molecular weights of 73, 87, 101 and 103, respectively, which as protonated ions would have m/z of 74, 88, 102 and 104, respectively.

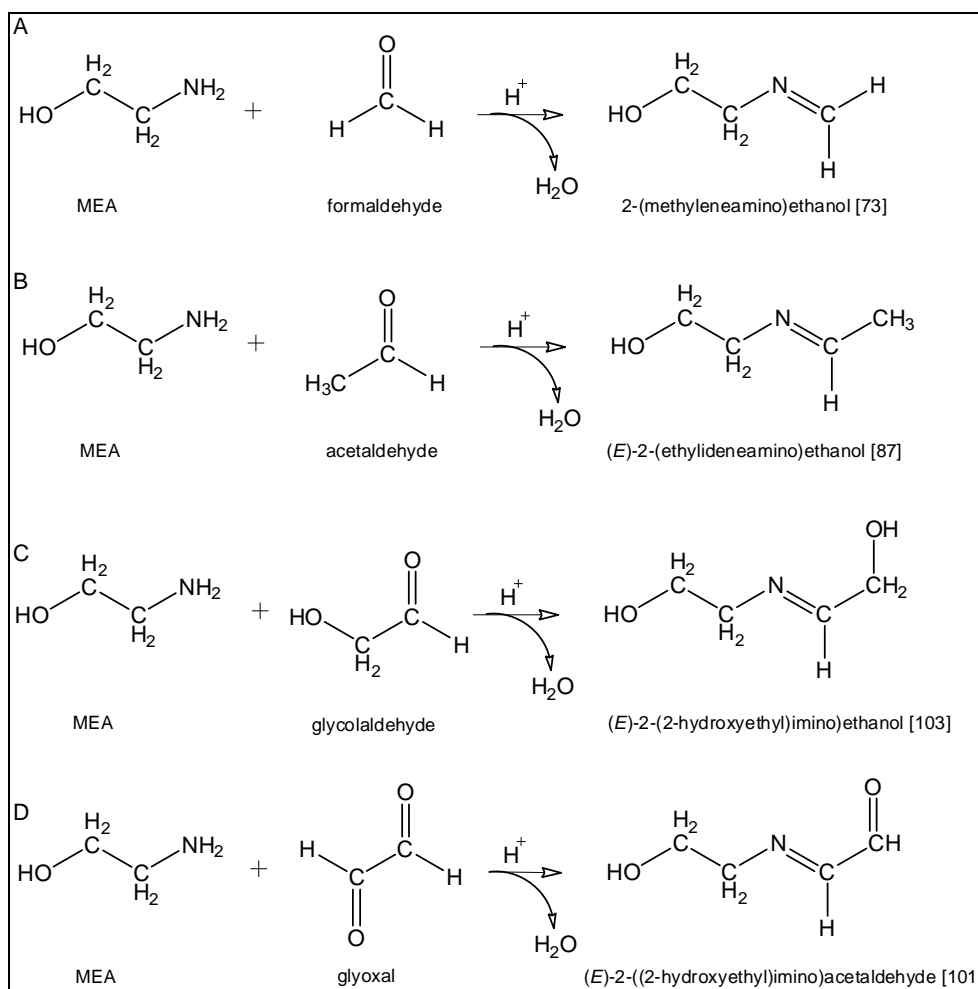


Figure 8 Scheme 6: Proposed formation of unidentified products of m/z 74, 88, 102 and 104 as detected by Nielsen et al. (2010)

3.2.4 Amino radical removal

Following OH abstraction of hydrogen from either MEA carbon, the formation of the NH_2 radical is predicted as shown in Scheme 1 and 2. As stated by Bråten et al. (2008) the lifetime of this radical is very short. The reaction of NH_2 radicals with NO and NO_2 is fast (Kuraskawa and Lesclaux, 1980) and are given in Scheme 7.

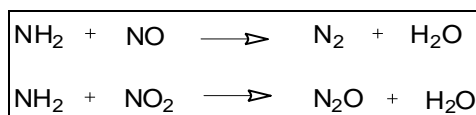


Figure 9 Scheme 7: Reaction of amino radicals with NO and NO_2

The significance of the reactions in Scheme 7 is unclear with respect to mass balance since the products are generally not measured in smog chamber photooxidation studies. A preliminary consideration of the existence of this radical in the MEA/ NO_x gas-phase system has also been made by Jackson and Attalla (2010).

3.2.5 Ammonia generation

Ammonia formation was observed by Nielsen *et al.* (2010) and Angove *et al.* (2010) during the photooxidation of MEA in NO_x and appeared to be light dependent. In the Angove *et al.* (2010) study, the increase in ammonia concentration was linear and after the lights were turned off its concentration remained unchanged.

Nielsen *et al.* (2010) suggested that it was likely that its formation was mediated by a surface reaction on the chamber walls. Angove *et al.* (2010) concurred with this suggestion but concluded that the main surface reaction was taking place on the surface of the aerosol rather than on the walls of the chamber alone, since the linear regression correlation coefficient (R) obtained by plotting the total aerosol surface area against the ammonia concentration was 0.992.

The observed concentration of ammonia in the Angove *et al.* (2010) matrix study indicated that for a fixed NO_x concentration that ammonia production was also dependent upon the initial concentration of MEA.

It is proposed that ammonia formation occurs on the surface of the aerosol by acting as a leaving group from the ethanol ammonium nitrate cation leaving behind a carbonium ion according to the reaction in Scheme 8.

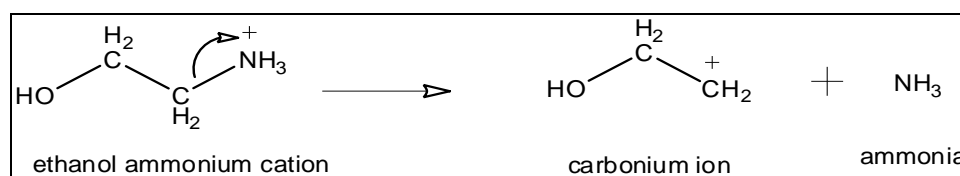


Figure 10 Scheme 8: Proposed reaction for the formation of ammonia from the ethanol ammonium nitrate cation

The light dependency probably arises as a result of the formation of ethanol ammonium nitrate which is dependent upon the light dependent production of HNO₃ (Akimoto *et al.*, 1987). Using the generalised mechanisms presented by Collins (1971), products expected to be formed from the carbonium ion in the aqueous phase are acetaldehyde, ethylene glycol (ethane-1,2-diol) and 2-hydroxyethyl acetate. On the assumption that the aerosol is principally ethanol ammonium nitrate (Murphy *et al.*, 2007), it is suggested that due to the probable close proximity of the nitrate group to the carbonium ion, they may react to form 2-hydroxyethyl nitrate.

Since ammonia formation in the MEA/NO_x system can be significant, its origin needs to be determined definitively in order to fully understand the carbon and nitrogen mass balances.

3.3 Nitrosamine and nitramine formation

The formation of nitrosamines and nitramines has been observed in the gas phase by reactions between the alkylamino radical, produced by N-H hydrogen abstraction of the parent amine, with NO to form nitrosamines and with NO₂ to form nitramines (Pitts *et al.*, 1978). It is known that while nitrosamines photolyse, nitramines are more resistant and it has been suggested that they could accumulate overtime (Grosjean, 1991). However, nitramines can also photolyse. Yields for formation of nitrosamines from alkyl amines have been determined to be in the range 1 to 2% by Pitts *et al.* (1978). Nielsen *et al.* (2010) estimated that the yield of nitroso compounds formed from MEA would be less than 3%.

The photolysis of dimethylnitramine ((CH₃)₂NNO₂) has been studied in the gas phase at 266 nm by Maillocq and Stephenson (1986) and at 248 nm by McQuaid *et al.* (1991). In both cases, dimethylnitramine was observed to photolyse and generate the dimethylamino radical ((CH₃)₂N[•]) + NO₂. It has also been suggested by Lazarou and Papagiannakopoulos (1990) that these products can undergo further reaction to form dimethylnitrosamine ((CH₃)₂NNO) and nitrodimehane ((CH₃)₂NO). The conversion from dimethylnitramine to dimethylnitrosamine has also been observed in alcohol solution solution after UV absorption at 240 nm by Suryanarayanan and Suryanarayanan (1970). It is postulated here that inter-conversion between the two species may be possible depending upon the wavelength of irradiation.

According to the theoretical mechanism proposed by Bråten *et al.* (2008), nitrosamines (Table 2, species J and K) and nitramines (Table 2, species G, H and I) could form in the gas phase after N-H hydrogen abstraction (Scheme 3). They also proposed that nitrosamines and nitramines may form after C2-H hydrogen abstraction but it is likely that this pathway is energetically unfavourable and will no longer be considered. In the CSIRO computational Study 1, Jackson and Attalla (2010), concluded that the formation of nitrosamine/nitramines in the gas phase was possible but that these species are likely to equilibrate with the hydroxydiazanyl (N=N-OH) and hydroxyoxidodiazanyl (N=N(OH)=O) forms.

When reviewing these compounds only references were found concerning species G, 2-nitroamino-ethanol and species K, 2-nitrosoamino-ethanol. Consequently, no further consideration will be given to the remaining species in Table 2 since nothing is known about them at this time other than, that they are likely to possess low vapour pressures. However, theoretical calculations of the form recommended by Lambropoulos (2010) [Study 2] can be used to investigate physical and chemical properties of these compounds.

In solution, primary amines react with nitrous acid to form N₂ and a mixture of alcohols and alkenes via the formation of a diazonium ion followed by a carbonium ion (Collins, 1971) which suggests that the yield of nitrosoamines from primary amines is likely to be low. There are some web references to studies using nitrosoethanolamine, however, all but one of these were transcription errors since, after direct reference to the work, it was found that the studies used nitrosodiethanolamine. The exception is the radiation biology study by Mothersill *et al.* (1989) who obtained nitrosoethanolamine, confirmed by CSIRO with the primary author, as bladder extracts from a US based collaborator.

The only reference found that refers to the preparation of the closely related compound to 2-nitrosoamino-ethanol was Challis and Shuker (1979) who successfully synthesised N-methyl-N-nitrosoethanolamine, which is a secondary amine. Since the nitrosoethanolamine used by Mothersill *et al.* (1989) was recovered as a bladder extract, it is hypothesised that it was stabilised as a ligand, which is a common configuration in biochemistry since it is unlikely to have been present as a stable conformer.

The formation of the nitramine, 2-nitroamino-ethanol is also a difficult multi-step synthesis which involves the nitration of 2-oxazolidone (Blatz *et al.*, 1953). It should be noted that this precursor has also been observed as an MEA degradation product in PCC process solutions as cited by Bello *et al.* (2005).

Nitrosamines were not detected by Nielsen *et al.* (2010) or Angove *et al.* (2010). The detection of 2-nitroamino-ethanol was confirmed by Nielsen *et al.* (2010), thus confirming that abstraction of hydrogen from the nitrogen atom had occurred under the conditions used in their experiments.

Nitrosoamine and nitramine formation from AMP, MDEA and PZ have not been observed in the gas phase. In a PCC context, this deficiency requires urgent attention both in the gas phase and the process liquid phase, from a primary emission perspective (Project B Task 3).

3.4 Aerosol formation and partitioning

Aerosol formation during MEA photooxidation in air in the presence of NO_x rapidly occurs after the lights are turned on. Shortly after nucleation most of the aerosol is conjectured to be ethanol ammonium nitrate, formed by the reaction between MEA and gas phase HNO₃ the latter which is formed when the lights are turned on. Only a small component of the aerosol is believed to be of non-salt organic origin. However, this is an estimate based on the findings of Murphy *et al.* (2007) who did not measure initial MEA but assumed 100% was injected without loss. A similar conclusion was also reached by Nielsen *et al.* (2010).

The total mass of aerosol observed by Angove *et al.* (2010) at low MEA concentration appeared to be independent of the NO_x concentration. However, at high MEA concentration it was strongly enhanced at low NO_x compared to high NO_x.

Silva *et al.* (2008) reported the appearance of mass fragments in aerosol formed in the trimethylamine system much larger than the parent amine. Similarly, Nielsen *et al.* (2010) observed that the composition of the aerosol appeared to change as their experiment proceeded, which included the formation of C3 and C4 fragments. They suggested that NH₄NO₃ may have condensed onto the surface of the aerosol. This is consistent with the conclusion by Angove *et al.* (2010) that ammonia formation is predominantly formed on the surface of the aerosol.

If ammonia formed on the aerosol surface then a variety of non-salt organic products would be incorporated into the aerosol. Including imines similar to that observed by Malloy *et al.* (2009). More complex reactions may take place, similar to that recently observed by Galloway *et al.* (2009), between glyoxal dimers/trimers with (NH₄)₂SO₄ seed aerosol.

The partitioning of species from the gas phase to the aerosol phase is unknown in the MEA system, although the method used by Murphy *et al.* (2007) to study partitioning in the triethylamine system is likely to be applicable to MEA. Since the mass of aerosol is probably dependent upon the concentration of gas-phase HNO₃. Aerosol studies have not been performed on AMP, MDEA and PZ.

If semi volatile compounds are present in the mixture, they can be present in both the gas and aerosol phases. Sampling of these two phases is important to examine the gas/aerosols partitioning where the selection of an appropriate method to desorb gaseous becomes highly requested.

4. ATMOSPHERIC LIFETIMES

The atmospheric lifetimes of compounds of interest, from a post-emission standpoint, have been considered from two aspects.

Table 4 compares nitrosated compounds identified as compounds of special interest in the Amine A specification. Table 5 lists oxidative degradation products of amines as cited in Project B Task 1.

Except in the case of ammonia, the lifetimes (τ) have been calculated using a daytime OH radical concentration of 1×10^6 radicals/cm³ and where published, the gas phase, OH rate constant, k_{OH} at 298K, where, $\tau = 1/(k_{OH} [OH])$. An OH radical concentration of 1×10^6 radicals/cm³ was also used by Finlayson-Pitts and Pitts (2000), which is close to the mean, OH diurnal concentration calculated for May in a tropospheric trend study by Isaksen and Hov (1987) at 60°N. The lifetimes listed do not take into account deposition or other atmospheric processes. Since the OH radical concentration decreases markedly at night, the lifetimes would be expected to increase by at least a factor of 10.

As shown in Table 4, except for N-nitrosodimethylamine, experimental, gas phase OH rate constant data are not available for the nitrosamines, hence lifetimes could not be calculated.

It should be noted that since nitrosamines such as N-nitrosodimethylamine and N-nitrosodiethylamine photolyse readily (Pitts et al., 1978; Tuazon et al. 1984), all nitrosoamines are expected to have short lifetimes of less than 3 hours during the daytime.

The lifetime for dimethylnitramine is ~72 hours (Tuazon *et al.*, 1984). The lifetime for the nitramine analogues of the other nitrosamines given in Table 4 are unknown.

Table 4 Atmospheric lifetimes of nitrosated-compounds of interest

Compound	Lifetime ^a (hours)	Reference
N-nitrosodimethylamine	~82 ^b	Tuazon <i>et al.</i> (1984)
N-nitrosodiethylamine	Note ^c	<i>unknown</i>
N-nitrosomorpholine	Note ^c	<i>unknown</i>
N-nitrosopiperidine	Note ^c	<i>unknown</i>
N-nitrosodiethanolamine	Note ^c	<i>unknown</i>
N-nitrosopiperazine	Note ^c	<i>unknown</i>
dimethylnitramine	~72 ^b	Tuazon <i>et al.</i> (1984)
diethylnitramine	-	<i>unknown</i>
nitromorpholine	-	<i>unknown</i>
nitropiperidine	-	<i>unknown</i>
nitramino-di-ethanol	-	<i>unknown</i>

^aCalculated as per Finlayson-Pitts and Pitts (2000)

^bCalculated based on rate constant determined by Tuazon *et al.* (1984)

^oN-nitrosamines are expected to photolyse under sunlight

Table 5 list those compounds, cited in Project B Task 1, as oxidative degradation products of amines. Those compounds for which an OH rate constant is not available are listed as having *unknown* lifetimes.

The lifetime for ammonia (Seinfeld and Pandis, 2006) is given in Table 5 as being less than 240 hours. This is the only species in Table 5 where the lifetime is dependent more on deposition than OH radical scavenging.

The lifetimes for methylamine, ethylamine and dimethylamine are 13, 10 and 4 hours, respectively (*cited in: Finlayson-Pitts and Pitts, 2000*).

Table 5 Atmospheric lifetimes of oxidative degradation products of amines identified in Project B Task 1

Compound	Lifetime ^a (hours)	Reference
AMINES		
ammonia	<240	Seinfeld and Pandis (2006)
methylamine, methanamine	13	<i>cited in</i> Finlayson-Pitts and Pitts (2000)
ethylamine, ethanamine	10	<i>cited in</i> Finlayson-Pitts and Pitts (2000)
dimethylamine, dimethanamine	4	<i>cited in</i> Finlayson-Pitts and Pitts (2000)
diethylamine, diethanamine	-	<i>unknown</i>
N-methylenethanamine	-	<i>unknown</i>
1-propylamine, 1-propanamine	-	<i>unknown</i>
ethane-1,2-diamine	-	<i>unknown</i>
piperazine	-	<i>unknown</i>
ALCOHOLS		
ethanol	72-96	Grosjean (1996), Good and Francisco (2003)
vinyl ethanol, ethenol	-	<i>See note^b</i>
1,2-ethanediol, glycol	~36	Grosjean (1996)
AMINO ALCOHOLS		
monoethanolamine, 2-aminoethanol (MEA)	1.1-2.5	This report
Diethanolamine (DEA)	-	<i>unknown</i>
Triethanolamine (TEA)	-	<i>unknown</i>
2-amino-2-methyl-1-propanol	-	<i>unknown</i>
N-methyldiethanolamine (MDEA)	-	<i>unknown</i>
2-(methylamino)ethanol	-	<i>unknown</i>
2-(dimethylamino)ethanol	-	<i>unknown</i>
2-((2-aminoethyl)amino)ethanol	-	<i>unknown</i>
2,2'-(2-(2-hydroxyethylamino)- ethylazanediy)diethanol	-	<i>unknown</i>
N,N,N-tris(hydroxyethyl)- ethylenediamine	-	<i>unknown</i>
N,N,N,N,- tetra(hydroxyethyl)ethylenediamine	-	<i>unknown</i>
2,2'-(ethane-1,2- diy)bis(azanediy)diethanol	-	<i>unknown</i>
N,N-bis(hydroxyethyl)- ethylenediamine	-	<i>unknown</i>
N-(hydroxyethyl)-ethylenediamine	-	<i>unknown</i>

Table 5 continued

AMIDES		
formamide	~55	Barnes <i>et al.</i> (2010)
acetamide	~79	Barnes <i>et al.</i> (2010)
propanamide	-	<i>unknown</i>
N-methylformamide	-	<i>unknown</i>
N-(2-hydroxyethyl) formamide	-	<i>unknown</i>
N-(2-hydroxyethyl) acetamide	-	<i>unknown</i>
2-hydroxy-N-(2-hydroxyethyl)-propanamide	-	<i>unknown</i>
3-(ethyl(hydroxy)amino)-N-(2-hydroxyethyl)-2-hydroxyethylamino-N-	-	<i>unknown</i>
ALDEHYDES		
formaldehyde	36°	Seinfeld and Pandis (2006)
acetaldehyde	11°	Seinfeld and Pandis (2006)
2-aminoacetaldehyde	<72	Bråten <i>et al.</i> (2008)
2-hydroxyacetaldehyde, glycolaldehyde	~22	Magneron <i>et al.</i> (2005)
2-imidazolecarboxyaldehyde	-	<i>unknown</i>
1-methyl-2-imidazolecarboxyaldehyde	-	<i>unknown</i>
ACIDS		
formic acid	~600 ^d	Seinfeld and Pandis (2006)
acetic acid, ethanoic acid	~350 ^d	Seinfeld and Pandis (2006)
propionic acid, propanoic acid	~227	Dagaut <i>et al.</i> (2005)
butyric acid	~140	Dagaut <i>et al.</i> (2005)
glycolic acid	variable	<i>See note^e</i>
glyoxylic acid	variable	<i>See note^e</i>
oxalic acid	variable	<i>See note^e</i>
glycine(2-aminoacetic acid)	-	<i>unknown</i>
2-aminosuccinic acid	-	<i>unknown</i>
1-(bis(2-hydroxyethyl)amino)acetic acid	-	<i>unknown</i>
2-(2-aminoacetamido)acetic acid	-	<i>unknown</i>
bicine(2-(bis(2-hydroxyethyl)amino) acetic acid)	-	<i>unknown</i>
5-aminopentanoic acid	-	<i>unknown</i>

Table 5: continued

OXAZOLIDINONES		
2-oxazolidone	-	<i>unknown</i>
oxazolidinone	-	<i>unknown</i>
4,4-dimethyloxazolidin-2-one	-	<i>unknown</i>
3,4-4-trimethyloxazolidin-2-one	-	<i>unknown</i>
3-hydroxyethyl-2-oxazolidinone	-	<i>unknown</i>
IMIDAZOLIDINONES		
1-(2-hydroxyethyl)-2-	-	<i>unknown</i>
1,3-bis(2-hydroxyethyl)-2-	-	<i>unknown</i>
1-(2-hydroxy-2-methylpropan-2-yl)-4,4-dimethylimidazolidin-2-	-	<i>unknown</i>
N-(hydroxyethyl) imidazolidone	-	<i>unknown</i>
N,N-bis(hydroxyethyl)	-	<i>unknown</i>
UREA COMPOUNDS		
Ethylurea	-	<i>unknown</i>
N,N'-di(2-hydroxyethyl)urea	-	<i>unknown</i>
CYCLIC COMPOUNDS		
N,N-bis(hydroxyethyl) piperazine	-	<i>unknown</i>
2,2'-(2-(piperazin-1-yl)ethylazanediyl) diethanol	-	<i>unknown</i>
N-(hydroxyethyl) ethyleneimine	-	<i>unknown</i>
N-(hydroxyethyl) piperazine	-	<i>unknown</i>

^aCalculated as per Finlayson-Pitts and Pitts (2000)

^bLikely to tautomerise to acetaldehyde

^cOH radical concentration of 1.5×10^6 molecules cm^{-3}

^dCalculated based on rate constant cited in Seinfeld and Pandis (2006)

^eNo clearly defined OH rate constants are available. These species are often associated with secondary organic aerosol formation

The lifetime for ethanol is 72-96 hours (Grosjean, 1996; Good and Francisco, 2003) and for 1,2-ethanediol, ~36 hours (Grosjean, 1996). The lifetime for the only amino alcohol in the list is for MEA which was determined computationally in Project B Task 2 as being 1.1-2.5 hours.

Recently, Barnes *et al.* (2010) estimated that the lifetimes for formamide and acetamide were ~55 and ~79 hours, respectively. The significance of this result for acetamide is unclear until an improved understanding of its role as a photo-degradation product is obtained. However, in the case of MEA, Nielsen *et al.* (2010) concluded that ~80% of MEA resulted in the formation of formamide, which, dependent upon mass of emission, may be problematic.

Although the lifetimes of formaldehyde and acetaldehyde are 36 and 11 hours (Seinfeld and Pandis, 2006), respectively, it should be noted that as a result of ongoing atmospheric reactions of all hydrocarbons, these compounds will be continually replaced, especially

formaldehyde. Bråten *et al.* (2008) estimated that the lifetime of 2-aminoacetaldehyde is <72 hours and that calculated from the OH rate constant determined by Magneron *et al.* (2005) for 2-hydroxyacetaldehyde was ~22 hours.

The lifetimes for formic acid and acetic acid are ~600 hours and ~350 hours (Seinfeld and Pandis, 2006), respectively. This is not surprising since they are near the end of the oxidative pathway and, similar to formaldehyde and acetaldehyde, are continually replaced. As the alkyl chain increase in length the lifetimes of carboxylic acids appears to decrease as demonstrated by propanoic acid and butyric acid, which have lifetimes of ~227 and ~140 hours (Dagaut *et al.*, 2005), respectively.

5. H&E RELEVANCE OF PROCESS AND ATMOSPHERIC CHEMISTRY

The composition and mass of emissions to atmosphere from energy production plants employing post-combustion amine-based technology are dependent on chemical and physical processes, the system dynamics of which are made complex by the possible inclusion of amines and products formed during amine degradation. Table 6 summarises the process degradation products and their potential fate in the environment.

Operational factors that affect the system dynamics are the energy demand required from the plant, hence, the mass of amine required and the conditions:

- In the absorber,
- In post-absorber mitigation (if installed),
- At the bottom of stack, and
- During stack transport (temperature gradient, surface interactions etc.).

Each of these process environments are expected to have different physical/chemical regimes and are considered as being distinct research areas. This is especially important for the transport of droplets since their pH may decrease markedly during stack transport.

During novel post-combustion capture plant design and development the only recourse is to make assumptions based on known processes. This leads to further assumptions about expected emissions rates and composition. Whilst this is logical methodology, the accurate prediction of abiotic fate can only be approached after emissions are fully characterised. Logically, this needs to be done prior to, or during commissioning. This sequence also ensures that emissions can be adequately controlled.

An air quality model, which utilises a validated reduced chemical mechanism, can be used as a screening tool to determine abiotic fate. The accuracy of prediction is dependent upon the quality of the embedded, reduced mechanism, which in turn is generated from a detailed, semi-explicit chemical mechanism. In an alkanolamine/piperazine atmospheric context, this is where the limitation exists. Even though some studies have been performed on MEA, verification of the mechanism of the atmospheric chemistry of MEA is still not well defined and, even less so for AMP, MDEA and PZ.

Consequently, the determination of the atmospheric fate of amine emissions can only be performed at this time with high uncertainty. Hence, since health and environmental impacts are dependent upon the mass and composition of emissions, it follows that process chemistry, including control, is more relevant. However, the role of atmospheric chemistry is also important since it can provide information to plant designers with regard to the efficiency of mitigation strategies as well as providing a means by which regulators can predict where adverse health and environmental effects may occur.

In summary, the most important limitations with regards to existing data is that the real world composition and mass of emissions from a PCC plant using solvents A, B and C is unknown. Some atmospheric gas phase MEA chemistry and even less of AMP is known. However, the atmospheric chemistry of MDEA and PZ is completely unknown. Only aerosol formation from MEA has been studied, but in a limited way. Currently, the data that is available does not provide a sound basis on which an accurate H&E risk assessments can be made.

THIS PAGE IS INTENTIONALLY LEFT BLANK

Table 6 Atmospheric fate of degradation products of amines (degradation products indentified from Kennard and Melsen, 1985; Strazisar, 2003; Goff and Rochelle, 2004; Bello and Idem, 2005; Supap, 2006; Bedell, 2009; Freeman, 2009; Lepaumier, 2009, Jackson and Attalla, 2010)

Degradation Products	Primary amines		Secondary amines		Tertiary amines	Atmospheric Emission and Fate
Compound class	MEA	AMP	DEA	PZ	MDEA	
Amines	Ammonia, ethanamine, methanamine, N-methylenethanamine, 1-propanamine		ethylenediamine			Vapour phase and droplet carry over. Atmospheric nitrosation
Diamines				ethylenediamine		Vapour phase and droplet carry over
Alcohols	vinyl ethanol, ethanol, 1,2-ethanediol				1,2-ethanediol	Vapour phase and droplet carry over
Amino Alcohols	2-(methylamino)ethanol, 2-((2-aminoethyl)amino)ethanol, 2,2'-(2-(2-hydroxyethylamino)ethylazanediy)diethanol	2-methyl-2-(methylamino)propan-1-ol	2-aminoethanol (MEA), N,N,N-tris (hydroxyethyl) ethylenediamine, N,N,N,N-tetra (hydroxyethyl) ethylenediamine, 2,2'-(ethane-1,2-diylbis (azanediy))diethanol, triethanolamine (TEA), N,N-bis(hydroxyethyl) ethylenediamine, N-(hydroxyethyl)ethylenediamine		diethanolamine, triethanolamine, 2-(methylamino)ethanol, 2-(dimethylamino)ethanol	Vapour phase and droplet carry over. Atmospheric nitrosation
Amides	N-(2-hydroxyethyl)formamide, N-(2-hydroxyethyl)acetamide, 2-hydroxy-N-(2-hydroxyethyl) propanamide, 3-(ethyl(hydroxy) amino)-N-(2-hydroxyethyl) propanamide, 2-hydroxyethylamino-N-hydroxyethylacetamide, N-methylformamide, acetamide					Vapour phase and droplet carry over.
Aldehydes	2-aminoacetaldehyde, formaldehyde, hydroxyacetaldehyde, acetaldehyde, 2-imidazolecarboxyaldehyde, 1-methyl-2-imidazolecarboxaldehyde					Vapour phase and droplet carry over

	MEA	AMP	DEA	PZ	MDEA	Atmospheric Emission and Fate
Acids	acetic acid, butyric acid, propionic acid, 2-aminosuccinic acid, 2-(2-aminoacetamido)acetic acid, oxalic acid, bicine (2-(bis(2-hydroxyethyl)amino)acetic acid), formic acid, glycolic acid, glycine (2-aminoacetic acid), glyoxylic acid, 5-aminopentanoic acid		2-(bis(2-hydroxyethyl)amino)acetic acid, acetic acid, formic acid, glycolic acid	formic acid	2-(bis(2-hydroxyethyl)amino)acetic acid, acetic acid, formic acid, glycolic acid	carry over
Oxazolidinones	2-oxazolidone	4,4-dimethyloxazolidin-2-one, 3,4,4-trimethyloxazolidin-2-one	oxazolidinone, 3-hydroxyethyl-2-oxazolidinone			carry over
Imidazolidinones	1-(2-hydroxyethyl)-2-imidazolidinone 1,3-bis(2-hydroxyethyl)-2-imidazolidin-2-one	1-(2-hydroxy-2-methylpropan-2-yl)-4,4-dimethylimidazolidin-2-one	N-(hydroxyethyl)imidazolidone, N, N-bis(hydroxyethyl)imidazolidone			carry over
Urea Compounds	ethylurea N,N'-di(2-hydroxyethyl)urea					carry over
Cyclic Compounds			N,N-bis(hydroxyethyl)piperazine 2,2'-(2-(piperazin-1-yl)ethylazanediyl)diethanol N-(hydroxyethyl)ethyleneimine N-(hydroxyethyl)piperazine	N,nitroso piperazine N,N-dinitrosopiperazine		Carry over. Atmospheric nitrosation

6. RANKING OF SOLVENTS

In Table 7 the expected range of vapour phase and droplet emissions is given. These have been calculated in Project B Task 1 for a variety of simulated process conditions based on the generic solvents A (=MEA), B (=AMP/PZ mixture), C (=MEA/MDEA mixture).

Dependent upon exposure, N-nitroso compounds are known to have a cancer risk. Accordingly, the solvents have been ranked on their propensity to form total N-nitroso compounds from the total mass of amine emitted into the atmosphere, based on ASAPEN modelling used in Project B Task 1.

If the solvents are first ranked on mass emission of amine then that ranking is clearly B>A>C. Since Solvent B contains second degree amines and the others don't, its rank stands. Solvent C contains a tertiary amine, hence no nitrosamine is expected, plus it also contains a primary amine with much less mass emission than that of Solvent A. Hence, Solvent C is expected to form less nitrosamine, than Solvent A, if at all. However, since Nielsen *et al.* (2010) did detect 2-nitraminoethanol in their MEA experiments, it is considered that from a cautionary standpoint that the ranking be made on the propensity to form total nitroso- compounds, hence, the ranking is still B>A>C which confirms the rank of A over C since a larger MEA emission is expected when using Solvent A compared to C.

In addition to the possibility that the solvents may produce N-nitroso compounds, they will also undergo complex chemical reactions in the presence of NO_x and sunlight to produce different pollutants such as ozone, aldehydes, amides and secondary particles. It is likely, that whilst nitrosamines and to some degree nitramines can be photolysed in sunlight, accumulation of N-nitroso compounds is expected under Nordic nights in the absence of sunlight.

Table 7 Atmospheric emissions of generic solvents and their contribution to the production of atmospheric pollutants

Solvent	Vapour Phase (per tonne of CO ₂ captured)	Droplets (per tonne of CO ₂ captured)	Total (per tonne of CO ₂ captured)	Contribution to atmospheric pollutants
Solvent A (Rank 2)				
Heat stable salts	Nil	0.1 to 0.5 mg	0.1 to 0.5 mg	particles
Ammonia	9 mg to 2.6 g	17 mg to 0.5 g	26 mg to 3.1 g	particles
MEA	12 mg to 11g	9 to 47 g	21 to 58 g	O ₃ , particles, aldehydes, formamide, formic acid, possibly nitrosated compounds
Solvent B (Rank 1)				
Ammonia	3.4 mg to 1 g	8 mg to 0.3 g	12 mg to 1.3 g	particles
AMP	0.7 g to 1.2 kg	15 to 127 g	16 g to 1.3 kg	particles, possibly nitrosated compounds
PZ	0.8 mg to 1.5 g	0.6 to 9.5 g	0.6 to 11 g	particles, possibly nitrosated compounds
Solvent C (Rank 3)				
Ammonia	0.4 mg 9 g	1 mg to 0.3 g	1.4 mg to 9.3 g	particles
MDEA	Nil	Nil	Nil	particles, possibly nitrosated compounds
MEA	0.9 mg to 0.9 g	0.6 to 2.1 g	0.6 to 3 g	O ₃ , particles, formaldehydes, formamide, formic acid methylamine, possibly nitrosated compounds

Most identified substances that are in Table 5 may affect human health and the environment if they exceed their threshold levels. Particles and ozone contribute to human health and environment and currently controlled under environmental regulations. NH₃ is a toxic that contributes to the particulate matter formation and has acidification potential as NH₄⁺. With respect to solvents and environmental regulations, the US laws regulate MEA by OSHA. However, the other solvents have not been enforced yet by US environmental regulations.

The formation of O₃ and oxygenated degradation products from AMP, MDEA and PZ in the gas phase is expected but yet to be observed.

A more thorough understanding of the fate of emissions and hence, risk to health and the environment can only occur after knowledge of process chemistry, composition of emissions and atmospheric chemistry/processes is improved well beyond current understanding.

7. COMPUTATIONAL CHEMISTRY STUDIES

The CSIRO, MEA theoretical kinetic studies performed by Jackson and Attalla (2010) [Study 1] and, Lambropoulos (2010) [Study 2] are presented as research addenda to this report. They differ from previous thermochemical studies (Bråten *et al.*, 2008) since their primary objectives were to derive OH radical hydrogen abstraction rate constants, since, at the time of writing, there were no kinetic results available.

The rate constants calculated from these studies are presented in Table 3, in Section 4.2.1 where they are compared with the “slower” estimates derived by Carter (2008) and Nielsen *et al.* (2010). The differences between the CSIRO quantum theoretically derived rate constants and those of Carter (2008) and Nielsen *et al.* (2010) are believed to have occurred because Carter (2008) used the structure-reactivity approach and Nielsen *et al.* (2010) used estimates based on a critical review of $\text{CH}_3\text{CH}_2\text{OH} + \text{OH}$ reactions.

The two CSIRO theoretical studies were performed using different methods, refer to Research Addenda, and produced overall k_{OH} that differed by a factor of two (see Table 3). Both methods suggest that hydrogen abstraction from the hydroxyl group is a major pathway. However, the Jackson and Attalla (2010) study produced branching proportions closer to that observed, for C1-, C2- and N-centred hydrogen abstraction, by Nielsen *et al.* (2010) than did Lambropoulos (2010).

Key findings from Study 1 (Jackson and Attalla, 2010)

- a. C2-abstraction is favoured kinetically.
- b. Predicted overall rate of OH abstraction of hydrogen from MEA is in agreement with experiment.
- c. Hydrogen abstraction at oxygen leads to immediate C-C bond breaking to form aminomethyl radical and formaldehyde.
- d. Abstraction at C1 is very slow (several orders of magnitude slower than C2, O abstraction).
- e. Formation of a C2-oxo derivative leads to immediate C-C bond breaking and formation of formamide plus hydroxymethyl radical
- f. Formation of a C1-oxo derivative to immediate C-C bond breaking and formation of formic acid plus aminomethyl radical.
- g. Reaction between the N-centred radical derivative of MEA and NO/NO₂ leads to formation of the nitrosamine/nitramine, but these species will equilibrate with the hydroxydiazanyl (N=N-OH) and hydroxyoxidodiazanyl (N=N(OH)=O) forms.
- h. Time-dependent density functional theory with a long-range exchange-correlation correction predicts the gaseous nitroso derivative of MEA will be unstable in UV-C light; however the efficiency of this decomposition route needs to be confirmed.
- i. Low energy pathways to 2-aminoacetaldehyde and 2-aminoethanol/2-iminoethanol could not be found (considering a single abstraction by OH radical and follow-up reaction with O₂).
- j. It is proposed that Nielsen *et al.* (2010) measured CH₃CN-H⁺-H₂O as the peak at *m/z* 60 using PTR-MS.

Key findings from Study 2 (Lambropoulos, 2010)

For the non-hydrated systems

- a. the C1- and N- abstraction were well within the order of experiment.
- b. The C2- abstraction differed by an order of 2 slower to that of experiment.
- c. The O- abstraction pathway differing by at most 3 orders of magnitude greater in rate to that of experiment.

For the hydrated systems

- d. The one noticeable difference with the non-hydrated systems was the dramatic increase in rate constants for each abstraction point. This may therefore infer the major role that water presence may have on rate constants (both from a theoretical and experimental perspective).

Additional observations

- e. The re-orientation of water molecules occurred between themselves and the MEA (with slight torsional changes), possibly due to hydrogen bonding;
- f. It is speculated that, the presence of molecular water near the path of a transition, which may effectively alter the energetics of the transition.
- g. An increase in free energy correction differences was observed between the transition state and starting reactants for each of the non-hydrated and hydrated models.

From the improvement observed in the modelling outcome for experiment E514, given in Figure 1, Section 4.2.1, it is concluded that both methods have much to offer.

Continued development of both methods will be ongoing to assist CSIRO in understanding the chemistry and kinetics of all amine-based solvents in both the liquid and gas phases. These findings will assist in deciding which form of useful output can be provided by these methods to assist in solvent evaluation and selection.

8. RECOMMENDATIONS

8.1 Modelling Context

The purpose of this introduction is to describe the difference between explicit and reduced chemical mechanisms and their relationship to predictive air quality modelling.

The objective of an explicit mechanism is to describe all possible reactions that are involved in the formation and/or degradation of a substance on a truly kinetic basis. An explicit mechanism should ideally describe such chemistry or fate, of a substance over a wide range of conditions. The resulting mechanism may involve many thousands of reactions. An explicit mechanism, such as the Master Chemical Mechanism (MCM) has a strong theoretical basis, except for amines at this time, and is built up of sub-mechanisms found in the literature. This is the preferred method for understanding the true fate of a substance.

The implementation of an explicit mechanism is computationally demanding which means that it is unsuitable for predictive air quality (AQ) models since they are required to perform mechanistic calculations at each grid point over the region of interest. In practice such models utilise a reduced mechanism which lumps reactions of similar species together and/or uses less reactions which approximate, for example, NO_x chemistry. Examples of these reduced mechanisms are SAPRC-07 and CB05.

Once an explicit mechanism for PCC amines has been developed which accurately describes their fate in the atmosphere, the explicit mechanism reaction set can be reduced in size, such reduction being limited of course to that which still accounts for their fate. Due in part to their empirical nature, reduced mechanisms can be more readily modified, to include for example, the photochemistry of PCC amines as more is learned about their fate from experiments designed to elucidate relevant explicit mechanisms by elucidating their decomposition pathways and kinetics.

The part to be embedded into the AQ model will be a modified reduced mechanism, such as SPARC-07 or CB05, which will include a PCC amine reaction set that is more accurately representative of the atmospheric chemistry of PCC amines. This PCC amine reaction set will be derived from the experiments referred to in the previous paragraph.

Input data into the explicit mechanisms as well as reduced mechanisms will be initial conditions used in smog chamber experiments. Input data into AQ models will be emissions factors and meteorological conditions. The AQ model will in turn input data into the reduced chemical mechanism embedded within. It should be noted that the reduced mechanism (e.g. SAPRC-07 or CB05) can be verified using chamber data as well as real world data, which is a powerful verification methodology.

The following recommendations are made by CSIRO for research to facilitate the elucidation of a more complete explicit chemical mechanism for the atmospheric photooxidation of PCC solvent components, which can be used to generate a more realistic, reduced mechanism than that which currently exists. Such a mechanism becomes the basis on which more rigorous abiotic fate studies can proceed.

The following recommendations are made by CSIRO for research to facilitate the elucidation of a more complete explicit chemical mechanism for the atmospheric photo-oxidation of PCC solvent components, which can be used to generate a more realistic, lumped mechanism than that which currently exists. Such a mechanism becomes the basis on which more rigorous abiotic fate studies can proceed.

8.2 Characterisation of PCC emissions to atmosphere

To facilitate the design of experiments, it is recommended that a complete composition matrix be developed that is representative of the range of concentrations expected from a PCC plant, similar to that employed by CSIRO during the recent MEA study for Norsk Energi/Gassnova. This matrix should include alkanolamines and their anticipated degradation products.

8.3 Elucidation of chemical mechanism

The elucidation of atmospheric chemical pathways can be a challenging task. Made more challenging in the case of alkanolamines, since they have not been studied extensively and a made more complex by the rapid formation of aerosol under some conditions

It is recommended that strategic, isotopic labelling of parent alkanolamines be prepared and used to assist in the elucidation of atmospheric chemical pathways, for example, as initiated by Nielsen *et al.* (2010) for MEA, in the EUPHORE chamber study. This may require multiple syntheses of the same species employing different isotopic configurations. CSIRO has also used this technique to study the photo-oxidation and production of SOA from ¹³C toluene during the recent Australian Government, Clean Air Program (Angove *et al.*, 2008).

Although it would be expensive to prepare the labelled alkanolamines, the advantages with respect to deduction efficiency and the expected reduction in time of conventional analysis is likely to offset this cost.

This approach is more likely to provide definitive smog chamber results with respect to determining the mass balance of alkanolamine/NO_x atmospheric reaction systems after comparison of naturally abundant and isotopically labelled alkanolamines. It may also be an advantage to employ isotopic studies to fast reaction flow techniques to investigate the significance of short life time species, such as NH₂ radicals, that may play a scavenging role.

Another advantage of using isotopes is that experimental verification of rate constants predicted using quantum computational techniques maybe more straightforward. Such knowledge is needed to optimise explicit chemical mechanisms.

8.4 Verification of explicit and reduced gas-phase mechanisms

It is recommended that, using the composition matrix, results from experiments that have been performed in a well characterised smog chamber, can be used to construct and verify a new or, modify an existing gas-phase, explicit mechanism for alkanolamine, atmospheric degradation. It should be noted that this will be a challenging task. Once the explicit mechanism has been validated for the range of the composition matrix, different conditions such as variations in light intensity and humidity can be used to further verify the explicit mechanism. At this point, the lumped mechanism can be constructed and verified against existing smog chamber results, before being embedded into a predictive, air quality model, which will enable abiotic fate studies of “amines” to proceed. This procedure has been employed by CSIRO

over many years, and was recently performed when the two widely used lumped mechanisms SAPRC07 and CB05 were recently updated to include an assumptive mechanism for MEA in the recent MEA smog chamber study performed by CSIRO (Angove *et al.*, 2010).

8.5 Aerosol formation

The formation of aerosol during the photo-oxidation of alkyl amines and MEA in the presence of NO_x is well established. It has been concluded that the aerosol, is predominantly a nitrate salt, such as ethanol ammonium nitrate, in the case of MEA. The mass of aerosol formed depends upon the concentration of gaseous HNO₃. Only one alkyl amine partitioning study has been performed, none have been performed using alkanolamines or piperazine. It is important to understand the aerosol formation chemistry of alkanolamines so that aerosol primary emissions can be controlled and the likelihood and fate of aerosol formed by secondary processes can be predicted, including the effect of humidity on aerosol formation. Therefore, it is recommended that in order to understand the chemistry and conditions required to form aerosol from the reaction between alkanolamines and HNO₃ and, other acids, that partitioning studies be performed on all solvents.

While partitioning studies will provide information regarding MEA incorporation into aerosol, only aerosol collection and analysis can provide knowledge with regard to the fate of products such as nitrosamines and nitramines, which maybe formed on the surface of aerosol prior to encapsulation. Therefore, it is recommended that a method be established for the collection of aerosol that minimises changes in morphology and, that after preliminary analytical method research, that an analytical method be developed to target species of concern, such as nitrosated compounds and oligomeric components.

Once the aerosol has been characterised to >80% of its mass has been identified, it is also recommended that an aerosol formation mechanism be developed drawing on results from the elucidated explicit gas phase mechanism and new aerosol partitioning studies.

The collection of SOA will also provide a means by which the role of aerosol formation plays in the subsequent formation of N-nitroso compounds and NH₃ can be determined.

8.6 Predictive dispersion modelling using the embedded mechanism

After the lumped mechanism has been optimised and embedded into the selected air quality model, it is recommended that regional air modelling be performed. Outcomes from the modelling should include normally expected profiles in addition to, as a minimum, distributions of ammonia, nitrosoamines, nitramines and aerosol formation. The role of humidity and precipitation and their effect on deposition need to be accommodated, which is a complex task and will be an objective of ongoing development.

In a Norwegian context, using an incomplete MEA mechanism, CSIRO capability was applied to a demonstration, case-study of the Kårsto plant (Angove *et al.*, 2010), which for example, produced modelled peak 1-hour concentrations of MEA, NH₄NO₃, NO₂ and HNO₃

8.7 Computational chemistry

The CSIRO theoretical studies have provided an additional insight into the chemistry and kinetics of MEA-degradation. It is recommended that the quantum-chemistry computational methods employed applied to AMP, MDEA and PZ systems. It is further recommended, that such studies be performed in a benchmarked environment to assist their development, thus ensuring a systematic approach when applied to amine chemistry. Study specific recommendations are provided in each Research Addendum.

8.8 Summary of recommendations

- a. It is recommended that a complete composition matrix be developed that is representative of the range of concentrations expected from a PCC plant, similar to that employed by CSIRO during the recent MEA study for Norsk Energi/Gassnova.
- b. It is recommended that strategic, isotopic labelling of parent alkanolamines be prepared and used to assist in the elucidation of atmospheric chemical pathways.
- c. It is recommended that, using the composition matrix, results from experiments that have been performed in a well characterised smog chamber, be used to construct and verify a new or, modify an existing gas-phase, explicit mechanism for alkanolamine and diamine, atmospheric degradation. The impact of amine emissions on more representative, ambient atmospheric systems should also be investigated.
- d. In order to understand the chemistry and conditions required to form aerosol from the reaction between alkanolamines/piperazine and HNO_3 and, other acids, it is recommended that gas phase/aerosol partitioning studies be performed on all solvents.
- e. It is recommended that a method be established for the collection of aerosol that minimises changes in morphology and, that after preliminary research, that an analytical method be developed to target species of concern, such as nitrosated compounds and oligomeric components.
- f. Once the aerosol has been characterised to >80% of its mass has been identified, it is also recommended that an aerosol formation mechanism be developed drawing on results from the elucidated explicit gas phase mechanism and new aerosol partitioning studies.
- g. After a lumped mechanism has been validated, optimised and embedded into the selected predictive air quality model, it is recommended that regional air modelling is performed. The predicted concentration profiles of the selected pollutants can be used to assess the exposure and potential environmental impacts of these pollutants. This model can be used as a step in the protocol developed in Project B Task 3 of this project.
- h. It is recommended that the quantum chemistry computational methods employed be reviewed and where suitable, applied to AMP, MDEA and PZ systems. It is further recommended, that such studies be performed in a benchmarked environment to assist their development, thus ensuring a systematic approach when applied to amine chemistry. Where possible, outcomes from computational methods should be verified by experiment.

9. ACKNOWLEDGEMENTS

The authors extend their thanks to Stephen White for his assistance in preparing this document as well as the CSIRO Library Services, notably Anne Stevenson, for their combined and extraordinary efforts. Thanks are also extended to Anne Tibbett, Stuart Day, Martin Cope and Paul Feron for their advice and to Anjana Narasimhan for project support.

10. REFERENCES

- Akimoto, H., Takagi, H., Sakamaki, F. (1987). *Photoenhancement of the nitrous acid formation in the surface reaction of nitrogen dioxide and water vapour: Extra radical source in smog chamber experiments*. Int. J. Chem. Kinetics., 19, 539-551.
- Angove, D. E., Fookes, C. J. R., Hynes, R. G., Walters, C. K., Azzi, M. (2006). *The characterisation of secondary organic aerosol formed during the photodecomposition of 1,3-butadiene in air containing nitric oxide*. Atmospheric Environment, 40, 4597–4607.
- Angove, D.E., White, S. J., Keywood, M. and Azzi, M. (2008). *Studies of the secondary organic aerosol component of PM_{2.5} arising from the NEPM air toxic precursors, toluene and m-xylene: Final Report, ET/IR 1035R*.
<http://www.environment.gov.au/atmosphere/airquality/publications/pubs/secondary-organic-aerosols.pdf>.
- Angove, D. E., Azzi, M., Tibbett, A., White, S., Cope, M., Lee, S. (2010). *Investigation of the atmospheric photochemistry of the CO₂ capture solvent, monoethanolamine (MEA) under controlled conditions*. CSIRO EP101723, Final Report to Norsk Energi and Gassnova SF.
- Azzi, M. , White, S., Angove, D., Jamie, I. and Kaduwela, A. (2010). *Evaluation of the SAPRC-07 mechanism against CSIRO smog chamber*. In Press: Atmospheric Environment.
- Barnes, I., Solignac, G., Mellouki, A., Becker, K. H. (2010) *Aspects of the atmospheric chemistry of amides*. ChemPhysChem, *In Press*.
<http://onlinelibrary.wiley.com/doi/10.1002/cphc.201000374/abstract>.
- Bello, A., Idem, R.O. (2005) *Pathways for the formation of products of the oxidative degradation of CO₂ loaded concentrated aqueous MEA solutions during CO₂ adsorption from flue gases*. Ind. Eng. Chem. Res. 44:945-969.
- Blatz, P.J., Elder, J. K., Fischer, J. R., Kispersky, J. P., O'Brien, J., Parrette, R. L., Tieman, C. H., Vanneman, C. R. (1953). *Research in nitropolymers and their application to solid smokeless propellants*. US Navy Department, Bureau of Aeronautics, Report No. 772.
- Bråten, H. B., Bunkan, A. J., Bache-Andreassen, L., Solimannejad, M., Nielsen, C. J. (2008) *Final report on a theoretical study on the atmospheric degradation of selected amines*. Report: NILU: OR 77/2008.
- Claeys, M., Graham, B., Vas, G., Wang, Wu., Vermeylen, R., Pashynska, V., Cafmeyer, J., Guyon, P., Andreae, M., Artaxo, P., Maenhaut, W. (2004). *Formation of Secondary Organic Aerosols Through Photooxidation of Isoprene*. Science, 303(5661), 1173-1176.
- Challis, B. C, Shuker, D. E., (1980). *Chemistry of nitroso-compounds. Part 16. Formation of N-nitrosamines from dissolved NOCL in the presence of alkanolamines and related compounds*. Cosmet. Toxicology, 18, 283-288.

Collins, C. J. (1971). *Reactions of primary aliphatic amines with nitrous acid*. *Accounts of Chemical Research*, 4 (9), 315–322.

Edney, E. O., Kleindienst, T. E., Jaouib, M., Lewandowska, M., Offenberga, J. H., Wang, W. Claeys, M. (2005). Formation of 2-methyl tetrols and 2-methylglyceric acid in secondary organic aerosol from laboratory irradiated isoprene/NOX/SO2/air mixtures and their detection in ambient PM2.5 samples collected in the eastern United States. *Atmospheric Environment*, 39, 5281–5289.

Finlayson-Pitts, B. J., Pitts, J. N. (2000). *Chemistry of the upper and lower atmosphere*. Academic Press, San Diego, US, p 969.

Gaind, V. S., Jedrzejczak, K., Chai, F., Guldner, B. (1992). *Gas-chromatographic determination of airborne monoethanolamine using reagent-coated absorbent tubes*. *Fresenius J. Anal. Chem.*, 342, 591-596.

Galano, A., Alvarez-Idaboy, J. R. (2008). *Branching ratios of aliphatic amines + OH gas-phase reactions: A variational transition-state theory study*. *J. Chem. Theory Comput.*, 4, 322-327.

Galloway, M. M., Chhabra, P. S., Chan, A. W. H., Surratt, J. D., Flagan, R. C., Seinfeld, J. H., Keutsch, F. N. (2009) *Glyoxal uptake on ammonium sulphate seed aerosol: reaction products and reversibility of uptake under dark and irradiated conditions*. *Atmospheric Chemistry and Physics*, 9 (10).

Gery, M.W., Whitten, G.Z., Killus, J.P., Dodge, M.C., (1989). *A photochemical kinetics mechanism for urban and regional scale computer modeling*. *Journal of Geophysical Research* 94 - (D10), 12925–12956

Glasson, W. A. (1979). *Experimental Evaluation of Atmospheric Nitrosamine Formation*, *Environmental Science and Technology*, 13(9) 1145-1147.

Grosjean, D. (1991). *Atmospheric chemistry of toxic contaminants. 6. Nitrosamines: Dialkyl nitrosamines and nitrosomorpholine*. *J. Air Waste manage. Assoc.* 41, 306-311.

Haddrell, A. E., Agnes, G. R. (2004). *A class of heterogeneous/multiphase organic reactions studied on droplets/particles levitated in a laboratory environment: aldehyde+1,8-diaminonaphthalene-imine*. *Atmospheric Environment*, 38, 545–556

IPCC, 2007: Summary for Policymakers. In: *Climate Change 2007: The Physical Science Basis. Contribution of Working Group I to the Fourth Assessment Report of the Intergovernmental Panel on Climate Change* [Solomon, S., D. Qin, M. Manning, Z. Chen, M. Marquis, K.B. Averyt, M. Tignor and H.L. Miller (eds.)]. Cambridge University Press, Cambridge, United Kingdom and New York, NY, USA.

Kohl, A., Nielsen, R. (1997) *Gas Purification*. 5th Ed. Gulf Professional Publishing, Texas, US, p 1395.

Kroll, J. H., Seinfeld, J. H. (2008) *Chemistry of secondary organic aerosol: Formation and evolution of low-volatility organics in the atmosphere*. *Atmospheric Environment*, 42, 3593-3624.

- Kurasawa, H., Lesclaux, R. (1980). *Rate constant for the reaction of NH₂ with ozone in relation to atmospheric processes*. Chem. Phys. Letters, 72(3), 437-442.
- Lalevee, J., Allonas, X., Fouassier, J. (2002) *N-H and α(C-H) bond dissociation enthalpies of aliphatic amines*. J. Am. Chem. Soc. 124, 9613-9621.
- Lawrence, S. A., (2004) *Amines: Synthesis, properties and applications*. Cambridge University Press, Cambridge., p 371.
- Lazarou, Y. G., Papagiannakopoulos, P. (1990). *Infrared multiphon decomposition of dimethylnitramine*. J. Phys. Chem., 94, 7114-7119.
- Lindley, C. R. C., Calvert, J. G., Shaw, J. H. (1979). *Rate studies of the reactions of the (CH₃)₂N radical with O₂, NO and NO₂*. Chemical Physics Letters, 67(1), 57-62.
- McCann, N., Maeder, M., Attalla, M. (2008). *Simulation of Enthalpy and Capacity of CO₂ Absorption by Aqueous Amine Systems*. Ind. Eng. Chem. Res. 47, 2002-2009.
- McCann, N., Phan, D., Wang, X.G., Conway, W., Burns, R., Attalla, M., Puxty, G., Maeder, M. (2009). *Kinetics and Mechanism of Carbamate Formation from CO_{2(aq)}, Carbonate Species and Monoethanolamine in Aqueous Solution*. J. Phys. Chem. A, 113, 5022-5029.
- McQuaid, M. J., Miziolek, A. W., Sausa, R. C., Mellow, C. N. (1991). *Photodissociation of dimethylanitramine at 248 nm*. J. Phys. Chem. 95, 2713-2718.
- Malloy, Q. G. J., Qi, Li., Warren, B., Cocker III, D. R., Erupe, M. E., Silva, P. J. (2009) *Secondary organic aerosol formation from primary aliphatic amines with NO₃ radical*. Atmospheric Chemistry and Physics, 9, 2051-2060.
- Mialocq, J., Stephenson, J. C. (1986). *Picosecond laser study of the collisionless photodissociation of dimethylnitramine at 266 nm*. Chemical Physical letters. 123(5) 390-393.
- Mothersill, C., Cusak, A., Seymour, C. B. (1989). *Enhanced proliferation of cells from human tissue explants following irradiation in the presence of environmental carcinogens*. Radiat. Environ. Biophys., 28, 203-212.
- Murphy, S. M., Sorooshian, A., Kroll, J. H., Ng, N. L., Chhabra, P., Tong, C., Surratt, J. D., Knipping, E., Flagan, R. C., Seinfeld, J. H. (2007) *Secondary organic aerosol formation from atmospheric reactions of aliphatic amines*. Atmos. Chem. Phys. 7:2313-2337.
- Nielsen, C. J., D'Anna, B., Dye, C., George, C., Graus, M., Hansel, A., Karl, M., King, S., Musabilla, M., Muller, M., Schmidbauer, N., Stenstrom, Y., Wisthaler, A. (2010). *Atmospheric Degradation of amines; Summary report: Gas-phase photo-oxidation of 2-aminoethanol (MEA)*. NILU, CLIMIT project no. 193438.
- Pitts, Jr. J. N., Grosjean, D., Cauwenberghe, K. V., Schmid, J. P., Fitz, D. R. (1978) *Photooxidation of aliphatic amines under simulated atmospheric conditions: formation of nitrosamines, nitramines, amides, and photochemical oxidant*. Environmental Science and Technology, 12(8), 946-953.

Schade, G. W., Crutzen, P. J. (1995). *Emission of aliphatic amines from animal husbandry and their reactions: Potential source of N₂O and HCN*. J. Atmos. Chem., 22, 319-346.

Seinfeld, J. H., Pandis, S. N. (2006). *Atmospheric chemistry and physics*. 2ndEd., John Wiley & Sons, NJ, USA, p 1203..

daSilva, E. F. (2005). *Comparison of quantum mechanical and experimental gas-phase basicities of amines and alcohols*. J. Phys. Chem A., 109, 1603-1607.

Silva, P. J., Erupe, M. E., Price, D., Elias, J., Malloy, Q. G. J., Li, Q., Warren, B., Cocker, D. R. (2008) *Trimethylamine as precursor to secondary organic aerosol formation via nitrate radical reaction in the atmosphere*. Environmental Science and Technology, 42, 4689-4696.

Spiegelhadler, B. (1984). *Occupational exposure to N-nitrosamines: Air measurements and biological monitoring*. Proceedings of the 8th International Symposia on N-Nitroso compounds, Banff, Canada. IARC Publication 57, Lyon, France. 937.

Suryanarayanan, K., Suryanarayanan, B. (1970) *Photo-chemical studies of secondary nitramine I. absorption spectra of nitramines and photolysis of dimethylnitramine in solution*. US Army, Technical Report 4068.

Thitakamol, B.; Veawab, A.; Aroonwilas, A. (2006) *Environmental Assessment of the Integration of Amine-based CO₂ Capture Unit to Coal-Fired Power Plants for Greenhouse Gas Mitigation* EIC Climate Change Technology, IEEE Volume , Issue , 10-12 May 2006 Page(s):1 – 7.

Thitakamol, B., Veawab, A., Aroonwilas, A. (2007) *Environmental impacts of adsorption-based CO₂ capture unit for post-combustion treatment of flue gas from coal-fired power plant*. Int J. Greenhouse Gas Control, 1:318-342.

Tuazon, E. C., Carter, W. P. L., Atkinson, R., Winer, A. M., Pitts Jnr. J., N. (1984) *Atmospheric reactions of N-nitrosodimethylamine and dimethylnitramine*. Environmental Science and Technology, 18, 49-54.

Vorobyoz, I., Yappert, M. C., DuPre, D. B. (2002). *Hydrogen bonding in monomers and dimers of 2-aminoethanol*. J. Phys. Chem., 106, 668-679.

Winberry, W. T., Murphy, N. T., Riggan, R. M. (1990). *Method for determination of toxic organic compounds in air*. EPA Methods. Noyes Data Corporation. New Jersey.

Yarwood G., Rao S., Yocke M., Whitten G. (2005) *Updates to the Carbon Bond chemical mechanism*.: CB05. Final report RT-04-00675 to U.S. Environmental Protection Agency, Research Triangle Park, NC 27703.

RESEARCH ADDENDUM – STUDY 1

Theoretical study of the atmospheric fate of 2-aminoethanol (MEA)

Authors: Phil Jackson and Moetaz I. Attalla

Summary

A theoretical study of the gas phase fate of 2-aminoethanol (ethanolamine or MEA) has been undertaken using state-of-the-art hybrid meta-density functional theory with a large basis set (M06-2X/cc-pVTZ). Transition structures were obtained for hydrogen abstraction by •OH at C1, C2, N and O centres. The computed rates of abstraction at 298 K are: C1 = 1.95×10^{-14} cm³/molec.s, C2 = 5.71×10^{-11} cm³/molec.s; O = 5.03×10^{-11} cm³/molec.s; N = 6.16×10^{-12} cm³/molec.s. Predicted branching ratios are C2: 50.3 %, O: 44.3 %, N = 5.4 %, C1 << 0.1 %. Assuming [•OH] = 10⁶ radicals/cm³, the atmospheric life time of MEA is ~2.5 hrs. This does not take into account surface processes, in particular partitioning between the condensed phase (droplets/aerosols) and the gas phase.

Further studies of the fate of various radicals derived from dehydro-MEA have also been undertaken. Abstraction from the oxygen centre leads almost exclusively to dissociation to form formaldehyde and methylamine radical (activation energy of +11.3 kJ, far less than the exoergicity of the hydrogen abstraction from the –OH group). A small fraction of the N-dehydro-MEA radicals will dissociate to form methanimine and •CH₂OH radicals, but N-dehydro-MEA radicals will be persistent relative to O-dehydro-MEA radicals. Following addition of molecular oxygen to radical C1, C2 centres of MEA (to form C1,C2-peroxo-MEA) and oxygen abstraction by NO to form NO₂, the resulting radicals C1, C2-oxo-MEA (oxidanyl species) are short-lived and decompose to formic acid (C1-oxo) and formamide (C2-oxo) respectively. The lowest activation energies for these reactions were found to be +1.8 kJ (C1-oxo-MEA → HCOOH + •CH₂NH₂) and 11.1 kJ (C2-oxo-MEA → H₂NC(O)H + •CH₂OH). 2-(nitrosoamino)ethanol was found to be stable in the gas (excluding the possibility of photolysis). However, some of the population of this species will undergo immediate isomerisation to 2-[(E)-hydroxydiazanyl]ethanol (-N=N-OH). Investigations of decomposition routes for this species are ongoing.

Finally, the energy demand for formation of 2-aminoacetaldehyde/2-aminoethanol/2-iminoethanol has been investigated. We conclude that the unreactive species corresponding to *m/z* 60 observed by Nielsen *et al.* (2010) in smog chamber experiments is a proton-bound cluster CH₃CN-H⁺-H₂O, and is thus an MS-artefact.

Introduction

This particular examination of the atmospheric degradation pathways of 2-aminoethanol (MEA) has been conducted independently by Jackson and Attalla (2010), as part of this report. The aim of this work is to capture the major degradation pathways of MEA with (i) due consideration of previous smog chamber (eg. Nielsen *et al.*, 2009) and theoretical (Bråten *et al.*, 2008) studies, and (ii) activation and reaction free energies generated as part of this study. Activation and reaction free energies will ultimately determine which reactions proceed/do not proceed. Due to time constraints, some potential pathways have been omitted. Photochemical activation of MEA and nitroso/nitro/aldehyde derivatives has not been considered. The latter requires recourse to configuration-interaction or random-phase approximation calculations, which are very time-consuming. This aspect of the work could be pursued in a follow-up study. The literature survey preceding this chapter, and previous atmospheric studies (Bråten *et al.*, 2008) have identified species likely to undergo photochemical activation.

The latest state-of-the-art hybrid meta-density functional has been used for this study (M06-2X, Truhlar and Zhao, 2008). Tests of this functional demonstrate it yields activation energies within 2 kcal/mol of the actual value (mean unsigned error for DBH76 test set, a set of 76 diverse barrier heights). A triple-zeta Dunning correlation-consistent basis set has also been used (cc-pVTZ), together with an exchange-correlation quadrature grid - recommended by the quantum chemistry software authors - that produces interpolation errors no larger than 1 microhartree. The CBS-Q model chemistry method has also been used to calculate reaction free energies of high accuracy.

Computational methods

- The level of calculation used was M06-2X/cc-pVTZ
- All optimised structures presented were verified by examination of the vibrational frequencies (hessian matrix). One imaginary frequency for transition structures (TS's), zero for minima (local, global)
- Rates of reaction were determined using standard transition state theory with the Wigner correction included to compensate for quantum tunnelling (Wigner, 1932)
- Excited states were determined using time-dependent DFT with long-range correlation corrections (LC-BOP/cc-pVTZ).
- These calculations were performed with the GAMESS software (Schmidt *et al.*, 1993) on the National Computing Infrastructure SGI-blade cluster (Australian National University, Canberra, Australia)
- Model chemistry calculations at the Complete Basis Set Quadratic Configuration Interaction level (CBS-Q) for reaction free energies were performed on an SG-Altix system (high performance supercomputing centre, CSIRO) located in Melbourne, Victoria.
- These calculations were done using the Gaussian 03 software suite (Pople *et al.*, 1993)

Assumptions: •OH is assumed to be the dominant radical species in the atmosphere, and is the only chemical initiator considered in this theoretical study. Other possible initiators not investigated include HO₂•, O₃ and •NO₃ radical; these are expected to -

but may not - be in lower abundance. Follow-up reactions involving O₂ and NO have also been modelled, primarily because of their anticipated high abundance in power station flue stack gas that has been scrubbed using amines within a post-combustion capture setting.

Results

A two-dimensional rendering of the MEA molecule with reference to the carbon positions is presented in Figure 1. The optimised structure at the M06-2X/cc-pVTZ level is presented alongside for reference.

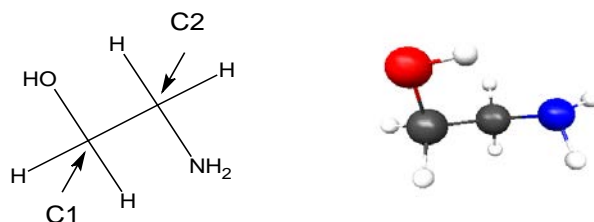


Figure 1. Two-dimensional and optimised gas-phase structures of MEA. In the gas phase, the most stable MEA conformer is hydrogen bonded through the nitrogen (proton acceptor) and hydroxyl group hydrogen (proton donor).

The CBS-Q reaction free energy changes for the degradation pathway initiated by H-abstraction from the carbon at position 2 in MEA, as presented on page 8 of the study of the atmospheric degradation of amines (Nielsen *et al.*, 2010), is presented below. The free energy changes associated with each step reveal this degradation pathway is possible, but without activation energies it is impossible to establish which pathways are preferred relative to abstraction at other positions in the MEA molecule.

In order to establish which hydrogen in the MEA molecule is likely to react with •OH, the potential energy surface for the •OH + MEA molecule was derived. All TS's are fully optimised (zero constraints). The surface for hydrogen abstraction (considering only •OH) is presented in Figure 3. The abstraction reactions begin with the separated reactants, which may or may not form a dipole-dipole complex through •OH forming a hydrogen bond with the MEA nitrogen atom; the reactants then pass through one of several transition states and proceed to the products (dehydro-MEA radical and water).

Abstractions from the carbon centres do not appear to proceed through a hydrogen-bonding intermediate. All energies are relative to the separated reactants (zero kJ/mol, reference point). Note that a minimum for •OH forming a hydrogen bond with the MEA oxygen centre was also found, however this has an energy of +20.6 kJ relative to the separated reactants.

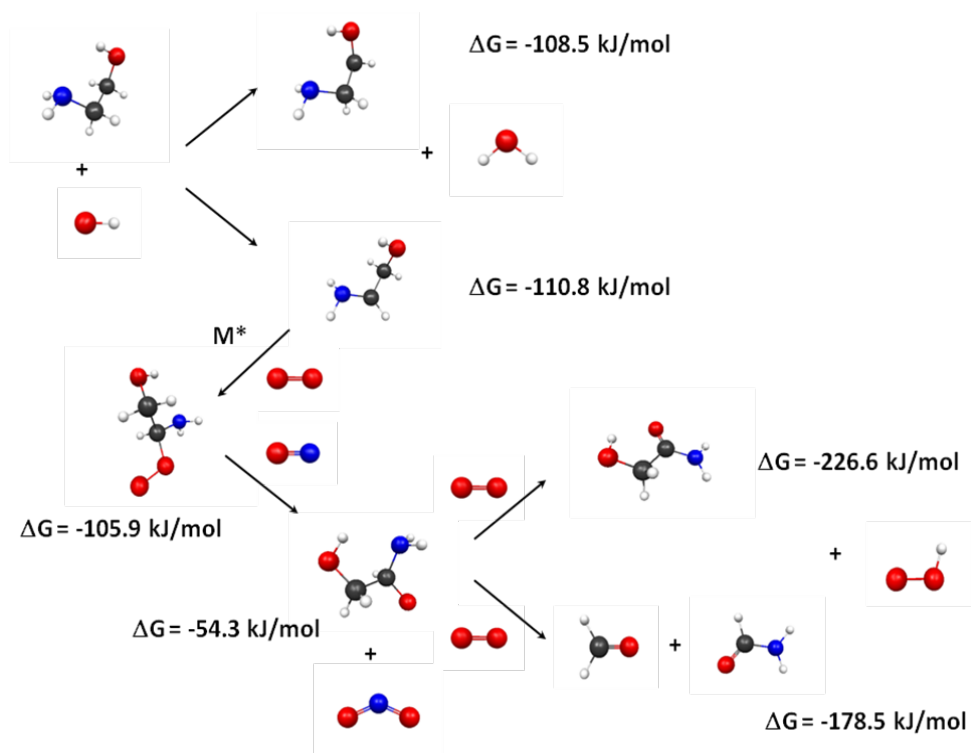


Figure 2. MEA degradation pathway after H-abstraction at C(2) by a reactive radical such as $\bullet\text{OH}$. Carbon atoms = black, nitrogen atoms = blue, oxygen atoms = red, hydrogen atoms = white.

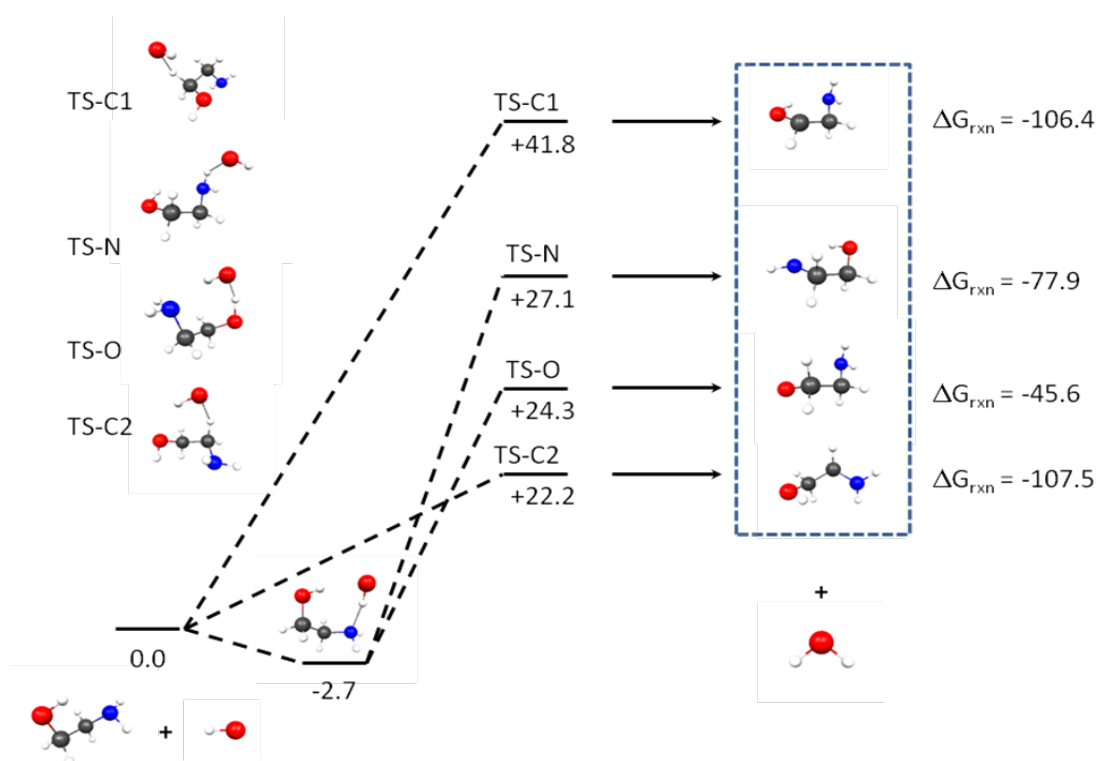


Figure 3. Energetics of the various $\text{MEA} + \bullet\text{OH} \rightarrow \text{dehydro-MEA}\bullet + \text{H}_2\text{O}$ hydrogen abstraction pathways computed at the M06-2X/cc-pVTZ level of theory. All energies are given in kJ relative to the separated reactants (MEA + $\bullet\text{OH}$). Carbon atoms = black, nitrogen atoms = blue, oxygen atoms = red, hydrogen atoms = white.

A second TS for abstraction from the oxygen centre was also found with an associated barrier of +45.6 kJ. Other low energy transition structures for abstractions from different centres may be located at a later date.

The imaginary frequencies associated with the transition structures located in Figure 3 are: C2 = 887i cm⁻¹; O = 1647i cm⁻¹; N = 618i cm⁻¹; C1 = 807i cm⁻¹. According to transition state theory, the rate constant for the reaction is given by:

$$k_r(T) = \Gamma(T)k_B T/h \exp(-\Delta G^\ddagger/RT)$$

where

$$\Gamma(T) = 1 + 1/24 * (h |v^\ddagger| / k_B T)^2$$

is the Wigner tunnelling correction. The other constants have their usual meanings. The results for the reaction rates are presented in Table 1 (corrected and uncorrected).

It can be seen that –uncorrected– the rate of abstraction at C2 relative to O is approximately 2 ~ 1. With the tunnelling correction included, the rates become comparable. The rate of abstraction from C1 is almost 3 orders of magnitude smaller than the rate of abstraction from C2. Based on these theoretical results, C2 and O abstraction reaction products should dominate smog chamber experiments.

Table 1. Reaction rates (corrected and uncorrected)

MEA abstraction centre	ω_{im} (cm ⁻¹)	Activation Energy	Wigner factor	Rate (10 ⁸ s ⁻¹ , uncorrected)	Rate (10 ⁸ s ⁻¹ , corrected)
C2	887	22.2	1.75	8.02	14.1
O	1647	24.3	3.60	3.44	12.4
N	618	27.1	1.37	1.11	1.52
C1	807	41.8	1.62	0.00295	0.00480

From these results, a branching ratio can be obtained: 50.3 % C2, 44.3 % O, 5.4 % N, 0 % C1. Although C1-centred radicals can be excluded on a kinetics basis, they are still considered in the event a lower energy transition structure is located at a later date.

The units for the corrected rates given above can be converted into cm³/molec.s by using the STP particle number density. This gives the following rates for •OH abstraction at: C2 = 5.71 x 10⁻¹¹ cm³/molec.s; O = 5.03 x 10⁻¹¹ cm³/molec.s; N = 6.16 x 10⁻¹² cm³/molec.s; C1 = 1.95 x 10⁻¹⁴ cm³/molec.s. The aggregate rate for disappearance of MEA in the atmosphere at STP due to reaction with •OH is 1.14 x 10⁻¹⁰ cm³/molec.s. If [•OH] = 10⁶ radicals/cm³ is assumed (Bråten *et al*, 2008), an atmospheric life time of 2.44 hrs is obtained.

Hydrogen abstraction at O

Hydrogen abstraction from the oxygen atom gives rise to a radical that represents a composite of two weakly-bound species: closed shell formaldehyde and aminomethyl radical. The activation barrier for the homolytic fission reaction leading to these products is +11.3 kJ, and the associated imaginary frequency has a value of 295i cm⁻¹

(see Figure 4). Given the exoergicity of formation of the oxygen-centred radical of MEA (-45.6 kJ/mol), it is likely that the oxygen-centred radical dissociates immediately to form formaldehyde and aminomethyl radical. The fate of aldehydes in the atmosphere is well established (Mouvier *et al*, 1986); the fate of aminomethyl radical is discussed below.

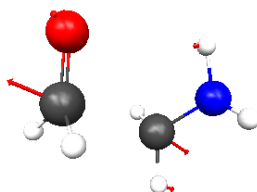


Figure 4. Transition structure for disproportionation of the oxygen-centred radical. Normal mode vectors are in red.

Hydrogen abstraction at N

The corresponding disproportionation reaction from the N-centred radical of MEA is associated with a significantly higher activation energy of +92.9 kJ. In order for the H-abstraction reaction to take place at the nitrogen centre of MEA, the activated complex must have >27.1 kJ internal energy, and when added to the reaction exoergicity (77.9 kJ), this gives a total of 105 kJ/mol distributed amongst the degrees of freedom of the departing water molecule and the N-centred radical. Thus, we conclude that this reaction is feasible but the N-centred radical will be long-lived relative to the O-centred radical. The lifetime of the N-centred radical will depend on how much energy is partitioned amongst the degrees of freedom of the water molecule, and how much of the reaction energy the radical retains prior to collisions and thermal equilibration.

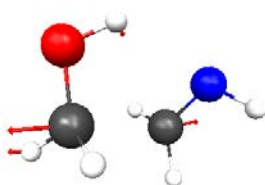


Figure 5. Transition structure for disproportionation of the nitrogen-centred radical. Normal mode vectors are in red ($\omega_{im} = 480 \text{ cm}^{-1}$).

Hydrogen abstraction at C1

The theory suggests that hydrogen abstraction from C1 is the slowest. In order to determine the fate of any C1 radicals produced, the O \rightarrow C1 hydrogen shift activation energy was determined. Depending on the extent to which energy is partitioned into the leaving water molecule, up to 148.2 kJ is available to C1-dehydro-MEA for further reaction. The activation energy was found to be +177.8 kJ ($\omega_{im} = 1885 \text{ cm}^{-1}$, transition structure not shown). On the basis of this value, this reaction will be extremely slow and is probably not feasible before C1-dehydro-MEA thermally equilibrates. Further possible reactions of the C1-dehydro-MEA radical are discussed below.

Double-bond formation?

According to PTRMS work conducted by Nielsen *et al.* (2010), an unidentified peak at m/z 60.044 (ion composition $C_2H_6NO^+$, neutral composition C_2H_5NO) appeared during photo-oxidation experiments on May 10 (p 16). As the degradation of MEA is initiated by a radical oxidant, it is not inconceivable that a hydrogen on an adjacent heavy atom is eliminated or abstracted (from N, C1 or C2; the O-centred dehydro-MEA radical is short-lived, see above).

Various isomers and conformers of $[C_2, H_5, N, O]$ have been investigated for their relative gas-phase stability. The results are presented in Figure 6.

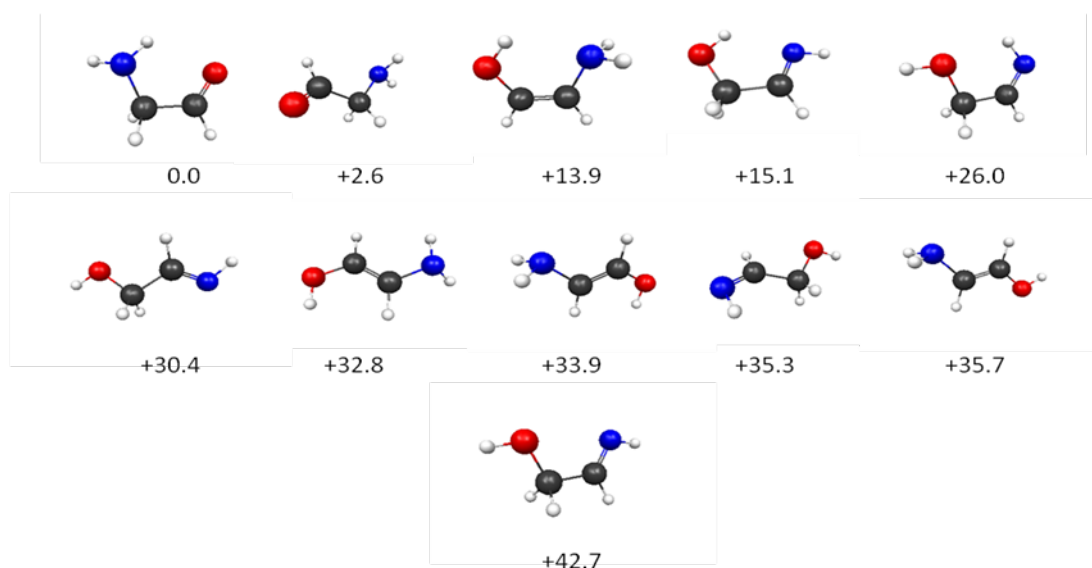
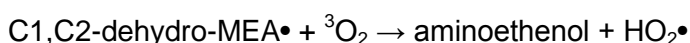
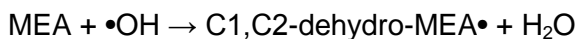


Figure 6. Isomers and conformers for $[C_2, H_5, N, O]$. Free energies relative to the most stable conformer of 2-aminoacetaldehyde (0.0) are also presented.

Formation of 2-aminoacetaldehyde would appear to be preferred to formation of *Z*-aminoethenol (+13.9 kJ) and 2-iminoethanol (+15.1). Given the relative instability of O-centred dehydro-MEA, formation of 2-aminoacetaldehyde would need to proceed by H-abstraction at C1 as the first step (slow according to rates in Table 1) or via a concerted photochemically-induced dihydrogen elimination reaction (unlikely). A further possibility is a surface-induced elimination (not investigated).

Formation of iminoethanol or aminoethenol conformers would seem more likely, especially considering the relative rates of H-abstraction from C2 and N. The following mechanism for the formation of aminoethenol is proposed:



Two transition structures were located, and are presented in Figure 7.

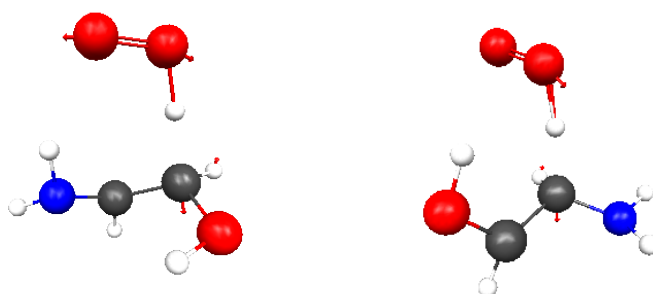


Figure 7. Transition structures for $^3\text{O}_2$ -mediated hydrogen abstraction from C2-dehydro-MEA (left) and C1-dehydro-MEA (right). Imaginary frequencies: $1672i\text{ cm}^{-1}$ (left) and $1720i\text{ cm}^{-1}$ (right).

The free energy of activation for these abstractions is relatively high: for radical abstraction from C1 in the C2-dehydro-MEA radical (left), +194.3 kJ; for radical abstraction from C2 in the C1-dehydro-MEA radical (right), +199.0 kJ. Thus, formation via this pathway would be negligible. Abstraction by NO_2 to form HONO (a stable neutral) could be more favourable energetically (not investigated), but it is unlikely to be low enough to make this pathway competitive.

To gain insight into which heavy atom-hydrogen covalent bonds could be activated (i.e. become more acidic) by dehydro-MEA radical formation, some auto-dissociative reaction barriers were modelled. The transition structures are presented in Figure 8.

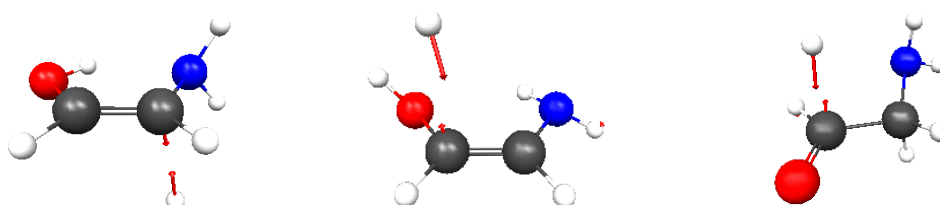


Figure 8. Transition structures for autodissociation involving C-H bonds adjacent to radical centres. Imaginary frequencies: $586i\text{ cm}^{-1}$ (left), $104i\text{ cm}^{-1}$ (centre), $1002i\text{ cm}^{-1}$ (right).

The free energies of auto-dissociative hydrogen loss were: +147.6 kJ (Figure 8, left), +144.3 kJ (Figure 8, centre) and +95.0 kJ (Figure 8, right). The oxygen-centred radical clearly has the most acidic hydrogen atom (at C1), however this pathway cannot compete effectively with O-centred MEA radical dissociation to produce formaldehyde and $\bullet\text{CH}_2\text{NH}_2$ radical. On the basis of these results, formation of aminoacetaldehyde, 2-iminoethanol or 2-aminoethenol should be extremely slow, unless significant surface or photolytic processes are at play.

The relative free energies of formation presented in Figure 6 suggest that 2-aminoacetaldehyde is energetically preferred if the $[\text{C}_2, \text{H}_5, \text{N}, \text{O}]$ system is in equilibrium. The lowest energy unimolecular decomposition pathway for this isomer corresponds to

formaldehyde elimination to produce CHNH₂, which presumably rearranges rapidly to form methanimine. According to the theory, the activation energy for first step is +169.1 kJ ($\omega_{im} = 692i \text{ cm}^{-1}$). The activation energy magnitude suggests this pathway will not be important, although open shell singlets could participate with lower activation energies under photolytic conditions. The aminoacetaldehyde-aminoethenol tautomerism pathway has a higher activation energy of +272.8 kJ, and is not considered feasible on the closed shell surface under STP conditions. Thus, we conclude any aminoacetaldehyde-aminoethenol-iminoethanol formed should be long-lived and observable in smog chamber experiments. However, their rates of formation would be extremely slow.

Nielsen *et al.* (2010) reported that there was no evidence of these species on cartridges used to sample the gas volume in their smog chamber experiments. Careful consideration of the PTRMS conditions suggests a peak at m/z 60 could arise from a proton-bridged molecular dimer, probably CH₃CN-H⁺-H₂O, which possesses the correct molecular composition. This species is commonly observed in API-mass spectrometry which employs acetonitrile as a mobile phase. Moreover, the Nielsen *et al.* (2010) study used CH₃CN as an unreactive tracer. The proton-bridged dimer would exhibit low reactivity as stated in the report, and would easily dissociate upon cartridge trapping. Thus, we conclude m/z 60 is an MS artefact.

Peroxo and oxo species

Dehydro-MEA radicals can react to form peroxo species via addition of ³O₂ at the radical centre. Oxo-derivatives can form by addition of either ³O₂ or NO₂ at the radical site, followed by ³O or NO elimination. The reaction free energies for formation of C1-, C2-peroxo species are presented in Table 2. Isoforms important in the gas-phase at 298 K are presented in Figure 9.

Table 2. Reaction free energies for formation of C1-, C2-peroxo species formed via C_x-dehydroMEA + O₂ + M → C_x-peroxoMEA + M*

X =	ΔG _r (298 K) kJ/mol (averaged)	Populations
1	-107.1	A = 58 %, B = 42 %, C < 0.2 %
2	-98.8	A = 78 %, B = 20 %, C = 2 %

The result obtained for formation of C2-peroxoMEA using the M06-2X/cc-pVTZ method compares well with the CBS-Q value (within 2 kcal/mol).

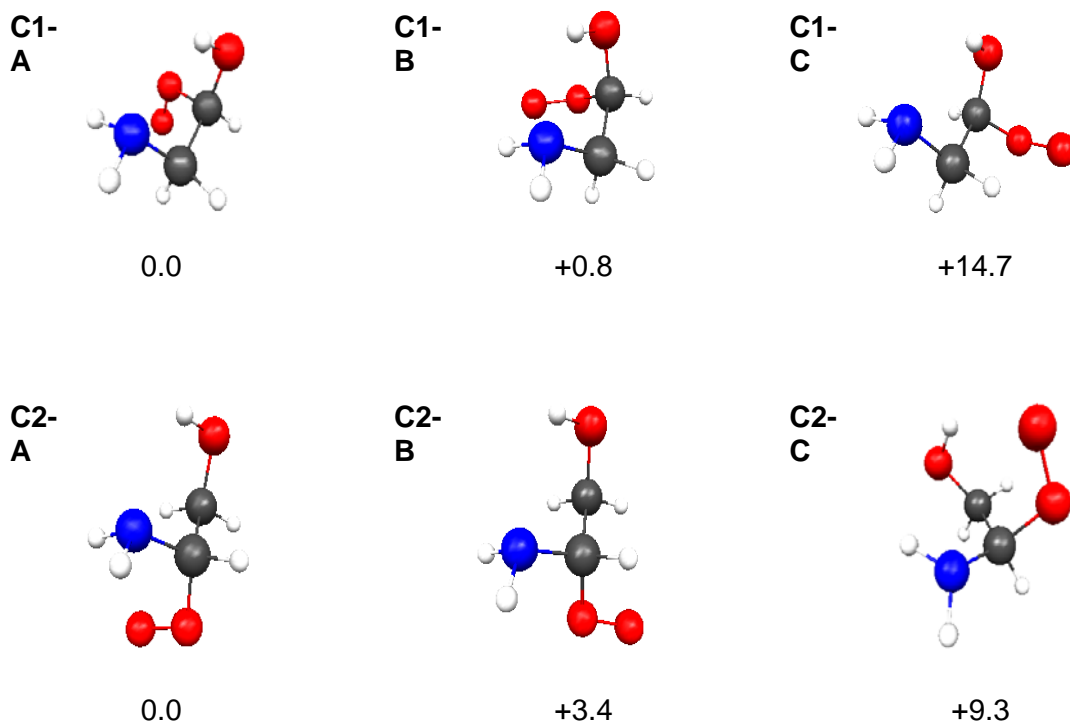


Figure 9. PES minima for C1-peroxo species (top) and C2-peroxo species (bottom). The lowest conformer for each peroxo form (C1-A and C2-A) have a free energy of 0.0 relative to other conformers.

Two pathways which could deplete the C_x-peroxoMEA population were investigated: the first involves abstraction of atomic oxygen by NO to generate NO₂ and an oxide of MEA; the second pathway involves disproportionation to yield either formic acid (from C1-peroxoMEA) or formamide (from C2-peroxoMEA).

The free energies of oxygen abstraction from C_x-peroxoMEA by NO are presented below in Table 3.

Table 3. Free energies of oxygen abstraction from C_x-peroxoMEA by NO via C_x-peroxoMEA + NO → C_x-oxoMEA + NO₂

X =	ΔG _r (298 K) kJ/mol (averaged)	Populations (refer to Figure 10)
1	-46.3	80 %, 20 %
2	-44.8	99 %, 1 %

The free energy changes for oxygen abstraction by NO are feasible. This reaction generates radicals which undergo low energy decompositions to form stable neutrals ie. formic acid and formamide.

Cx-oxoMEA (oxidanyl radicals) and associated unimolecular decomposition

Two isomers were modelled for both C1-oxoMEA ((2-amino-1-hydroxethyl)-oxidanyl) and C2-oxoMEA ((1-amino-2-hydroxethyl)-oxidanyl). These are presented in Figure 10, together with their relative energies.

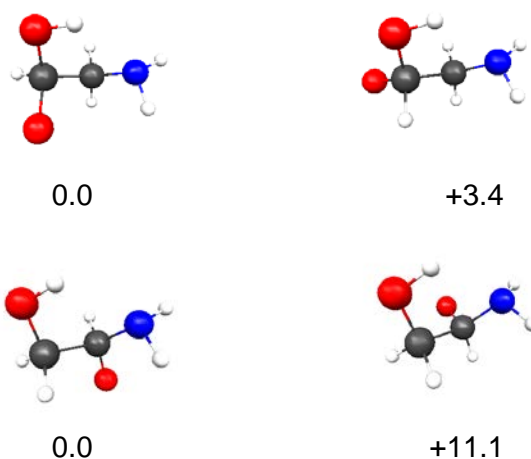


Figure 10. Isomers and relative energies (in kJ/mol) for C1-oxoMEA (top) and C2-oxoMEA (bottom).

The molecular connectivity of C1-oxo species suggests decomposition to formic acid and $\bullet\text{CH}_2\text{NH}_2$ (aminomethyl) could be feasible. The transition structures and imaginary modes associated with this reaction are presented in Figure 11. The free energies of activation for these reactions were found to be +1.8 kJ and +9.1 kJ.



Figure 11. Transition structures for elimination of formic acid from C1-oxoMEA isomers. Imaginary frequencies: $383i\text{ cm}^{-1}$ (left) and $315i\text{ cm}^{-1}$ (right).

Based on these activation energies and the exoergicity of oxygen abstraction from C1-peroxoMEA (Table 3), the C1-oxoMEA species will decompose to yield formic acid. This reaction will be a source of $\bullet\text{CH}_2\text{NH}_2$ radicals.

Transition structures were also located for the decomposition of C2-oxoMEA isomers to formamide and $\bullet\text{CH}_2\text{OH}$ radicals. These are presented in Figure 12.



Figure 12. Transition structures for elimination of formamide from C2-oxoMEA isomers. Imaginary frequencies: $340i\text{ cm}^{-1}$ (left) and $367i\text{ cm}^{-1}$ (right).

The associated activation energies are +11.1 kJ (left, Figure 12) and +19.3 kJ (right, Figure 12). The activation energies for these decompositions are also relatively low, so it can be assumed that formation of C1- or C2-oxoMEA species leads to decomposition to formic acid and formamide, respectively (although the C2-oxoMEA species could be slightly longer lived). These reactions are sources of the radicals $\bullet\text{CH}_2\text{OH}$ and $\bullet\text{CH}_2\text{NH}_2$, the fates of which are discussed in the following sections.

In order to account for any ammonia that might be produced, one additional TS was located, which corresponds to loss of ammonia and formaldehyde to produce HCO radicals (not shown) from C2-oxoMEA. The activation energy is 52.4 kJ/mol ($\omega_{\text{im}} = 414i\text{ cm}^{-1}$), so this pathway is of little importance and cannot compete with the pathways described above.

Decomposition of Cx-peroxoMEA

Two transition structures were located for the intramolecular rearrangement of the C2-peroxo-MEA radicals to form C2-hydroperoxy radicals (hydrogen abstraction from the C2, C1 centres). These are presented in Figure 13.



Figure 13. Transition structures for the intramolecular conversion of C2-peroxo radicals to C2-hydroperoxy radicals (C-centred radicals). Imaginary frequencies: $1825i\text{ cm}^{-1}$ (C2-abstraction, left) and $1861i\text{ cm}^{-1}$ (C1-abstraction, right).

The activation energies for these abstraction reactions were found to be +188.1 kJ (C2-abstraction) and +118.5 kJ (C1-abstraction), both with respect to the most stable C2-peroxo-MEA conformer. The condensation reaction between the C2-centred MEA radical is exoergic by 98.8 kJ/mol, so the C2-abstraction pathway can be ruled out; the C1-abstraction also appears implausible, as (i) additional energy in excess of the condensation reaction exoergicity is needed, and (ii) the third body will leave the condensation reaction with a finite amount of the 98.8 kJ.

Fate of •CH₂OH (hydroxymethyl) radicals

This radical will survive to react with other molecules/radicals present in the atmosphere. For the purposes of this study, follow-up chemistry with water and ³O₂ (a radical molecule of high atmospheric abundance) are considered.

According to the calculations, the reaction between ³O₂ and •CH₂OH is exoergic at 298 K ($\Delta G_{\text{rxn}} = -105.7$ kJ/mol, averaged over •O₂CH₂OH isomer populations). Isomers of •O₂CH₂OH and their relative free energies are presented in Figure 14.

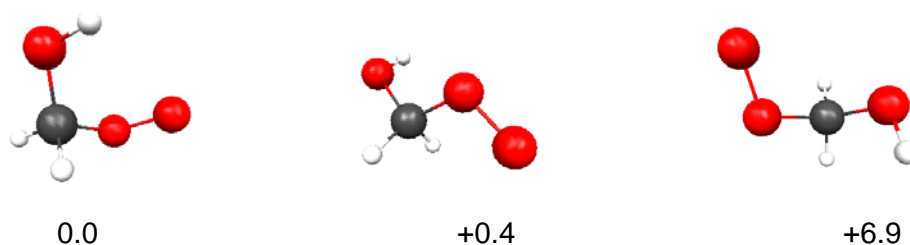


Figure 14. Conformers of •(O₂)CH₂OH and their relative energies (kJ). Relative gas-phase populations at 298 K: 53 % (left), 44 % (centre) and 3 % (right).

The following unimolecular decompositions were considered for •O₂CH₂OH:

- (1) loss of •HO₂ to form formaldehyde
- (2) loss of water to form HCOO•
- (3) loss of •OH to form [H₂C, O₂] (which can undergo rearrangement)

The three transition structures located are presented in Figure 15. Loss of HO₂• to produce formaldehyde requires an activation energy of +191.9 kJ, well in excess of the exoergicity of •O₂CH₂OH formation, so this pathway can be discounted. Water loss to produce ²HCOO requires a free energy of activation of +346.8 kJ, so this pathway can also be discounted. The activation energy associated with the final pathway is the smallest (+104.1 kJ, Figure 15), and is almost equal to the O₂/•CH₂OH association energy. This is the most feasible pathway for dissociation of the •O₂CH₂OH radical, and (i) regenerates •OH radicals, and (ii) leads to either formic acid and/or CO₂ and H₂ (not modelled).

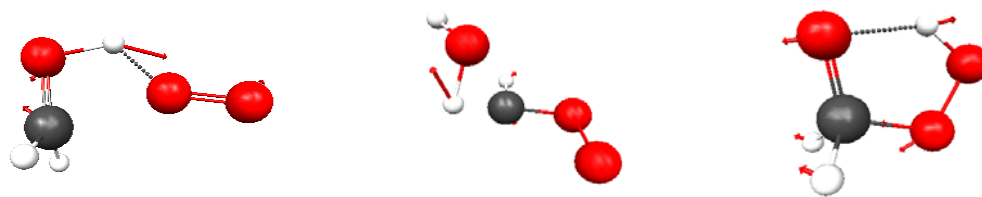


Figure 15. Transition structures located for pathways: 1 (left), 2 (centre) and 3 (right). Imaginary frequencies: 1331 cm^{-1} (left), 1324 cm^{-1} (centre), 1146 cm^{-1} (right).

The reaction of hydroxymethyl radical with water has also been modelled. In this case, the hydroxymethyl radical abstracts a hydrogen atom from water to produce $\bullet\text{OH}$ radicals and methanol. The calculated activation energy is $+120.5\text{ kJ}$ ($\omega_{\text{im}} = 525i\text{ cm}^{-1}$, transition structure not shown), so formation of methanol does not appear to be feasible unless $\bullet\text{CH}_2\text{OH}$ is formed “hot” as the product of a reaction not investigated.

Fate of $\bullet\text{CH}_2\text{NH}_2$ (aminomethyl) radicals

This radical can also undergo addition of molecular oxygen, however the final product is likely to be formamide.

Two minima were located for $\bullet\text{O}_2\text{CH}_2\text{NH}_2$, which are presented in Figure 16.

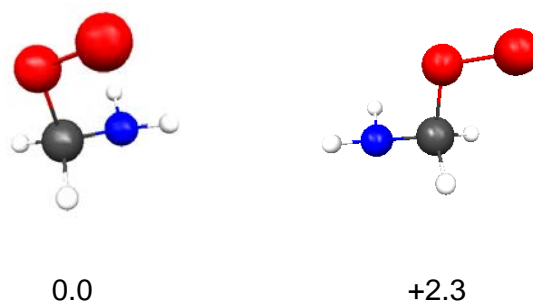


Figure 16. Minima located for $\bullet\text{O}_2\text{CH}_2\text{NH}_2$ and their relative energies (in kJ/mol)

The free energy of reaction for $\bullet\text{CH}_2\text{NH}_2 + \text{O}_2 + \text{M} \rightarrow \bullet\text{O}_2\text{CH}_2\text{NH}_2 + \text{M}^*$ (weighted over both radical product populations) is -96.2 kJ/mol , so the addition of O_2 is feasible.

The addition of O_2 at the carbon centre of aminomethyl radical should enhance the acidity of one of the hydrogen atoms also attached to the carbon; one possible pathway for reaction of this radical is abstraction of H from the carbon atom and elimination of $\bullet\text{OH}$ radical to produce formamide. Two transition structures were located, and these are presented in Figure 17.



Figure 17. Transition structures located for the intramolecular rearrangement of $\bullet\text{O}_2\text{CH}_2\text{NH}_2$ to form aminohydroperoxymethyl radical ($\text{HOOC}\bullet\text{HNNH}_2$). Imaginary frequencies: 1570 cm^{-1} (left), 1562 cm^{-1} (right).

The corresponding free energies of activation for these rearrangements are +178.2 kJ and +184.1 kJ. On the basis of these energies, this pathway can be discounted.

The reaction of water with aminomethyl radical has also been modelled. The computed activation energy was found to be +133.1 kJ ($\omega_{\text{im}} = 525i\text{ cm}^{-1}$, transition structure not shown), so formation of methylamine from water and aminomethyl radical does not appear to be feasible.

Formation of C- and N-nitroso species

With the exception of O-centred MEA radicals (which are short-lived according to the results presented above), C1-, C2- and N-centred MEA radicals can combine with $\bullet\text{NO}$ radical to form C- and N-centred nitrosamines. In the first instance, the thermochemistry of addition of $\bullet\text{NO}$ to MEA radicals has been investigated. Optimised structures for various nitrosamines are presented below in Figure 18.

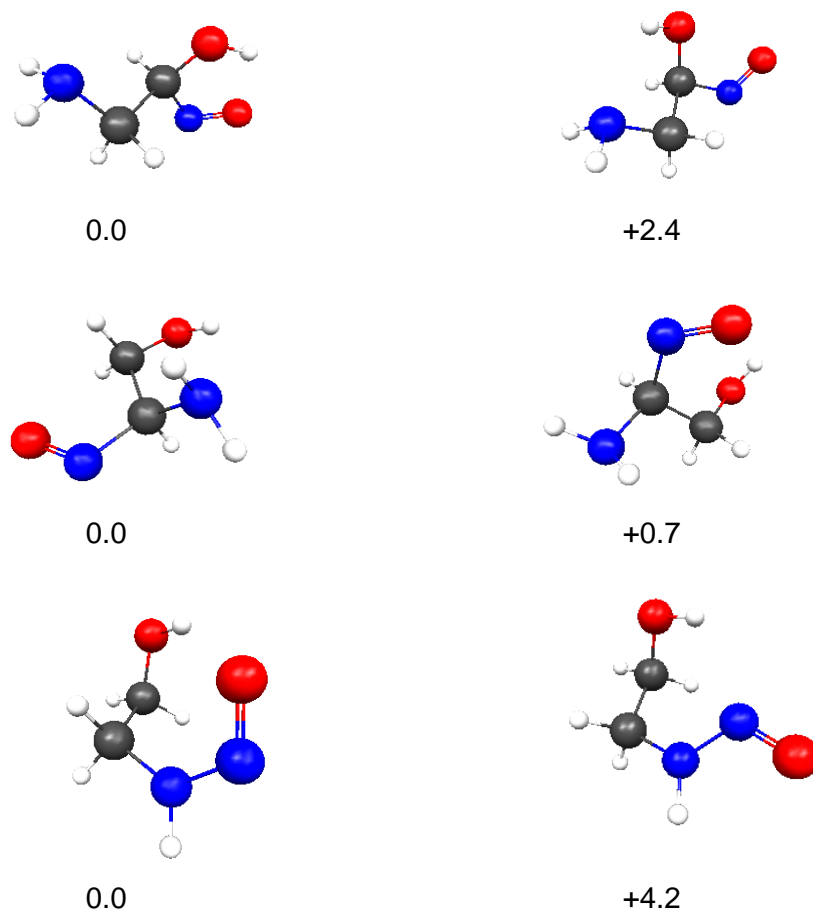


Figure 18. Stable conformers (minima) located for C- and N-nitrosamine derivatives of MEA and their relative energies (in kJ/mol): C1-nitrosamines (top), C2-nitrosamines (centre) and N-nitrosamines (bottom).

The free energy of the addition of •NO to MEA-centred radicals are presented in Table 4. The addition reaction is feasible for all radical centres, however, the NO - N-centred radical (MEA) interaction is more favourable, due to the closed-shell resonance:

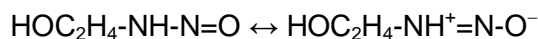
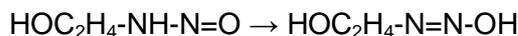


Table 4. Free energy of the addition of •NO to MEA-centred radicals formed via C,N-dehydroMEA + NO + M* → C,N-oxoMEA + M*

Nitroso centre =	ΔG_r (298 K) kJ/mol (averaged)	Populations (refer to Figure 16)
C1	-99.8	72 % (LHS), 28 % (RHS)
C2	-95.7	57 % (LHS), 43 % (RHS)
N	-148.7	84 % (LHS), 16 % (RHS)

Although the formation of the nitrosamines is feasible, the kinetic stability of each molecule needs to be established. For this reason, the intramolecular rearrangement of N-nitrosamine to an (*E*) N-hydroxydiazene has been investigated:



The transition structure for this rearrangement is presented in Figure 19.

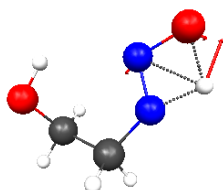


Figure 19. Hydrogen-shift transition structure for the intramolecular rearrangement from 2-nitrosaminoethanol to 2-[(*E*)-hydroxydiazenyl]ethanol. Imaginary frequency $\omega_{im} = 1901 \text{ cm}^{-1}$

This hydrogen shift, which leads exclusively to an *E*-hydroxydiazenyl conformation, has a free energy of activation of +130.8 kJ. Overall, this transformation is only slightly exoergic (-2.1 kJ/mol). The free energy of reaction leading to formation of N-nitrosoMEA is -148.7 kJ/mol (averaged over the gas phase conformational populations of N-nitrosoMEA); depending on the amount of reaction energy partitioned amongst the degrees of freedom of the third body (M^*) and N-nitrosoMEA, there is sufficient energy for at least a fraction of the N-nitrosoMEA product to undergo this rearrangement immediately following formation, prior to thermal equilibration.

The conformer of N-nitrosoMEA on the left hand side of Figure 18 is slightly more stable in the gas phase, due to hydrogen-bond formation between the hydroxyl group hydrogen and the oxygen of the nitroso group. The proximity of these groups suggests that hydrogen transfer from the -OH to the -NO group could be the first step in formation of a hydroxydiazene functionality. This reaction was also investigated.

The *E*-hydroxydiazenyl isomer can undergo intramolecular rearrangement via hydrogen shift from the C1-centred OH to the nitrogen of the diazenyl group, which could lead to formaldehyde elimination. The transition structure located for this rearrangement is presented in Figure 20:

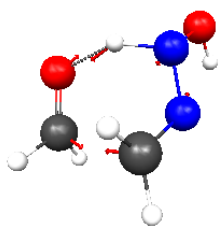


Figure 20. Hydrogen-shift transition structure for the intramolecular elimination of CH_2O from 2-[(E)-hydroxydiazenyl]ethanol. Imaginary frequency $\omega_{\text{im}} = 813 \text{ cm}^{-1}$.

This elimination reaction is associated with an activation energy of +188.1 kJ, and is not feasible without photolytic activation or surface catalysis.

The elimination reaction above produces formaldehyde hydroxyhydrazone ($\text{CH}_2\text{N}_2\text{HOH}$) as a by-product; in turn, this molecule can eliminate water to yield diazomethane, a potent alkylating agent. This process is associated with an activation energy of +188.0 kJ (1585 cm^{-1}); if the preceding elimination of CH_2O was feasible, then the follow-up water-elimination step could also be considered feasible; without photolytic or surface activation, the decomposition of N-nitrosoaminoethanol to diazomethane is presumed not to be feasible in the gas phase. Photolysis of the HN-(N=O) bond is the most probable mechanism of nitrosamine decay, and this apparently occurs with high efficiency for many nitroso species.

Time-dependent DFT studies using the LC-BOP/cc-pVTZ level of theory reveal that there are two low-lying singlet excited states for the hydrogen-bonded 2-(nitrosamino)ethanol conformer at 3.45 eV (360 nm) and 6.34 eV (196 nm), for the non-hydrogen bonded conformer at 3.37 eV (369 nm) and 6.32 eV (197 nm). The first excited singlet state ($S_1 \leftarrow S_0$) is accessed by absorption of light in the UVA region, however this transition is associated with a low oscillator strength (~ 0.001). The UVC $S_2 \leftarrow S_0$ transition is associated with a much larger oscillator strength (~ 0.1), so it is more likely to be observed spectroscopically.

The character of the UVC $S_2 \leftarrow S_0$ transition is presented in Figure 21. The excitation is $n \rightarrow \pi^*$, where π^* is the LUMO and n has contributions from the two orbitals shown.

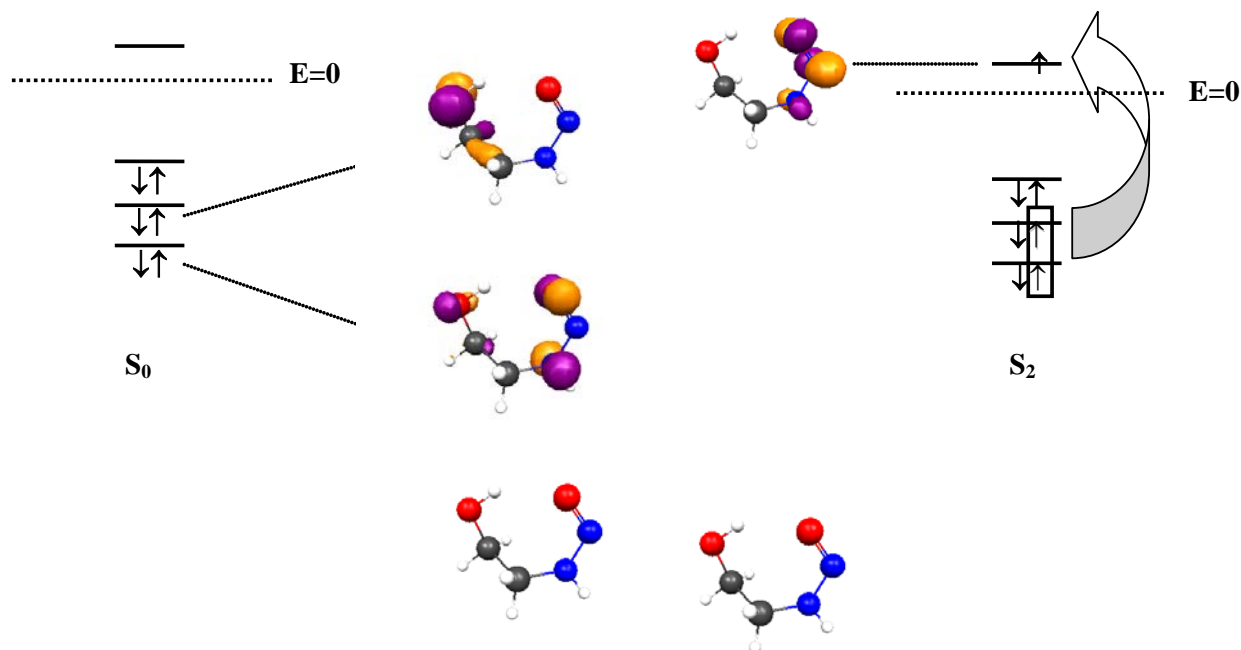


Figure 21. The character of the $S_2 \leftarrow S_0$ for N-nitrosoMEA predicted by TD-DFT. The orbitals are imposed on the optimised N-nitrosoMEA structures (shown at the bottom).

The transition described by Figure 21 is expected to induce vibrational excitation of the N-NO bond. However it may/may not lead to dissociation (this depends on the nature of the excited state ie. whether it is bound, and whether it correlates –in an orbital sense- with the dissociation asymptote). The triplet excited states were also calculated for the same structure. Two triplet states of importance for inter-system crossing were located at 3.86 eV and 6.53 eV. The triplet state at 6.53 eV is close in energy to the 6.32 eV open-shell singlet state ($\Delta E = 0.21$ eV or 20.4 kJ), and has almost identical character to the open-shell singlet transition. Inter-system crossing is expected to be facile in this instance, and might lead to dissociation. The lowest triplet excited state is 2.46 eV (239.4 kJ) vertically above the ground state N-nitrosoMEA singlet structure, which is higher in energy than the N-nitrosoMEA bond strength (1.53 eV, 148.7 kJ). The lowest energy triplet structure was optimised in order to locate its energy relative to the N-nitrosoMEA bond dissociation asymptote. This was found to lie 187.9 kJ (1.93 eV) above the ground state, and is probably metastable with respect to dissociation. The process for the photolysis of N-nitrosoMEA is presented in Figure 22.

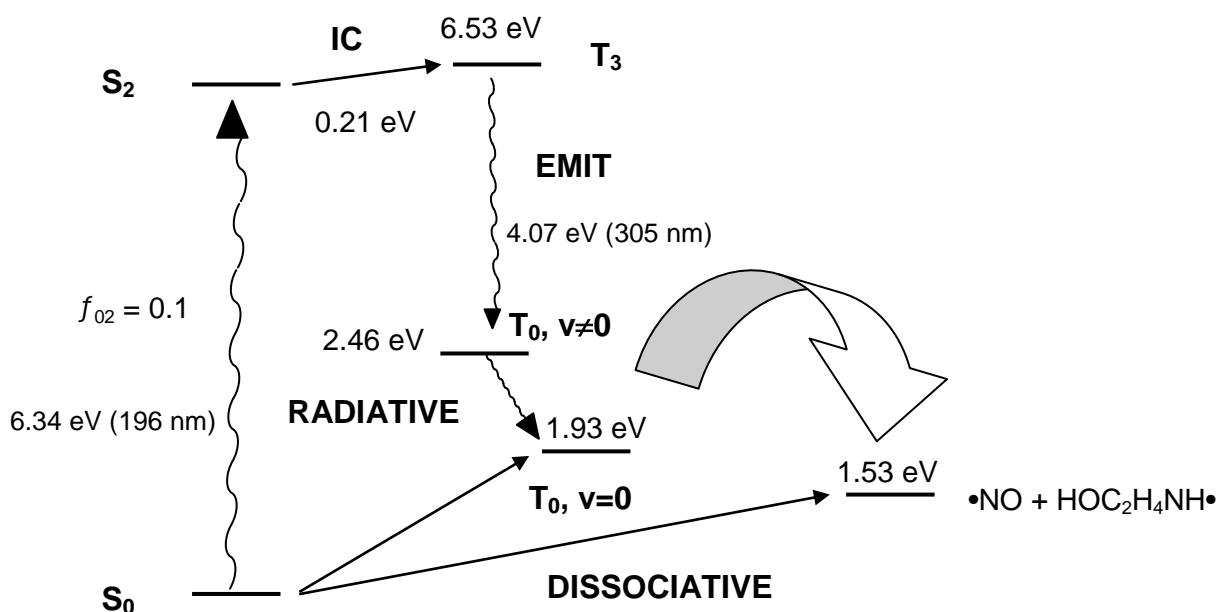


Figure 22. Most likely photolysis pathway for ground state N-nitrosoMEA according to TD-DFT predicted oscillator strengths.

Formation of C- and N-nitro, nitrite species

Both nitro- and -yl nitrite species have been investigated in order to establish the most likely products of reaction between C1-, C2- and N-centred MEA radicals and NO_x . Nitro-species possess connectivity of R- NO_2 , whereas -yl nitrite species have connectivity R-ONO. Although the nitrogen atom in R- NO_2 is formally in oxidation state +5 and +3 in the R-ONO, in free $\bullet\text{NO}_2$ the oxidation state is +4. In principle, reactions between MEA-centred radicals and $\bullet\text{NO}_2$ could lead to both nitro- and -nitrite products. Moreover, interconversion between the two isoforms could well be important to the gas phase chemistry of MEA.

The most stable C1,2-ONO conformer, the most stable C1,2-NO₂ conformer and their relative energies are presented in Figure 23.

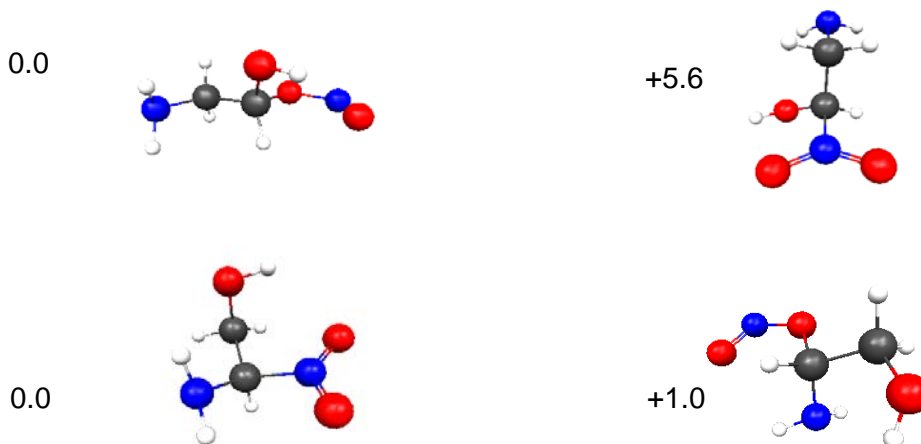


Figure 23. C1,C2-nitro and -yl nitrite structural isomers and their relative free energies (kJ/mol). Top row: C1 isoforms, bottom row: C2 isoforms.

It is evident from this figure that the two forms are almost isoenergetic (although a full conformational search is still in progress). The nitrite forms can be generated by a condensation of ONO at the radical site, or by addition of •NO to an MEA-oxo radical. The nitro isoforms could be formed by condensation of •NO₂ at the radical site, or by oxidation of C,N-N=O groups. Using weighted populations, the addition of either •ONO or NO₂ to C1 or C2 radical centres is exoergic by 204.7 and 204.3 kJ/mol, respectively ($\Delta_{GC1}(298\text{ K}) = -204.7\text{ kJ/mol}$, $\Delta_{GC2}(298\text{ K}) = -204.3\text{ kJ/mol}$). Collisional cooling will be needed to stabilise the product, or decomposition could ensue to •NO and C1,C2-oxo species.

As is the case for the 2-(nitrosoamino)ethanol converting to a hydroxydiazene, 2-(nitroamino)ethanol can undergo intramolecular conversion to 2-(2-hydroxy-2-oxido-2 λ^5 -diazene-1-yl)ethanol immediately after condensation of •NO₂ at the N-radical centre (free energy of activation +151.5 kJ; imaginary frequency = 1931i cm⁻¹). The transition structure for intramolecular isomerisation is presented in Figure 24.

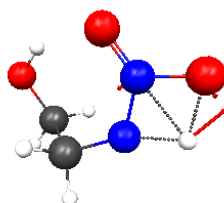


Figure 24. Transition structure for isomerisation of *N*-nitroMEA to *N*-hydroxynitrosoMEA.

Aminyl ($\bullet\text{NH}_2$) radicals

Although not expected to be present in significant abundance, the fate of aminyl radical has been investigated, specifically in relation to formation of nitrosoamine (the most fundamental nitrosamine). It is possible that certain surface processes or photochemical reactions could give rise to this highly reactive species. The potential energy surfaces for the reaction of $\bullet\text{NH}_2$ and $\bullet\text{NO}/\bullet\text{NO}_2$ are presented in Figures 25 and 26. The free energy of reaction of $\bullet\text{NH}_2$ and NO suggests some nitrosoamine will convert to hydroxydiazene ($\text{HN}=\text{N}-\text{OH}$), and populations of both species will be present. Some nitrosoamine will also proceed to decompose to H_2O and N_2 . The amount of each product formed will depend on the energy partitioning between the third body (M^*) and the reactant couple. A similar fate is envisaged for nitrosamine, with a fraction undergoing decomposition to N_2O and H_2O , and populations of hydroxydiazene-oxide and dihydroxydiazene co-existing with nitrosamine if equilibration is rapid. Pathways which are not considered feasible under standard conditions are marked with an 'X' in Figures 25, 26.

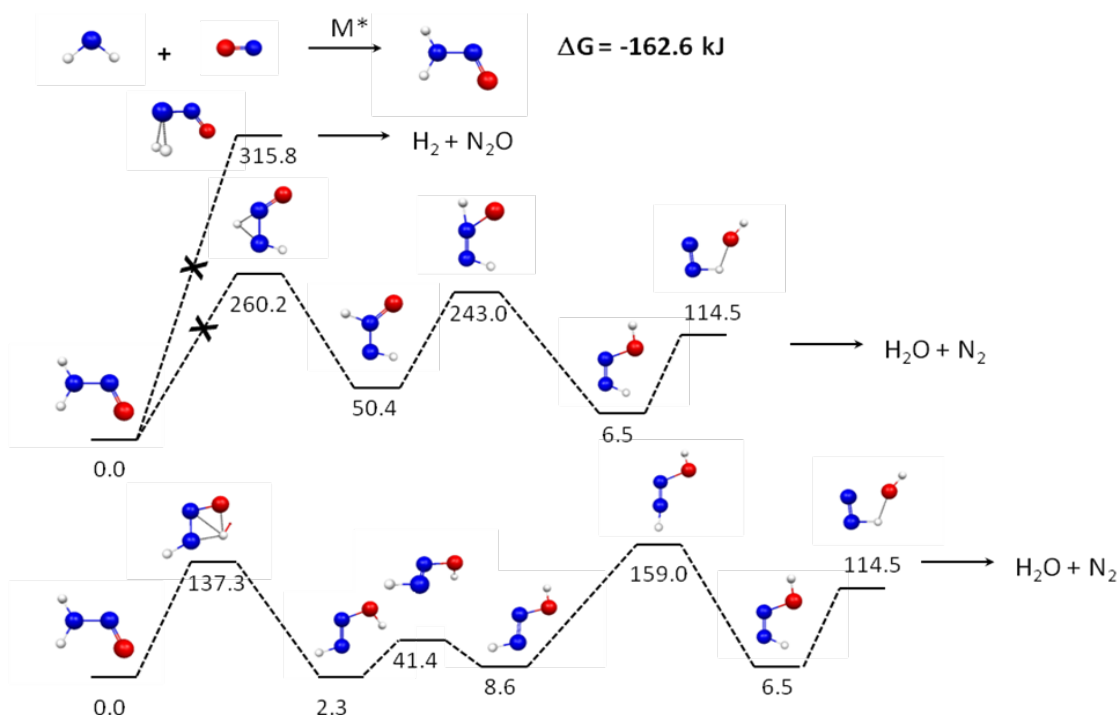


Figure 25. Potential energy surface for the reaction of aminyl radical and NO.

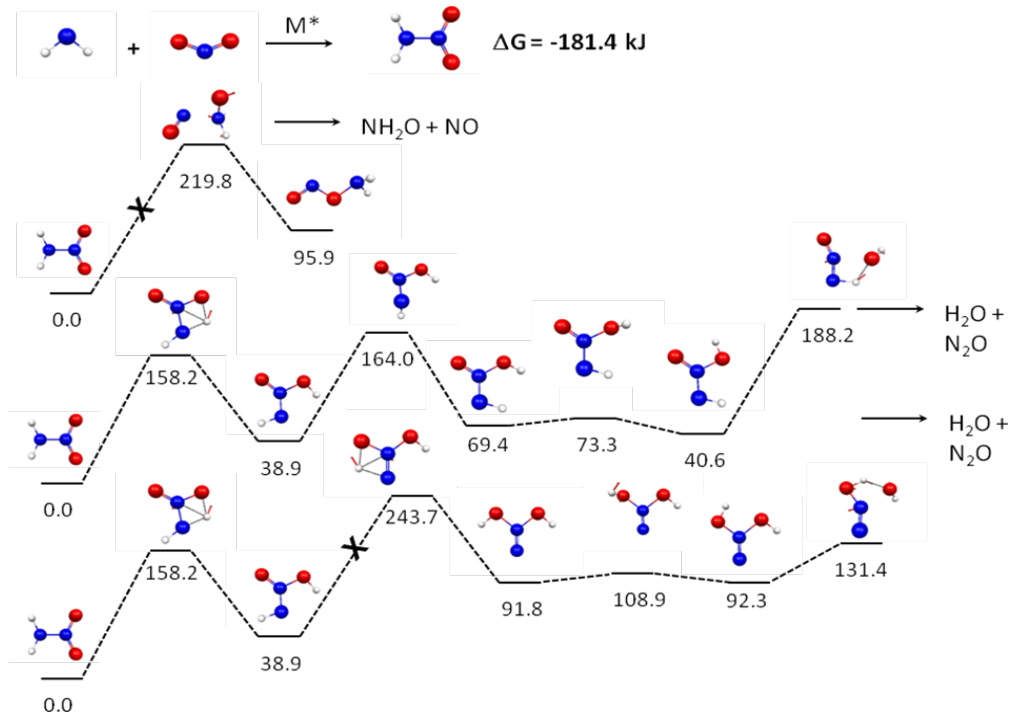


Figure 26. Potential energy surface for the reaction of aminyl radical and NO.

References to Study 1

Bråten, H.B, Bunkan, A.J., Bach-Andreassen, L., Solimannejad, M., Nielsen, C.J. (2008). *Final report on a theoretical study on the atmospheric degradation of selected amines*. NILU OR 77/2008.

Carlier, P., Hannachi, H., Mouvier, G. (1986) *Atmospheric Environment* 20, 2079-2099.

Frisch, M. J., Trucks, G. W., Schlegel, H. B., Scuseria, G. E., Robb, M. A., Cheeseman, J. R., Montgomery, Jr., J. A., Vreven, T., Kudin, K. N., Burant, J. C., Millam, J. M., Iyengar, S. S., Tomasi, J., Barone, V., Mennucci, B., Cossi, M., Scalmani, G., Rega, N., Petersson, G. A., Nakatsuji, H., Hada, M., Ehara, M., Toyota, K., Fukuda, R., Hasegawa, J., Ishida, M., Nakajima, T., Honda, Y., Kitao, O., Nakai, H., Klene, M., Li, X., Knox, J. E., Hratchian, H. P., Cross, J. B., Bakken, V., Adamo, C., Jaramillo, J., Gomperts, R., Stratmann, R.E., Yazyev, O., Austin, A. J., Cammi, R., Pomelli, C., Ochterski, J. W., Ayala, P. Y., Morokuma, K., Voth, G. A., Salvador, P., Dannenberg, J.J., Zakrzewski, V. G., Dapprich, S., Daniels, A. D., Strain, M. C., Farkas, O., Malick, D. K., Rabuck, A. D., Raghavachari, K., Foresman, J. B., Ortiz, J. V., Cui, Q., Baboul, A. G., Clifford, S., Cioslowski, J., Stefanov, B. B., Liu, G., Liashenko, A., Piskorz, P., Komaromi, I., Martin, R. L., Fox, D. J., Keith, T., Al-Laham, M. A., Peng, C. Y., Nanayakkara, A., Challacombe, M., Gill, P. M. W., Johnson, B., Chen, W., Wong, M. W., Gonzalez, C., Pople, J. A. (2004) *Gaussian 03, Revision C.02*. Gaussian, Inc., Wallingford CT.

Nielsen, C.J, D'Anna, B., Dye, C., George, C., Graus, M., Hansel, A., Karl, M., King, S., Musabila, M., Müller, M., Schmidbauer, N., Stenstrøm, Y., Wisthaler, A. (2010). *Atmospheric degradation of amines*. NILU OR 8/2010.

Schmidt, M.W., Baldridge, K.K., Boatz, J.A., Elbert, S.T., Gordon, M.S., Jensen, J.H., Koseki, S., Matsunaga, N., Nguyen, K.A., Su, S.J., Windus, T.L., Dupuis, M., Montgomery, J.A.(1993) *Journal of Computational Chemistry* 14, 1347-1363.

Wigner, E.P. (1932) *Z. Phys. Chem.* B19, 203.

Zhao, Y., Truhlar, D.G.(2008) *Accounts of Chemical Research* 41, 157-167.

RESEARCH ADDENDUM – STUDY 2

First principles determination of rate constants – MEA degradation

Author: Nicholas Lambropoulos

Introduction

In the atmosphere, oxidation of most amines results from the complex interactions between these amines and the following oxidants OH, O₃ and HNO₃ during the day and NO₃ during night-time, leading to the formation of different secondary pollutants. One of the most important identified chemical reactions leading to the degradation of amines is the reaction between amine and OH. This reaction is controlled by the rate constant of this reaction that is not very well established. Less attention was given to the other expected chemical reactions with O₃, HNO₃ and NH₃, and their roles in atmospheric pollutants formation. Currently, there is crucial need to determine these rate constants and other kinetic parameters affecting the fate of amines in the atmosphere and the potential formation of secondary pollutants.

In the aim of achieving an improved understanding the accuracy of the rate constants that control the rates of chemical reactions, we have proposed to assess the suitability of theoretical approaches to determine these rate constants. Given the imperative requirement to interactively qualify theoretical outcomes, the need for an experimental program is also necessary.

The content of this component of the report deals with the determination of rate constants derived from a first principles perspective related to the degradation of a selected amine, in this case we have considered MEA, in an atmospheric environment. The targeted selection of MEA was more so due to the complexity of the subject and the limited time of the project delivery where we could not investigate other molecules.

In tandem with the parallel theoretical investigation which has applied the methodologies and levels of theory drawn from the discipline of computational chemistry (QC), the computational methods applied here are primarily taken from the discipline of theoretical physics applied traditionally to the study of solid state matter (crystals, clusters, metals, semiconductors, etc) and most recently 'soft matter' (such as polymer and biological materials).

Computational methods for calculating Minimum Energy Paths (MEPs) are widely used in the fields of theoretical chemistry, physics, and materials science. In general, the MEP describes the mechanism of reaction, and in thermal systems, the energy barrier along the path which can be used to calculate the reaction rate. In this approach, we utilise two codes to map out MEPs in which both initial and final optimised structural states required. Our goal is then to find the MEP between states to a specified accuracy with the smallest amount of computational effort. Of the number of periodic and cluster based codes available, the CSIRO has a strong capability with two mature codes, VASP and Dmol³. The primary code engaged to predictively calculate reaction barriers for the series of reactions between MEA with OH was Dmol³ though VASP to a lesser extent (due to time restrictions) was utilised to initiate an alternative approach to evaluating rate constants of molecular systems.

Transitions state search methods

With respect to the computational approach applied for this study, each of the codes tabled offer either a direct (the VASP code[Kresse, 1993, 1996]) or indirect (the Dmol³

code[Delley, 1990]) derivative of the Nudged Elastic Band (NEB)[Mills, 1994] method towards calculating MEPs. The NEB method is an efficient method for finding the MEP between a given initial and final state of a transition. In essence, the NEB method introduces a fictitious spring force that connects neighbouring points on the path to ensure continuity of the path and projection of the force so that the system converges to the MEP. Furthermore, a possible advantage of the NEB algorithm is that it provides a computationally cost competitive (based on time) qualitative examination of MEPs compared to QC related approaches.

The difference however is that whilst the direct derivative approach implemented in VASP locates a transition state (TS) and reaction pathway based on two endpoints, the indirect derivative approach implemented in Dmol³ commences with a TS obtained by using The LST/QST algorithms (discussed in more detail below) and returning the Intrinsic Reaction Path (IRP) through the three points (Reactant, TS, Product). This is the path that would be produced by a molecular dynamics (MD) simulation starting at the TS using completely damped velocities and infinitesimal steps. Each point on the IRP is an energy minimum in all directions except one, which defines the direction of the IRP. This pathway also corresponds to the MEP connecting two structures.

As implemented in Dmol³, Synchronous Transit Methods are used to find transition states when reasonable structures for the reactants and products exist, whereby the location of the TS is unknown. Commencing from reactants and products, synchronous transit methods interpolate a reaction pathway to find the TS. A Linear Synchronous Transit (LST)[Halgren, 1977] method constructs the reaction path by interpolating between the reactant and product structure, and determines the point of maximum energy on the path as a guess for the TS. Furthermore, a Quadratic Synchronous Transit (QST)[Peng, 1993] method interpolates the reaction path between three structures whereby an intermediate geometry is required in addition to the reactant and product structures.

The Linear Synchronous Transit (LST) is a method that interpolates geometrically between a reactant and a product to generate a reaction pathway. It can be used, in conjunction with single point energy calculations, to perform transition state searches. In the original LST method, an idealized set of structures connecting reactants and products is obtained by linearly interpolating all distances between pairs of atoms (in this respect resembling the "total connection scheme") in the reactant and product. In essence, the LST path point is defined by locating the molecular geometry with inter-nuclear distances as close as possible to the geometry obtained by interpolating the Cartesian coordinates between reactant and product. Such an interpolation is purely geometrical without the need to calculate energy. When the potential energy is calculated at points along a given pathway, the maximum total energy is located which is considered as the LST maximum approximation to the transition state.

Whilst the LST method generates the paths points by interpolating between the start and end points, the QST method makes an interpolation between three points, requiring a third "intermediate" point. The QST algorithm begins with a maximum search from the intermediate point, imposing the constraint that the resulting geometry has the same path coordinate as the initial point of optimization. The QST optimization procedure offers an upper bound to the TS under the applied constraint.

It is possible to combine the improved LST algorithms involving constrained minimizations with the QST algorithm: complete LST/QST begins by performing an LST/Optimization calculation. Complete LST/QST begins by performing an LST/Optimization calculation. The TS approximation obtained in that way is used to perform QST maximisation. From that point, another conjugate gradient minimization is performed. The cycle is repeated until a stationary point is located or the number of

allowed QST steps is exhausted. This is claimed to be considerably more accurate than the other methods, yielding results close to those obtainable using eigenvector following methods. It is this approach that has been utilised for our study.

Model scenarios investigated

Eight scenarios were investigated as summarised in Table 6. Pathway reactions depicting the degradation process of MEA were undertaken in both a hydrated and non-hydrated environment.

Table 6 Pathway Scenarios Modelled

Without Hydration		With Hydration	
A	MEA -H abstraction from C2 with neutral hydroxyl radical	E	MEA.2H ₂ O -H abstraction from C2 with neutral hydroxyl radical
B	MEA -H abstraction from C1 with neutral hydroxyl radical	F	MEA.2H ₂ O -H abstraction from C1 with neutral hydroxyl radical
C	MEA -H abstraction from amino end with neutral hydroxyl radical	G	MEA.2H ₂ O -H abstraction from amino end with neutral hydroxyl radical
D	MEA -H abstraction from alcohol end with neutral hydroxyl radical	H	MEA.2H ₂ O -H abstraction from alcohol end with neutral hydroxyl radical

Introduction of molecular water allows for improved energy landscape accuracy with respect to the interacting MEA and neutral radical reactants. In the case of the hydrated scenarios, two water molecules were included which offers stabilisation of the radicals surrounding the MEA group as shown in Figure 11.

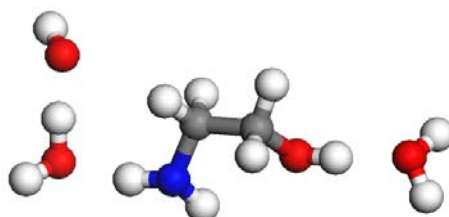


Figure 11 MEA and Neutral Hydroxyl Radical Surrounded by Molecular Water

This allows for inclusion of perturbations with respect to binding between reactant and product and possible shifts in transition state structures which may ultimately shift final barrier energies and rate constants. To corroborate this approach, we have just become aware of a recent study [Du, 2009] which investigated electronic structure, stability, and dynamics of interaction and recombination of free radicals such as HO₂ and OH influenced by water. Results indicated that a significant interaction, overcoming the repulsive Coulombic barrier, occurs at a separation distance between the radicals of 5.7Å.

Computational methodology

Geometry optimizations were carried out to locate minima and saddle points at the level of DFT by using initially using the *Perdew-Wang GGA-PW91* generalized-gradient approximation functional[Perdew, 1992] in combination with a double-numerical with polarisation (DNP) basis set as detailed in Table 7 and all electron potential (where all electrons are treated as valence electrons which offers good accuracy suited towards hydrogen bonding applications).

Table 7 Double Numerical plus Polarization

DNP	Double Numerical. MIN + a second set of valence AOs. Includes d-function on all non-hydrogen elements and polarization p-function on all hydrogen atoms.	H: 1s 1s' 1p C: 1s 2s 2p 2s' 2p' 3d Si: 1s 2s 2p 3s 3p 3s' 3p' 3d
-----	--	---

Further refinement of structure was made available by the *Revised Perdew-Burke-Ernzerhof GGA-RPBE* correlation functional[Hammer, 1999], which is noted as considerably improving on predicting thermodynamic properties[Yang, 2010], in combination again with a DNP basis set and treated this time with semi-core pseudopotentials (DSPPs) - a variant form of norm conserving pseudopotentials [Bachelet, 1988] which greatly assisted with decreasing computational cost whilst maintaining accuracy.

Convergence thresholds for energy change, maximum force, and maximum displacement during geometry optimization cycles were taken through progressively from coarse, medium and finally fine convergence with each convergence threshold given in the Table 8:

Table 8 Geometry Optimisation Thresholds

Value	Coarse	Medium	Fine
Energy (Hartree)	1×10^{-4}	2×10^{-5}	1×10^{-5}
Max. force (Hartree \AA^{-1})	0.02	0.004	0.002
Max. displacement (\AA)	0.05	0.005	0.005

The search for saddle points is performed by using the LST and QST algorithm approach as discussed Section 2. Harmonic frequencies are calculated analytically for all species at the same level and are used un-scaled throughout the work. The frequencies of the minima are all real, and the saddle points exhibit only one imaginary frequency. Again, qualities of settings were that of medium level for the smaller model systems (scenarios [a] to [d]) and coarse level for the larger hydrated model systems

(scenarios [e] and [h]). The threshold values utilised are summarised in Table 9. Both reactants and products are structurally optimised prior to determination of transition state.

Table 9 LST and QST Thresholds

Quality	Energy (Hartree)	Force (Hartree/Å)	Displacement (Å)
Coarse	10^{-4}	0.02	0.05
Medium	2×10^{-5}	0.004	0.005

There was an operational requirement to implement a fractional occupancy, which effectively mixes some virtual orbitals into the occupied space. This is more so the case when the HOMO-LUMO gap is small and there is significant density of states in the vicinity of the Fermi level. In such situations, one may achieve SCF convergence by incorporating smearing techniques [Delley, 1995]. Such a technique tends to shift up the virtual orbitals, or fixing (freezing) occupancy. Typically, this is useful during problems with SCF convergence especially for open-shell systems such as this case dealing with neutral hydroxyl radical systems. The level of smearing used for our modelled MEA-hydroxyl system was set at 0.005 during geometry optimisations when using the GGA-PW91 / GGA-RPBE functionals and changed to 0.01 Ha during the transition structure search.

All model zero charge free radical scenarios were treated as spin unrestricted open shell doublet systems (equating to a multiplicity of two).

Derived rate constants using synchronous direct methods

To calculate reaction rate constants from the model runs, the well-known Wigner expression for the reaction rate constant of a bimolecular reaction $A + B \rightleftharpoons AB^\ddagger$ was implemented [McQuarrie, 1997, Aguilera-Lparraaguirre, 2008]:

$$k = V_m \frac{k_B T}{h} \exp\left(\frac{-\Delta G_{B,0}}{RT}\right)$$

Equation 1

where R is the gas constant; k_B is the Boltzmann constant; h is the Planck constant; and V_m is the molecular volume of the model system. $\Delta G_{B,0}$ is defined as the electronic barrier height $\Delta G_{B,e}$ inclusive of the zero-point vibrational energy (ZPVE) which is computed at the GGA-RPBE/DNP level for all the methods under this study.

Table 10 Constants & Nomenclature used in the Wigner expression

Constants	Nomenclature
h = 6.626×10^{-34} J.s	h : Planck Constant
k_B = 1.381×10^{-23} J.K ⁻¹	k_B : Boltzmann Constant
T = 298.15 K	T : Temperature
R = 8.314 J.mol ⁻¹ .K ⁻¹	R : Gas constant
	Ha: Hartree (atomic unit of energy)
	$\Delta G_{B,0}$: Free Energy Barrier Height (inclusive of ZPVE)
	V_m : Molecular Volume
	k : Rate Constant

Calculated rate constants (in units of cm³.molecule⁻¹.s⁻¹) are derived from the model simulations using Synchronous Direct Methods (for the first tier of the MEA degradation scenarios shown in Table 6) and summarised in Table 11 for the non hydrated systems (scenarios [a] to [d]) and in Table 12 for the hydrated systems (scenarios [e] to [h]). Molecular volumes have been calculated using the approaches of Jalbout [Jalbout, 2003] and Wong [Wong, 1995] whilst all other constants required for the Wigner expression from Equation 1 are summarised in Table 10.

Transition states were located using the approaches and methodologies discussed in sections 2 and 4. Electronic and temperature corrected free energies (inclusive of ZPVE) were calculated and stated as $G_{\text{tot-reactants}}$ and $G_{\text{tot-transition}}$ for both initial reactants and transition state for each scenario respectively. Structures of reactant, transition state and products have been included in Figure 2.

Table 11 Transition State Theory Derived Rate Constants for Non-Hydrated MEA Scenarios

		Non Hydrated			
		A	B	C	D
		C2	C1	Amino	Alcohol
V_m	$cm^3.molecule^{-1}$	1.06×10^{-22}			
ΔG_{tot-} reactants	Hartrees	-286.1625	-286.1633	-286.1687	-286.1694
ΔG_{tot-} transition	Hartrees	-286.1578	-286.1589	-286.1668	-286.1680
$\Delta G_{correction}$	$kJ.mol^{-1}$	6.590	2.628	1.946	9.355
$\Delta G_{B,0}$	$kJ.mol^{-1}$	12.453	11.523	5.155	3.436
k	$cm^3.molecule^{-1}.s^{-1}$	4.31×10^{-12}	6.28×10^{-12}	8.19×10^{-11}	1.64×10^{-10}

Table 12 Transition State Theory Derived Rate Constants for Hydrated MEA Scenarios

		Hydrated			
		E	F	G	H
		C2	C1	Amino	Alcohol
V_m	$cm^3.molecule^{-1}$	1.69×10^{-22}			
ΔG_{tot-} reactants	Hartrees	-439.0539	-439.0534	-439.0459	-439.0529
ΔG_{tot-} transition	Hartrees	-439.0550	-439.0525	-439.0524	-439.0660
$\Delta G_{correction}$	$kJ.mol^{-1}$	-2.523	3.883	17.945	26.895
$\Delta G_{B,0}$	$kJ.mol^{-1}$	-2.754	2.444	-17.067	-34.535
k	$cm^3.molecule^{-1}.s^{-1}$	3.18×10^{-09}	3.90×10^{-10}	1.02×10^{-06}	1.18×10^{-03}

Scenario	Reactant	TS	Product
<i>a</i>			
<i>b</i>			
<i>c</i>			
<i>d</i>			
<i>e</i>			
<i>f</i>			
<i>g</i>			

Figure 2 Reactant, TS and Product Structures of MEA and radical groups

Observations

Firstly on the non-hydrated systems modelled (scenarios [a] to [d]). Surprisingly, use of the RPBE functional with DNP basis set and DSPPs resulted with the calculated rate constants agreeing well to experiment, to an extent, for each abstraction pathway modelled. The C1 and N (amino end) abstraction were well within the order of experiment whilst the C2 abstraction differed by an order of 2 slower to that of experiment whereas the alcohol (O) abstraction pathway differing by at most 3 orders of magnitude greater in rate to that of experiment.

Secondly with respect to the hydrated systems modelled (scenarios [e] to [h]), the one noticeable difference was the dramatic increase in rate constants for each abstraction point. By placing one additional water molecule on each side of the MEA (as depicted in Figure 11), an increase in magnitude of 3, 2, 4 and 7 was observed for each of the abstractions occurring at C2, C1, N and O respectively. Exactly the same functional, basis set and pseudopotentials were applied as was with the non-hydrated scenarios. This may therefore infer the major role that water presence may have on rate constants (both from a theoretical and experimental perspective).

Other observations include:

- The re-orientation of water molecules between themselves and the MEA (with slight torsional changes), possibly due to hydrogen bonding;
- The presence of molecular water near the path of a transition which may be effectively altering the energetics of the transition (this is drawn from a speculative perspective) and;
- An increase in free energy correction differences between the transition state and starting reactants for each of the non-hydrated and hydrated models, as noted by $\Delta G_{\text{correction}}$ in both Table 11 and
- Table 12. Absolute mean and standard deviations were calculated to be $5.1 \pm 3.5 \text{ kJ.mol}^{-1}$ and $12.8 \pm 11.7 \text{ kJ.mol}^{-1}$ for each scenario respectively.

The purpose of introducing water is not to quantify the difference between vacuum and hydrated environments though to emphasise the impact that atmospheric water has on the outcome. The addition of molecular water to the model systems was not to simulate to effect of saturated solvation effects (i.e., in solvated liquid environments), but to investigate the change in energetics when atmospheric water presence becomes part of the reactant make-up. Follow-up to this observation is briefly tabled in the section on recommendations in the study.

Improved NEB - The Dynamical Matrix Approach

An alternative approach to the synchronous direct method, which was detailed and implemented in Section 5, is by way of harmonic transition state theory (*hTST*) approximation using a dynamical matrix. Traditionally implemented in the solid state discipline, the method has been used in conjunction with plane wave based electronic structure calculations derived from DFT calculations.

Firstly, an improved implementation of the NEB method would be specifically applied to a benchmark model system, utilising a technique referred to as the climbing image [Henkelman, 2000] (Stage I). This is a small modification to the NEB method in which the highest energy image is driven up to the saddle point. This image does not feel the spring forces along the band. Instead, the true force at this image along the tangent is inverted. In this way, the image tries to maximize its energy along the band, and minimize in all other directions. When this image converges, it will be at the exact saddle point. The MEP is found by constructing a set of images (replicas) of the

system, typically in the order of 4–20, between the initial and final state. A spring interaction between adjacent images is added to ensure continuity of the path, thus mimicking an elastic band. The MEP can then be used to estimate the activation energy barrier for transitions between the initial and final states within the *hTST* approximation. Any maximum along the MEP is a saddle point on the potential surface, and the energy of the highest saddle point gives the activation energy needed for the *hTST* rate estimate.

Because the highest image is moved to the saddle point and it does not feel the spring forces, the spacing of images on either side of this image will be different. It can be important to do some minimization with the regular NEB method before this flag is turned on, both to have a good estimate of the reaction co-ordinate around the saddle point, and so that the highest image is close to the saddle point. If the maximum image is initially very far from the saddle point, and the climbing image was used from the outset, the path would develop very different spacing on either side of the saddle point.

Secondly, upon completing the saddle point search using the improved NEB method, VASP's implementation of a dynamical matrix code would therefore allow for the calculation of harmonic frequencies and the prefactor of a reaction (Stage II). The formalism was developed by Vineyard[Vineyard, 1957], and the Arrhenius rate includes the Vineyard prefactor. The general idea is that the potential is assumed to be harmonic at both initial and transition states. With this assumption, one may formulate the migration prefactor (the product of the attempt frequency and the exponential of the migration entropy over k) as the ratio of the products of the frequencies of the normal modes of the initial state over the transition state. In essence, the entropy of the initial and transition state is evaluated using a harmonic approximation.

As briefly tabled in the introduction, a preliminary investigation was initiated during the course of this study to investigate an alternative approach to evaluating rate constants of molecular systems. Due to the well known time restrictions of the project, only the first stage of mapping out the energy-pathway of the reactant-transition mechanism was completed.

The model system selected was that of the abstraction of hydrogen from ethane by a neutral hydroxyl radical. The calculated reactant to product pathway is shown in Figure 3, where it can be seen that location of a transition state and other 'quasi-transition' states is possible. Molecular layout of the reactants (commencement of the NEB analysis) and products (completion of the NEB analysis) is shown in Figure 4.

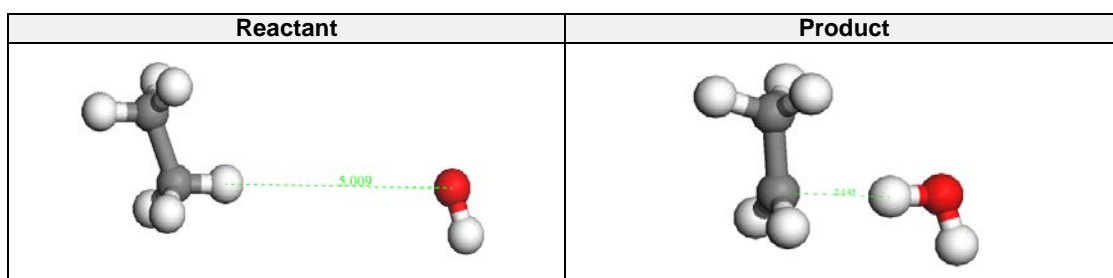


Figure 3 Reactant and Product Structures of Ethane and Neutral Radical Hydroxyl

Ground-state DFT calculations are performed using VASP along with the projected augmented wave method [Blochl, 1994] with an energy cut-off of 432.37eV. Real space is sampled with a Monkhorst-Pack k-point mesh of 3x3x3 per unit cell. The generalized gradient approximation (GGA) was implemented with the parametrized Perdew–Burke–Ernzerhof (PBE) functional for atomic structures and relative energetics between the reactants and products.

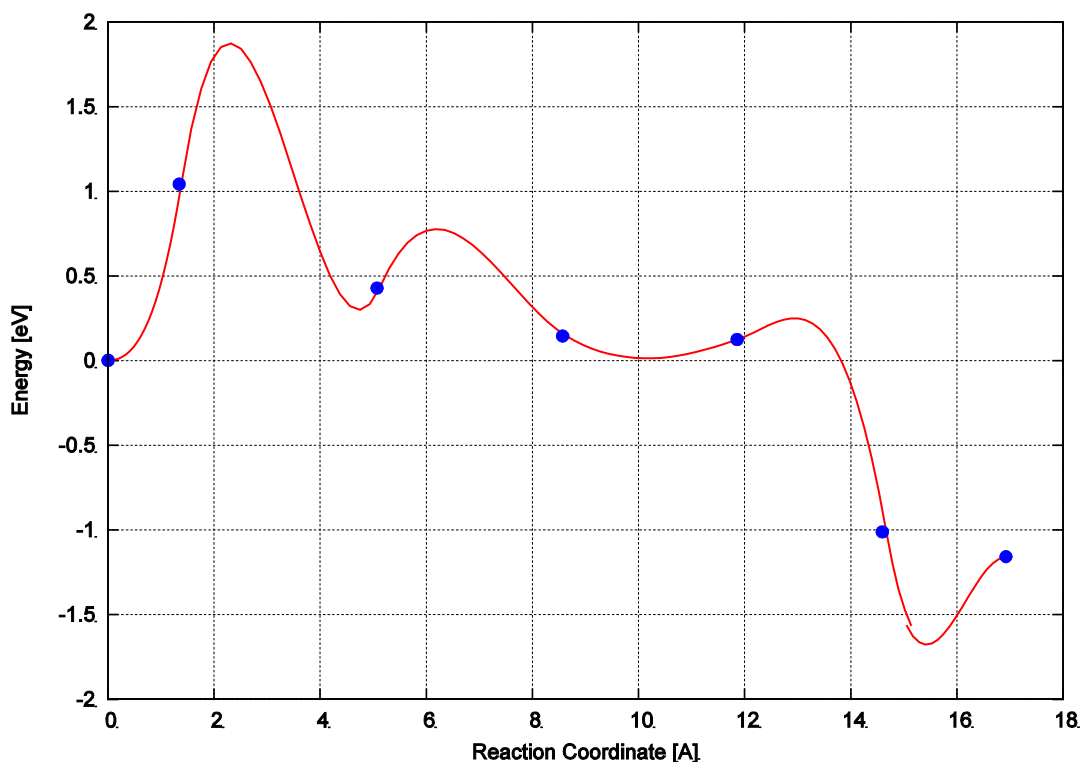


Figure 4 Calculated Reactant to Product Pathway for Ethane using the Improved NEB Method

The intention is to extract these states in the foreseeable future and apply a dynamical matrix scheme whereby calculation of a Vineyard prefactor will allow calculation of kinetic rates.

Preliminary Recommendations

- ♦ Continue further rate constant studies whereby the presence of water is essential within the models;
- ♦ Determination of rate constants for other atmospheric species as directed by Gassnova using the established synchronous direct method for the MEA pathways;
- ♦ Allow for further development of using the dynamical matrix approach outlined in section 6 to determining rate constants.

With respect to integrating first principles modelling with empirical based Aspen One process modelling, CSIRO will use quantum mechanical modelling of the compounds in question resulting from the conceptual PFD to access attributes of the solvents. Outputs may include determination of:

- ♦ Vapour pressure
- ♦ Free energy of solvation
- ♦ Activity coefficients
- ♦ Partition coefficients
- ♦ Solubility and solid-liquid equilibria (SLE).
- ♦ Liquid-liquid equilibrium (LLE) and vapour-liquid equilibrium (VLE)
- ♦ Phase diagrams, azeotropes, miscibility gaps, excess enthalpies and excess free energies
- ♦ pKa of acids and bases
- ♦ Various QSPR models
- ♦ Reaction constants
- ♦ Liquid extraction equilibria

Note that this semi-empirical approach is derived from quantum mechanical modelling of compounds in a solvated environment using the Turbomole code (COSMO solvation level of theory used) and then combined with an electrostatic theory of locally interacting molecular surface descriptors (which are available from QM calculations) with a statistical thermodynamics methodology to derive the attributes mentioned above.

References to Study 2

1. Kresse, G. and J. Hafner, Ab initio molecular dynamics for liquid metals. *Phys. Rev. B*, 1993. 47(558).
2. Kresse, G. and J. Furthmüller, Efficiency of ab-initio total energy calculations for metals and semiconductors using a plane-wave basis set. *Comput. Mat. Sci.*, 1996. 6(15).
3. Delley, B., *J. Chem. Phys.*, 1990. 92(508).
4. Mills, G. and H. Jonsson, *Phys. Rev. Lett.*, 1994. 72(1124).
5. Halgren, T.A. and W.N. Lipscomb, The Synchronous Transit Method for Determining Reaction Pathways and Locating Transition States. *Chem. Phys. Lett.*, 1977. 49(225).
6. Peng, C. and H.B. Schlegel, Combining Synchronous Transit and Quasi-Newton Methods for Finding Transition States. *Israel J. Chem.*, 1993. 33.
7. Du, S., J.S. Francisco, and S. Kais, Study of electronic structure and dynamics of interacting free radicals influenced by water. *J. Chem. Phys.*, 2009. 130(124312).
8. Perdew, J.P. and Y. Wang, *Phys. Rev. B*, 1992. 45(13244).
9. Hammer, B., L.B. Hansen, and J.K. Norskov, *Phys. Rev. B*, 1999. 59: p. 7413.
10. Yang, K., et al., Tests of the RPBE, revPBE, tau-HCTHhyb, omega B97X-D, and MOHLYP density functional approximations and 29 others against representative databases for diverse bond energies and barrier heights in catalysis. *Journal of Chemical Physics*, 2010. 132(16): p. -.
11. Bachelet, G.B., D.R. Hamann, and M. Schluter, Pseudopotentials That Work - from H to Pu - Reply. *Physical Review B*, 1988. 37(9): p. 4798-4798.
12. Delley, B., *Modern Density Functional Theory: A Tool for Chemistry*, in *Theoretical and Computational Chemistry*, J.M. Seminario and P. Politzer, Editors. 1995, Elsevier Science: Amsterdam.
13. McQuarrie, D.A. and J.D. Simon, *Physical Chemistry: A Molecular Approach*. 1997: University Science Books: Sausalito.
14. Aguilera-Iparraguirre, J., et al., Accurate Benchmark Calculation of the Reaction Barrier Height for Hydrogen Abstraction by the Hydroperoxyl Radical from Methane. *J. Phys. Chem. A*, 2008. 112: p. 7047-7054.

15. Jalbout, A.F., Theoretical calculations of the molar volumes of atoms and molecules. *Journal of Molecular Structure-Theochem*, 2003. 624: p. 81-85.
16. Wong, M.W., K.B. Wiberg, and M.J. Frisch, Ab-Initio Calculation of Molar Volumes - Comparison with Experiment and Use in Solvation Models. *Journal of Computational Chemistry*, 1995. 16(3): p. 385-394.
17. Henkelman, G. and H. Jónsson, Improved tangent estimate in the nudged elastic band method for finding minimum energy paths and saddle points. *J. Chem. Phys.*, 2000. 113(9978).
18. Vineyard, G.H., *J. Phys. Chem. Solids*, 1957. 3(121)
- .19. Blochl, P.E., *Phys. Rev. B*, 1994. 50: p. 17953.



Contact Us

Phone: 1300 363 400
+61 3 9545 2176

Email: enquiries@csiro.au

Web: www.csiro.au

Your CSIRO

Australia is founding its future on science and innovation. Its national science agency, CSIRO, is a powerhouse of ideas, technologies and skills for building prosperity, growth, health and sustainability. It serves governments, industries, business and communities across the nation.